UNIVERSIDADE FEDERAL DE MINAS GERAIS
Instituto de Geociências
Programa de Pós-graduação em Geologia

Raphael do Carmo Fernandes

EVOLUÇÃO ESTRUTURAL DO DEPÓSITO AURÍFERO CUIABÁ E PERSPECTIVAS EXPLORATÓRIAS CIRCUNJACENTES, QUADRILÁTERO FERRÍFERO, BRASIL

Belo Horizonte
2022

Raphael do Carmo Fernandes

EVOLUÇÃO ESTRUTURAL DO DEPÓSITO AURÍFERO CUIABÁ E PERSPECTIVAS EXPLORATÓRIAS CIRCUNJACENTES, QUADRILÁTERO FERRÍFERO, BRASIL

Versão final

Dissertação apresentada ao Programa de Pós-graduação em Geologia da Universidade Federal de Minas Gerais como requisito parcial para obtenção de título de Mestre em Geologia Econômica Aplicada.

Orientador: Prof. Dr. Jorge Geraldo Roncato Júnior

Coorientador: Prof. Dr. Rodrigo Sérgio de Paula

Belo Horizonte

2022

F363e
2022

Fernandes, Raphael do Carmo.

Evolução estrutural do depósito aurífero Cuiabá e perspectivas exploratórias circunjacentes, Quadrilátero Ferrífero, Brasil [manuscrito] / Raphael do Carmo Fernandes. – 2022.

99 f., enc. il. (principalmente color.)

Orientador: Jorge Geraldo Roncato Junior.

Coorientador: Rodrigo Sérgio de Paula.

Dissertação (mestrado) – Universidade Federal de Minas Gerais, Instituto de Geociências, 2022.

Área de concentração: Geologia Econômica Aplicada.

Bibliografia: f. 88-97.

Inclui anexos.

1. Geologia – Velhas, Rio das (MG) – Teses. 2. Ouro – Minas e mineração – Teses. 3. Metalogenia – Quadrilátero Ferrífero (MG) – Teses. I. Roncato, Jorge. II. Paula, Rodrigo Sérgio de. III. Universidade Federal de Minas Gerais. Instituto de Geociências. IV. Título.

CDU: 553.078(815.1)

Ficha catalográfica elaborada por Elisabete Quatrini Vieira – CRB-6/2210
Biblioteca “Vitória Pedersoli”, Instituto de Geociências da UFMG

UNIVERSIDADE FEDERAL DE MINAS GERAIS

PROGRAMA DE PÓS-GRADUAÇÃO EM GEOLOGIA DO IGC-UFMG

FOLHA DE APROVAÇÃO

Evolução estrutural do depósito aurífero Cuiabá e perspectivas exploratórias circunjacentes, Quadrilátero Ferrífero, Brasil

RAPHAEL DO CARMO FERNANDES

Dissertação submetida à Banca Examinadora designada pelo Colegiado do Programa de Pós-Graduação em GEOLOGIA, como requisito para obtenção do grau de Mestre em GEOLOGIA, área de concentração GEOLOGIA ECONÔMICA E APLICADA, pelo Programa de Pós-graduação em Geologia do Instituto de Geociências da Universidade Federal de Minas Gerais.

Aprovada em 27 de outubro de 2022, pela banca constituída pelos membros:

Prof. Jorge Geraldo Roncato Júnior – Orientador
UFMG

Profa. Flávia Cristina Silveira Braga
UFMG

Prof. Alexandre Uhlein
UFMG

Prof. Issamu Endo
UFOP

Belo Horizonte, 27 de outubro de 2022.

À população de Sabará e Caeté dedico este trabalho.

Com todo respeito e admiração.

AGRADECIMENTOS

Gostaria de expressar os meus agradecimentos a diversas pessoas sem os quais esse trabalho não poderia ser executado.

À minha esposa Lívia pelo amor, paciência, compreensão, companhia, confiança e motivação. A meus filhos Mateus e Maria, que me ensinam diariamente a não perder o espírito da infância e a manter a ausência de preconceitos, ambos imprescindíveis para se manter a alegria no dia a dia e a observar um fenômeno da natureza de maneira imparcial.

À minha família. Em especial a meus pais Djalma e Maria Aparecida que me privilegiaram com uma base de amor e educação. A meus irmãos, cunhados, sobrinhos e sogros, que me propiciam praticar a união, partilha, e respeito ao próximo.

À minha *alma mater* Universidade Federal de Minas Gerais, a Pró-reitoria de Pós-graduação (PRPg) da UFMG e ao Programa de Pós-graduação em Geologia do Instituto de Geociências (IGC) da UFMG, em especial aos meus orientadores e professores Dr. Jorge Roncato e Rodrigo Sérgio de Paula. Vocês são espelho de como eu gostaria de ser caso tenha a honra de me tornar um professor futuramente. Aos professores de geologia pelo aprendizado acadêmico e por compartilhar experiências profissionais que nos auxiliam a trilhar o "caminho das pedras", em especial à Dra. Rosaline Cristina Figueiredo e Silva e aos Drs. Fabrício Caxito, Tiago Novo e Paulo Galvão.

À Universidade Federal de Ouro Preto onde pude cursar algumas disciplinas e compartilhar a experiência e vivência em uma outra universidade: aos professores doutores Fernando Flecha Alkmim, Leonardo Lagoeiro e em especial ao Issamu Endo, sendo um ouvinte bastante assíduo de

minhas expectativas geológicas referente a esse trabalho e que me ajudou na elaboração de uma metodologia de estudo para a caracterização do arcabouço estrutural.

Aos membros da banca pelo qual pude ser avaliado e cujas observações foram muito importantes para a melhoria deste trabalho: a professora Dra. Flávia Cristina Braga e aos professores Dr. Alexandre Uhlein e Dr Issamu Endo.

À AngloGold Ashanti por propiciar o meu desenvolvimento profissional com qualidade, a apoiar esse trabalho de mão dupla e permitir que o artigo fosse publicado, em especial ao Diogo Afonso Costa, pela confiança durante a minha contratação, treinamento e orientação profissional durante os primeiros anos de trabalho na empresa; aos geólogos, em especial ao Anderson Gonçalves Cândido, Avled Vilela Oliveira, Fred Vinícius Rodrigues Ribeiro, Frederico Wallace Reis Vieira, Rhuan Carlos Vidal Rocha, Roberto Moreno Prado Pereira, André Luiz Vitorino, Luiz Gustavo Dal'bo da Costa e Suellen Olívia Cândida Pinto que contribuíram com proveitosas discussões e propiciaram construir uma base sólida que sustentasse um modelo geológico coerente ao observado; ao geólogo Pedro Dumond Barroso pela leitura crítica do artigo que se encontra nessa dissertação; aos técnicos de Geologia e equipe de GIS que contribuem e contribuíram, em especial ao Geraldo Guilherme da Silva e Sidney Marcos de Carvalho, Mirian Regina Corradi e Leandro Lopes; a toda equipe de amostragem, sondagem e topografia, responsáveis diretos pela geração da informação geológica; a toda operação de mina, sem os quais esse trabalho seria inviabilizado.

Enfim, agradeço a todos os amigos e colegas além da geologia, sem os quais não seria possível tornar essa caminhada mais tranquila e prazerosa.

“O saber a gente aprende com os mestres e com os livros.

A sabedoria, se aprende é com a vida e com os humildes”

Cora Coralina

Resumo

O entendimento estrutural de um depósito orogênico é fundamental para a sua compreensão metalogenética, uma vez que ambos os assuntos estão interligados nesse tipo de ambiente. O depósito aurífero Cuiabá, localizado em rochas arqueanas do *greenstone belt* Rio das Velhas no Quadrilátero Ferrífero, é alvo de inúmeros estudos focados sobretudo na caracterização metalogenética. Estas mineralizações estão hospedadas essencialmente em sulfetos nas formações ferríferas bandadas e encaixadas em xistos de composição máfica. Do ponto de vista da caracterização estrutural, dois modelos divergentes têm sido estudados: o modelo de dobra em bainha e o modelo de redobramento, trazendo diferentes perspectivas exploratórias para a região. Como forma de suprir esta lacuna, o principal objetivo desse trabalho é caracterizar a geologia e definir um novo modelo para o depósito de forma que haja uma melhor compreensão a respeito de seu arcabouço. Para isso, as metodologias aplicadas neste trabalho foram: mapeamento geológico em subsolo nas galerias de minério acessíveis e definição de domínios geológicos-estruturais cujos principais critérios estão relacionados à determinação de assimetria de dobramentos e indicadores estratigráficos observados no plano de simetria da dobra no sentido de caimento do eixo de dobra. A geologia estrutural é caracterizada por 3 fases deformacionais relacionadas a 2 eventos tectônicos. O primeiro evento possui duas fases deformacionais progressivas dúcteis (D1 e D2), com tectônica transpressiva e direção de transporte NE-SW, com geração de padrões de interferência de dobras coaxiais com geometria cilíndrica e caimento de eixo para ESE, sendo o principal agente formador da estrutura principal. O segundo evento, possui uma fase deformacional rúptil-dúctil a rúptil (D3) com tectônica inversa e vergência para W, possivelmente relacionado à tectônica Brasiliana na borda do cráton São Francisco. A mineralização aurífera está associada a

introdução de fluidos hidrotermais ricos em sílica e enxofre durante as fases D1 e D2 ao longo das foliações plano-axiais. A fase D1 está associada a mineralização pirrotítica, com ouro grosso (entre 50 e 500 μm). A fase D2 está associada a mineralização pirítica com ouro fino (entre 10 e 100 μm). Não há mineralização aurífera na fase D3, embora haja sulfetos tardi-tectônicos. As observações de campo demonstram a presença de padrões de redobramento coaxiais associados a mineralização, eixos de dobramento constantes com caimento para ESE, ausência de dobras em bainha e estruturas sedimentares preservadas. Desta forma, não há evidências de campo que demonstrem a existência de dobramento em bainha para o depósito, modelo este utilizado há muitas décadas. A morfologia do depósito associada a interferências de dobras sugere potenciais prospectivos a SW e a N do depósito Cuiabá, com sugestão de forte conexão estrutural entre outros depósitos auríferos, como os alvos Lamego e Descoberto.

Palavras-chave: Depósito de ouro orogênico. Plano de simetria. Análise estrutural. Metalogenia estrutural. Padrão de interferência de dobras. Greenstone belt Rio das Velhas.

Abstract

The structural architecture of an orogenic deposit is essential for its metallogenetic understanding, as both subjects are interconnected in this type of environment. Cuiabá gold deposit, located in Archean rocks from Rio das Velhas Greenstone belt, is the subject of numerous studies focused mainly on metallogenetic issues. These mineralizations are hosted essentially at sulfides inside banded iron formations and surrounded in schists of mafic composition. From the point of view of structural characterization, two divergent models have been studied: the sheath-fold model and the refolding model, bringing different exploratory perspectives to the region. As a way of filling this gap, the main objective of this work is to characterize the geology and define a new deposit model so that there is a better understanding of its framework. For this, the methodologies applied for this work were: underground geological mapping in accessible ore galleries and definition of geological-structural domains whose main criteria are related to down-plunge view of fold asymmetry and stratigraphic indicators in the fold symmetry plane. Structural geology is characterized by 3 deformation phases related to 2 tectonic events. The first event has two ductile-progressive deformation phases (D1 and D2), with NE-SW strike-slip direction of transport associated coaxial fold interference patterns with cylindrical geometry plunging to ESE, which represents the main structure and gold mineralization at the mine. The second event is a brittle-ductile deformational phase (D3) with W-verging reverse fault systems, probably associated to Brasiliano Pan-African Orogeny. Gold mineralization is associated with silica and sulfide-rich hydrothermal fluid introduction through D1 and D2 axial-plane foliation. Phase D1 is pyrrhotite-associated mineralization, with coarse gold presence (from 50 to 500 μm). D2 phase has pyrite-associated mineralization with fine gold (from 10 to 100 μm). There is no gold in phase D3, although it has late tectonic sulfide formation. Field observations demonstrate the existence of

coaxial refolding patterns associated with mineralization, constant fold axes plunging to ESE, absence of sheath folds and preserved sedimentary structures. Therefore, there is no field evidence that corroborate the existence of sheath folds for the deposit. Fold interference patterns associated to deposit morphology suggests SW and N prospective targets, with strong possibility of structural connection between other gold deposits, such as Lamego and Descoberto targets.

Keywords: Orogenic gold deposit. Symmetry plane. Structural analysis. Structural metallogenesis. Fold interference pattern. Rio das Velhas greenstone belt.

LISTA DE ILUSTRAÇÕES

LISTA DE TABELAS

SUMÁRIO

1. INTRODUÇÃO

A região do Quadrilátero Ferrífero (QF) é uma das maiores províncias minerais do mundo, tendo mais de 300 anos ininterruptos de exploração mineral, em especial ouro e recentemente ferro. No século XXVIII era a região do Brasil que mais produzia ouro (Ruchkys e Machado, 2013).

Os principais depósitos auríferos em atividade são o depósito Cuiabá (5.49 Moz de recurso com 5.87 g/t), Lamego (1.07 Moz de recurso com 2.96 g/t), Córrego do Sítio (3.33 Moz de recurso com 3.68 g/t, incluindo a antiga mina de São Bento com 0.69 Moz de recurso, AngloGold Ashanti, 2021). Além destes depósitos ativos, a maior e mais profunda jazida aurífera do Brasil está localizada nessa província, denominada depósito Morro Velho, paralisada no ano de 2004 com 2400m de profundidade e com produção histórica de mais de 12 Moz (Vial, 2007).

O depósito Cuiabá pertence a empresa sulafricana AngloGold Ashanti, e já produziu mais de 6 Moz desde o início da década de 1980, com produção anual de 250 kOz (2021). Atualmente (AngloGold Ashanti, 2021) possui 5.49 Moz em recursos, sendo considerado um depósito de classe mundial. Cuiabá é a maior e mais profunda mina de ouro subterrânea do Brasil em atividade, possuindo 22 níveis e com 1460 m de profundidade abaixo da superfície (AngloGold Ashanti, 2021).

Depósitos orogênicos possuem uma clara relação entre a mineralização e estruturas geológicas previamente formadas. Todavia, essa relação não tem recebido a devida importância, fazendo com que modelos prévios de exploração mineral sejam adotados sem uma visão crítica do ponto de vista estrutural (Cowan, 2017, 2018).

Por ser dos mais representativos depósitos de ouro do Grupo Nova Lima, pertencente ao *greenstone belt* Rio das Velhas, o depósito de ouro orogênico Cuiabá tem sido continuamente

estudado nas últimas décadas (*e.g.* Vial, 1980; Ladeira, 1991; Xavier *et al.* 2000; Vieira, 1988, 1992; Lobato *et al.* 1998, 2001a, b, 2007; Martins, 2000; Costa, 2001; Martins *et al.* 2016; Araújo e Lobato, 2019; Kresse *et al.* 2020 e Sena, 2021). Muitos trabalhos foram publicados explicando o mecanismo de enriquecimento em ouro com foco especialmente na geoquímica das alterações hidrotermais (Vial, 1980, Vieira, 1988, Martins, 2000, Costa, 2001, Lobato, 2001 e Kresse *et al.* 2018). No entanto, poucos trabalhos realmente focados na caracterização do arcabouço estrutural desse depósito foram realizados. Vieira (1988) introduz a hipótese de redobramentos coaxiais, mas a hipótese de dobramento em bainha (Toledo, 1997, Ribeiro-Rodrigues, 1998) foi a adotada logo após esse mecanismo ter sido difundido por Skjernaa, (1989). O modelo de dobra em bainha é o modelo até então aceito para o depósito Cuiabá, entretanto sem consenso definitivo (Kresse, 2018).

Com isso muitas dúvidas ainda persistem quanto a evolução estrutural de sua geometria, fazendo com que haja diferentes perspectivas geológicas, principalmente prospectivas para além de seus domínios. No modelo de redobramento coaxial as rochas hospedeiras são contínuas ao longo da direção da camada com proposição de campanhas exploratórias laterais ao depósito. No modelo de dobra em bainha as rochas hospedeiras são contínuas em subsuperfície, com possibilidade da existência de corpos mineralizados não aflorantes aos arredores do depósito.

1.1. Objetivos e justificativa

O objetivo principal deste trabalho refere-se à proposição de um modelo estrutural-metalogenético do depósito que vise orientar a exploração mineral. A discussão nesse trabalho endereça a controvérsia entre os dois modelos existentes (“redobramentos coaxial” versus “dobra em bainha”).

A proposição de um modelo estrutural auxilia na descoberta de novos alvos de prospecção através do estudo de continuidade do horizonte mineralizado, extrapolando a área de exploração atual.

1.2. Localização e vias de acesso

O depósito Cuiabá está localizado a 30km de distância do centro de Belo Horizonte, capital do estado de Minas Gerais, Brasil (Figura 1). O depósito está localizado entre 2 cidades históricas a saber: Caeté e Sabará. Para acessar a mina deve-se percorrer a estrada que conecta essas duas cidades, a GT-262, popularmente conhecida como estrada Mestre Caetano.

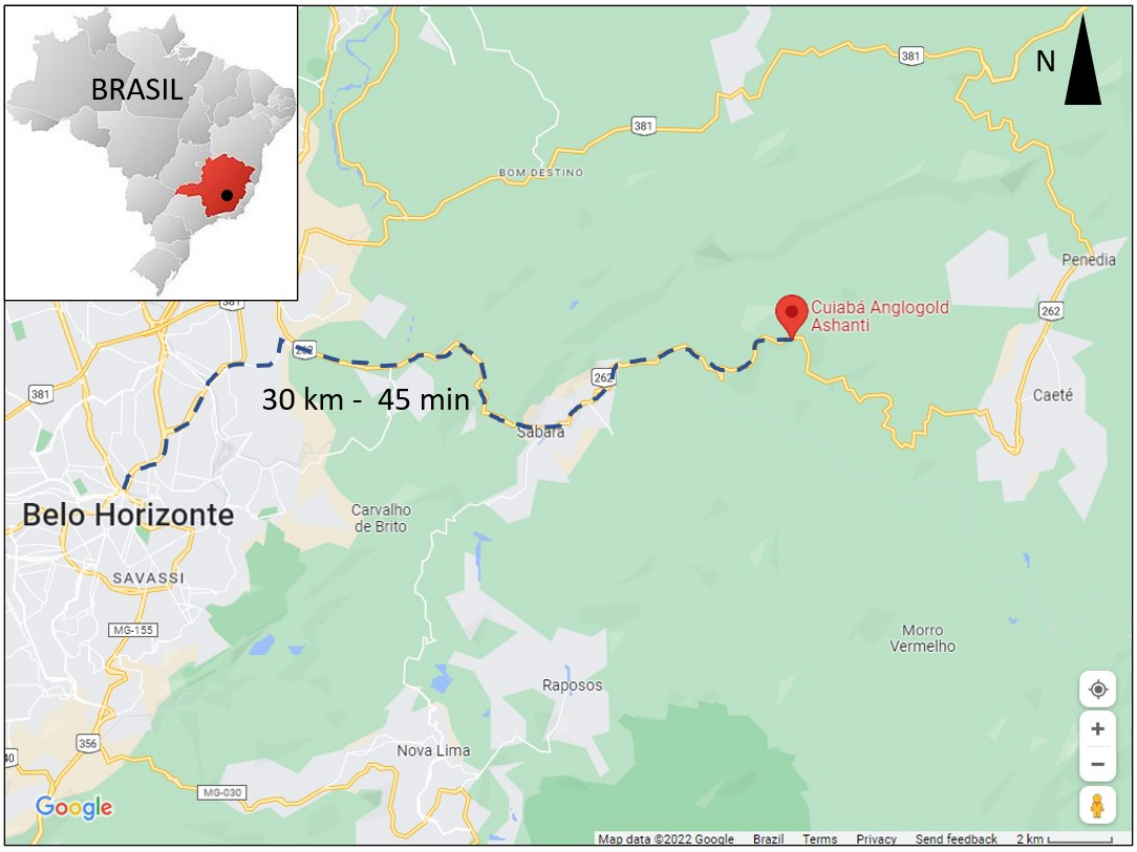

Figura 1. Localização e vias de acesso para o depósito Cuiabá (Fonte: Google Maps)

1.3. Estrutura da dissertação

Este estudo é apresentado sob a forma de capítulos e um artigo científico da seguinte forma:

- Capítulo 1: Introdução – apresenta os aspectos econômicos das principais jazidas auríferas do QF, bem como o contexto e objetivos do trabalho e localização da área de estudo.
- Capítulo 2: Metodologia – apresenta as técnicas utilizadas para se chegar aos resultados: em especial a técnica de mapeamento geológico em subsolo associado aos levantamentos estruturais.
- Capítulo 3: "*Structural model and features of the world-class Cuiabá orogenic gold deposit, Rio das Velhas greenstone belt, Quadrilátero Ferrífero region, Brazil*". Descreve as feições estruturais policíclicas em escala de depósito associados a uma deformação polifásica relacionada a redobramentos coaxiais e suas relações com as fases de mineralização. Esse artigo foi submetido ao periódico *Journal of South American Earth Sciences (*ISSN 0895-9811 – Qualis CAPES A2 – ANEXO 1) e aceito pelo mesmo periódico, com endereço no link https://doi.org/10.1016/j.jsames.2023.104201 (ANEXO 2).
- Capítulo 4: Considerações finais – exibe a síntese das conclusões finais desse trabalho e possíveis trabalhos futuros que podem ser realizados a partir dessa dissertação.

2. MÉTODOS DE TRABALHO

O trabalho tem como base a cartografia geológica subterrânea, caracterização do arcabouço estrutural e divisão dos domínios geológico-estruturais.

2.1. Cartografia geológica subterrânea

O mapeamento em subsolo no depósito Cuiabá foi realizado na escala 1:200 utilizando-se como base cartográfica o levantamento topográfico de piso das galerias e amostras de canal realizadas nas zonas mineralizadas. As amostras de canal são espaçadas a cada 3 metros ao longo da direção da camada (*strike*) da rocha hospedeira, o que gera uma grande densidade de informações geológicas, que possibilita uma representação bastante confiável da geologia local. Os canais e contatos litológicos são projetados segundo a atitude do eixo de dobra em uma superfície imaginária horizontal localizada a 3 metros do piso (Figura 2).

2.2. Caracterização do arcabouço estrutural

Durante o mapeamento geológico e marcação dos contatos são observados elementos geopetais e estruturais com o objetivo de se entender a topologia local.

Os elementos geopetais são utilizados para se determinar critérios de topo e base e localização de flanco normal ou invertido. Eles são caracterizados na mina através do empilhamento estratigráfico definido previamente por Vial (1980), Vieira (1988), Vieira (1992) e Toledo (1997), que consideram as rochas internas ao núcleo do depósito (rochas metamáficas de composição andesítica) como sendo mais antigas que as rochas externas (rochas metassedimentares pasmo-pelíticas). Como forma de se confirmar essa hipótese, critérios estratigráficos em fluxos turbidíticos definidos por Bouma (1962) também são utilizados nas rochas metassedimentares, localizadas nas porções externas ao núcleo do depósito.

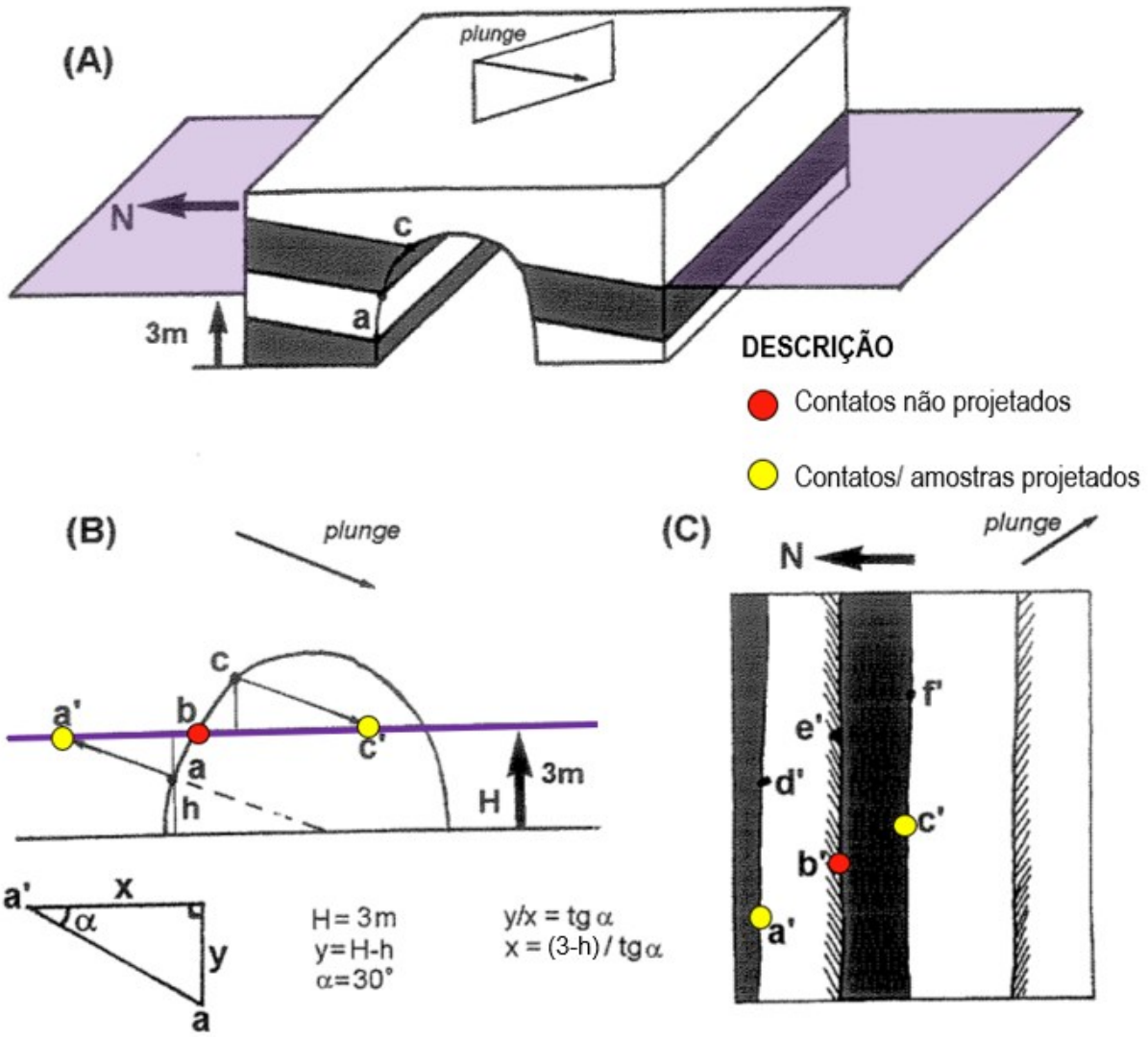

Figura 2. Representação esquemática do método de mapeamento em subsolo. A. Os pontos a, b e c estão localizados nos contatos litológicos e devem ser projetados na superfície imaginária. B. Os pontos projetados passam a ocupar as posições a', b' e c'. O ponto b está projetado exatamente no plano imaginário a 3 metros do piso e, portanto, não precisa ser projetado. C. Os contatos litológicos são traçados no mapa unindo-se os pontos projetados. Modificado de Toledo (1997).

Os elementos estruturais planares e lineares foram medidos utilizando-se o método de *dip direction* (McClay, 1987). Os dados de produção são apresentados no item 2.5.

A metodologia de caracterização do arcabouço estrutural é determinada pela:

- Análise da estrutura através da observação no plano de verdadeira grandeza ou ao seu correto plano de simetria (Cowan,2016a; Ramsay e Huber, 1987), representado pelo plano "ac" e ortogonal ao eixo "b" de dobramento (Figura 3);
- Levantamento das assimetrias de dobra através da Regra de Pumpelly. A regra de Pumpelly (nome atribuído ao geólogo americano do século XIX, Raphael Pumpelly, descobridor deste método de trabalho) demonstra que "*a orientação de estruturas de menor escala é representativa da orientação de estruturas regionais*" de mesma geração tectônica (Pluijm e Marshak, 2004, pag. 248);
- A análise de assimetria de dobras parasíticas é feita sempre observadas no sentido de caimento do eixo de dobra ("*down-plunge*") ou da lineação de interseção (Mackin, 1950, Ramsay e Huber, 1987, Cowan, 2014 e Piassa, 2018). Desta forma, os padrões de dobra em "S" e "Z" são indicativos de zonas de flancos, enquanto as dobras em "M" ou "W" são indicativas de zonas de charneira.

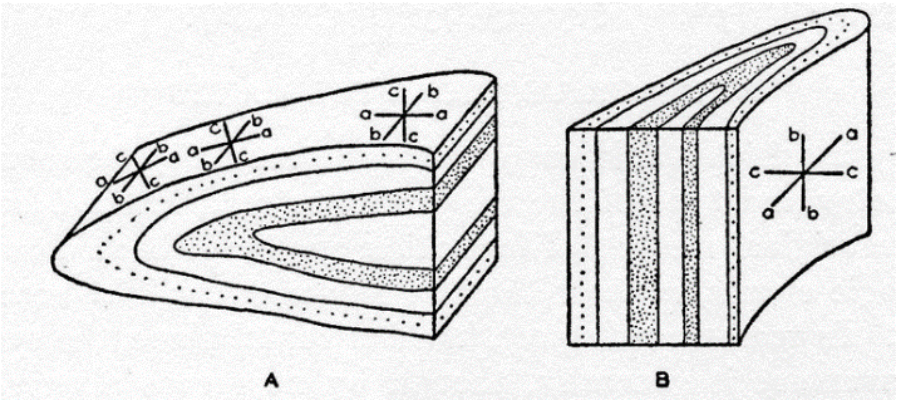

Figura 3. A discussão do plano de simetria em sistemas dobrados em um dos primeiros textos sobre geologia estrutural (Knopf and Ingerson, 1938, p. 57 *apud* Cowan, 2016a). O plano de simetria da dobra é representado pelo plano "ac" e ortogonal ao eixo "b" de dobramento. Para a figura A, o plano é vertical. Para a figura B o plano de simetria é horizontal. Em ambos os casos o plano de simetria representa o plano de deformação.

A lista de medidas realizadas neste trabalho está organizada em um banco de dados que contêm as informações estruturais de forma a auxiliar as análises subsequentes.

Para a organização do acervo estrutural foi utilizado o programa Microsoft Excel®. Para a análise estatística dos dados estruturais foi utilizado o programa Leapfrog Geo®, através de projeção estereográfica de igual área no hemisfério inferior e média associada a tabela de distribuição de Fisher.

O sistema de coordenadas geográficas utilizadas é um sistema de coordenadas local (coordenada SW) histórico utilizado pela empresa.

2.3. Divisão de domínios estruturais

O banco de dados proveniente do mapeamento geológico é reunido em uma tabela e os corpos mapeados são caracterizados em domínios estruturais seguindo os critérios estratigráficos (flanco normal ou invertido) e assimetria de dobra (S, Z, M ou W). Da mesma forma que os contatos geológicos são projetados e observados no plano de verdadeira grandeza, os corpos mineralizados também o são, de modo que corpos mapeados em diferentes níveis sejam projetados e analisados na mesma visada, permitindo um entendimento geológico mais amplo entre os diferentes domínios caracterizados. A dificuldade em se mapear domínios diferentes em um mesmo nível se deve ao fato da dinamicidade das operações da mina.

2.4. Metodologia de distinção de estruturas progressivas mineralizadas

A distinção em campo entre as estruturas mineralizadas das fases 1 e 2 é bastante dificultada devido à similaridade física, subparalelismo nas zonas de flanco e caráter coaxial entre elas. Sendo assim, seguindo a metodologia científica proposta por Feynman (1964) opta-se em inicialmente classificar estas estruturas subparalelas à fase “21”. Com posterior análise dos dados em gabinete e, em caso de inconsistência observada em campo, a classificação é ajustada para que o modelo

seja aproximado da realidade. Em alguns casos é possível distingui-las através da utilização de critérios básicos de relação de corte e de dobramentos tais como:

- Observação de padrão de interferência de dobras, apresentando redobramentos coaxiais do tipo 3 observados, onde seja fácil a distinção entre as fases de deformação D1 e D2;
- Indicadores de padrões de interferência de dobras não observados como as inconsistências entre assimetrias de dobras parasíticas e seus respectivos sentidos de fechamento nas charneiras das dobras principais.

O único domínio onde é possível fazer essa distinção de forma clara é o setor central do depósito, alvo VQZ conforme dados apresentados e discutidos *a posteriori*. Após a análise estrutural de todos os domínios relacionados a partir da fase "21", estes são interpretados com sua respectiva fase.

2.5. Caracterização metalogenética-estrutural

Para a caracterização metalogenética-estrutural, adotou-se principalmente pela descrição macroscópica dos tipos de minério. Além desta metodologia, foi também utilizado os dados de geoquímica de amostras de canal coletadas no depósito Cuiabá e localmente foram feitas análise microestruturais das principais tipologias de minério, com foco na construção de uma cronologia entre os tipos de mineralização e as estruturas presentes.

A descrição macroscópica dos tipos de minério durante o processo de mapeamento geológico foi realizada fazendo associações das estruturas geológicas com suas paragêneses minerais.

Como historicamente no depósito Cuiabá há um conhecimento sobre a correlação entre os elementos enxofre (S) e ouro (Au) optou-se neste trabalho em demonstrar a geoquímica de

amostras de canal do minério. Para que essa correlação pudesse ser identificada em diferentes litologias, foi utilizado o método *Fire Assay* através de um espectrômetro de massa (LA-ICP-MS) para determinação do elemento ouro (Au) e, para a determinação do elemento enxofre (S), o analisador LECO foi utilizado.

A análise microestrutural foi realizada através da descrição de algumas seções polidas-delgadas não-orientadas em microscópio de luz refletida e transmitida para as tipologias de minério em diferentes fases mineralizadas, visando a caracterização microestrutural dos sulfetos (tamanho, geometria, contato entre grãos e porosidade) e do ouro (tamanho e grau de liberação das partículas).

2.6. Dados de produção

Este trabalho é fruto de um total de 52 galerias mapeadas em diferentes setores da mina ao longo de 11 anos de trabalho (entre 2009 e 2020). Foram realizadas 2795 medidas estruturais, desde o nível 07 (590m acima do nível do mar) ao nível 19 (200m abaixo do nível do mar) totalizando uma variação de 800m em desnível (**Figura 4**).

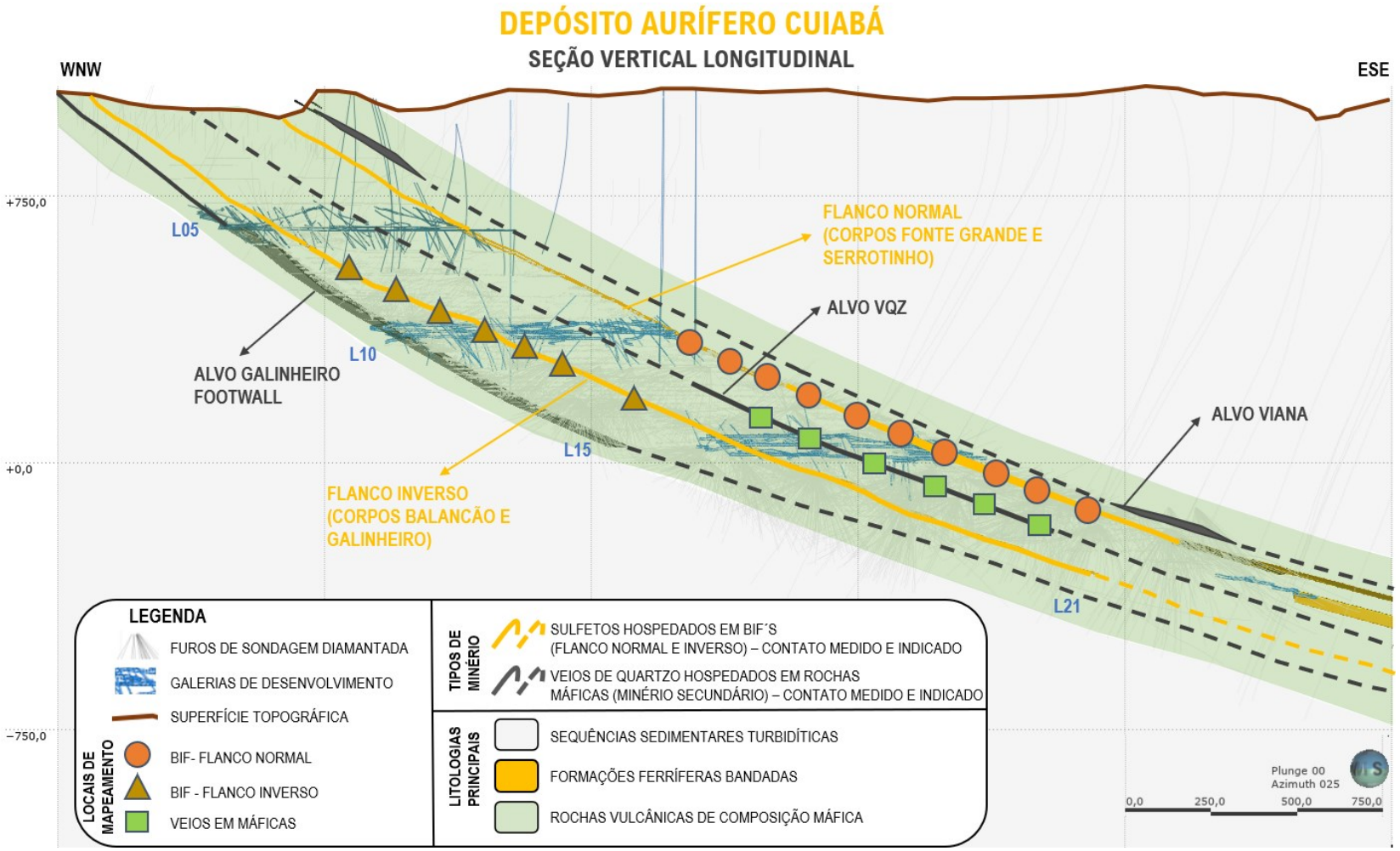

Figura 4. Seção geológica longitudinal simplificada do depósito aurífero Cuiabá contendo os locais de mapeamento e coleta de dados estruturais.

3. STRUCTURAL MODEL AND FEATURES OF THE WORLD-CLASS CUIABÁ OROGENIC GOLD DEPOSIT, RIO DAS VELHAS GREENSTONE BELT, QUADRILÁTERO FERRÍFERO REGION, BRAZIL

Raphael do Carmo Fernandes[1,2], Jorge Roncato[2], Rodrigo Sérgio de Paula[2]

[1]Anglogold Ashanti, Cuiabá Mine, Estrada Mestre Caetano, s/n Cuiabá, Sabará - MG, 34505-320.
[2]Instituto de Geociências-Centro de Pesquisa Manoel Teixeira da Costa, Departamento de Geologia, Universidade Federal de Minas Gerais, Av. Antônio Carlos 6627, Campus Pampulha, 30130-009, Belo Horizonte, Minas Gerais, Brazil.
Corresponding author: Raphael do Carmo Fernandes |Tel: +55-31-997068805|
E-mail address: rcfernandes@anglogoldashanti.com.br; raphaeldocarmo@yahoo.com.br

3.1. ABSTRACT

The structural architecture of an orogenic deposit is essential for its metallogenetic understanding, as both subjects are interconnected in this type of environment. Cuiabá gold deposit, located in Archean rocks from Rio das Velhas Greenstone Belt, is the subject of numerous studies focused mainly on metallogenetic issues. From the point of view of structural characterization, two divergent models have been studied: the sheath-fold model and the refolding model. Such hypothesis is different in terms of defining an exploratory research plan and, therefore, the detailed structural characterization is still not well understood. As a way of filling this gap, the main objective of this work is to propose a structural characterization of the entire deposit to demonstrate evidence for a new model of tectonic evolution. For this, the methodologies applied for this work were: underground geological mapping in all available ore galleries and definition of geological-structural domains whose main criteria are related to down-plunge view of fold asymmetry and stratigraphic indicators. Structural geology is characterized by 3 deformation phases related to 2 tectonic events. The first event has two ductile-progressive deformation phases (D1 and D2), with NE-SW strike-slip direction of transport associated coaxial fold interference patterns with cylindrical geometry plunging to ESE, which represents the main structure at the mine. The second event is a brittle-ductile deformational phase (D3) with W-verging reverse fault systems, probably associated to Brasiliano Pan-African Orogeny. Gold mineralization is associated with silica and sulfide-rich hydrothermal fluid introduction through D1 and D2 axial-plane foliation. Phase D1 is pyrrhotite-associated mineralization, with coarse gold presence. D2 phase has pyrite-associated mineralization with fine gold. There is no gold in phase D3, although it has late-tectonic sulphides formation. Therefore, there is no field evidence that corroborate the existence of sheath folds for the deposit. Fold interference patterns associated to deposit morphology suggests SW and N prospective targets, with strong possibility of structural connection between other gold deposits, such as Lamego and Descoberto targets.

Keywords: Orogenic gold deposit, fold interference pattern, structural model, structural metallogenesis.

3.2. HIGHLIGHTS

- Geological mapping reveals a pre-Cambrian fold interference pattern with no field evidence for sheath folds.
- Gold inside BIF is related to this framework at two stages: (1) pyrrhotite with coarse gold and (2) pyrite with fine gold.
- A NE-SW ductile strike-slip transport at a convergent tectonic setting with inclined folds plunging to ESE is suggested.
- Gold was transported throughout axial-plane foliation and were placed where coaxial refolding was locally presented.
- A post-mineralization tectonic event was responsible for orthogonal displacements at the entire deposit.

3.3. INTRODUCTION

The Quadrilátero Ferrífero region is one of the great mineral provinces of the planet, being more than 300 years of continuous mineral exploration, especially gold and iron (Dorr, 1957, Dorr, 1969, Vieira, 2000, Lobato et al., 2001a, Vial, 2007, Baltazar and Lobato, 2020, Castro et al., 2020). In the eighteenth century it was the region of Brazil that produced the most gold (Ruchkys & Machado, 2013).

The Cuiabá gold deposit is owned by the South African company AngloGoldAshanti. This deposit has already produced more than 6MOz in its history, producing annually (AngloGold Ashanti, 2021) 250 kOz, being considered the company's main gold mine in South America (AngloGold Ashanti, 2021). Currently (AngloGold Ashanti, 2021) it has 5.49MOz resources, which is

considered a world-class deposit. The deposit is the major gold producer and the largest active underground mine in Brazil, having 22 levels with 1,450 m in depth below surface.

As one of the most representative orogenic gold deposits in the Nova Lima Group, the orogenic Cuiabá gold deposit has been studied continuously in the last decades (*e.g*. Vial, 1980; Ladeira, 1991; Xavier et al. 2000; Vieira, 1988, 1992; Ribeiro-Rodrigues, 1998, 2007; Lobato et al. 1998, 2001a, b, 2007; Martins et al. 2016; Vitorino, 2017; Araújo and Lobato, 2019; Kresse et al. 2020).

Gold production in the QF Archean Rio das Velhas greenstone belt is significant worldwide (Ribeiro Rodrigues, 1998), with the Algoma-type, magnetite- and-or siderite-rich BIFs, being one of the most important host to gold mineralization (e.g., Lobato et al., 2001; Araújo and Lobato, 2019). The main gold deposits described are the world-class Cuiaba deposit (5.49 MOz resources with 5.87 g/t), Lamego (1.07MOz resources with 2.96 g/t), Córrego do Sítio (3.33 Moz resources with 3.68 g/t including 0.69 Moz resources from São Bento target) and current closed world-class deposits such as Raposos and Morro Velho (Figure 5).

This paper aims at providing a review of deposit-scale structural features that control the continuity and geometry of ore domains assessing the structural evolution and placing it in a tectono-metallogenic context. A better understanding of structural ore controls will provide a basis for focusing exploration programs at Cuiabá deposit. Awaits too helps to discover new prospecting targets through the study of continuity of the mineralized horizon, extrapolating the current exploration area.

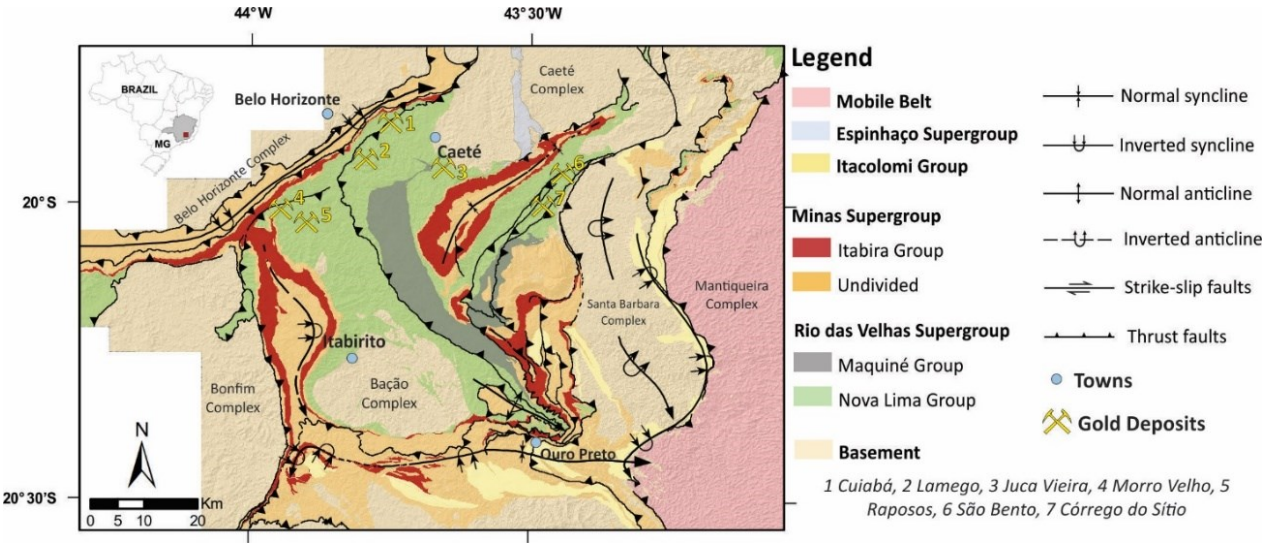

Figure 5. Geological map of the Quadrilátero Ferrífero region with main gold deposits of the Rio das Velhas greenstone belt (modified from Araujo, 2018 and Endo et al., 2019).

3.4. REGIONAL GEOLOGICAL SETTING

The Quadrilátero Ferrífero region (QF; Figure 5 and Figure 6) is situated in the southern portion of the São Francisco craton (Almeida, 1977) and is composed of the Archean Rio das Velhas greenstone belt (Schorscher et al., 1982), the paleoproterozoic Minas Supergroup and the Itacolomi Group. These supracrustal units are surrounded by granite-gneiss domes (Dorr 1969, Lana *et al.,* 2013), which consist of poly-deformed unit (Baltazar and Lobato, 2020). The regional basement metamorphic complexes outcrop out in several distinct domes and with metamorphic grades ranging from greenschist to granulite facies (Herz, 1970).

The Rio das Velhas greenstone belt corresponds to a metavolcanosedimentary sequence composed from the base to the top of the Nova Lima and Maquiné groups, respectively (Dorr *et al.,* 1957; Almeida, 1977; Schorscher, 1978). The Nova Lima Group, shown on figure 2, comprises a basal unit formed by tholeiitic-komatiitic volcanic rocks, associated with chemical sedimentary rocks; a volcaniclastic intermediate unit, associated with felsic volcanism; and an upper unit with clastic

sedimentary rocks (Ladeira, 1980; Ladeira, 1991; Zucchetti and Baltazar 2000; Baltazar and Zucchetti 2007). Schorscher (1978) described komatiites at the base of the sequence, naming them the Quebra Osso Group. The Maquiné Group, shown in figure 2, is composed (Gair, 1962) of sequences of graywacke and conglomerates deposited at ca. 2.73 Ga (Moreira et al., 2016). The Rio das Velhas rocks was classified by Baltazar & Zucchetti (2007) according to its volcano-sedimentary characteristics in lithofacies associations (Figure 6) and summarized by Roncato et al. (2015; 2020):

(1) Mafic-ultramafic: lavas with minor intrusions of gabbro, anorthosite and peridotite, as well as intercalations of Banded Iron Formation (BIF), ferruginous chert, carbonaceous pelite, turbidites, and rare felsic volcanoclastic rocks. It corresponds to the Quebra Ossos Group and Ouro Fino unit of the Nova Lima Group. (2) Volcano-chemical-sedimentary: tholeiites intercalated with BIF and ferruginous chert and less fine-grained clastic sedimentary rocks, such as carbonaceous turbidites and pelites, intercalated with chemical sedimentary rocks. (3) Clastic-chemical sedimentary: typified by alternating fine-grained, clastic and chemical rocks. Pelites (micaceous and chloritic schists) are intercalated with lesser BIF, subordinate chert and carbonaceous phyllites. (4) Volcaniclastic: made up of volcaniclastic felsic and mafic rocks. (5) Resedimented: widely distributed in the Quadrilátero Ferrífero, it includes three different sequences of graywacke-argillite, two metamorphosed in the greenschist facies in the N and E sectors (they are composed mainly of graywackes, quartz graywackes, sandstones and siltstones, with cyclic layers and abrupt basal contacts between cycles) and one in the amphibolite facies in the south. (6) Coastal: restricted to a small area, with sandstones exhibiting preserved sedimentary structures. (7) Non-marine: conglomerate-sandstone; coarse-grained sandstone, fine- to medium-grained sandstone; it includes the Casa Forte Formation of the Maquiné Group (Dorr et al., 1957).

The U-Pb ages of detrital zircon from volcaniclastic rocks of the Nova Lima Group indicate felsic volcanism between 2.79-2.75 Ga (Machado and Carneiro, 1992; Noce 1998; Noce et al., 2007), a minimum depositional age of 3.02 Ga (Machado et al., 1992) and the maximum depositional age of the metapsamite from Córrego do Sítio unit 2, 81 ± 31 Ga (Sepulveda et al. 2021).

Published U-Pb ages data from the basement of the QF allowed for the identification of four main magmatic events (Lana et al., 2013; Romano et al., 2013; Farina et al., 2015). Periods of magmatic activity, which registers the tectonomagmatic Archean history of the QF, was described as the Santa Bárbara, Rio dasVelhas I, Rio das Velhas II and Mamona, spanning from 3220 to 2770 Ma (Lana et al., 2013).

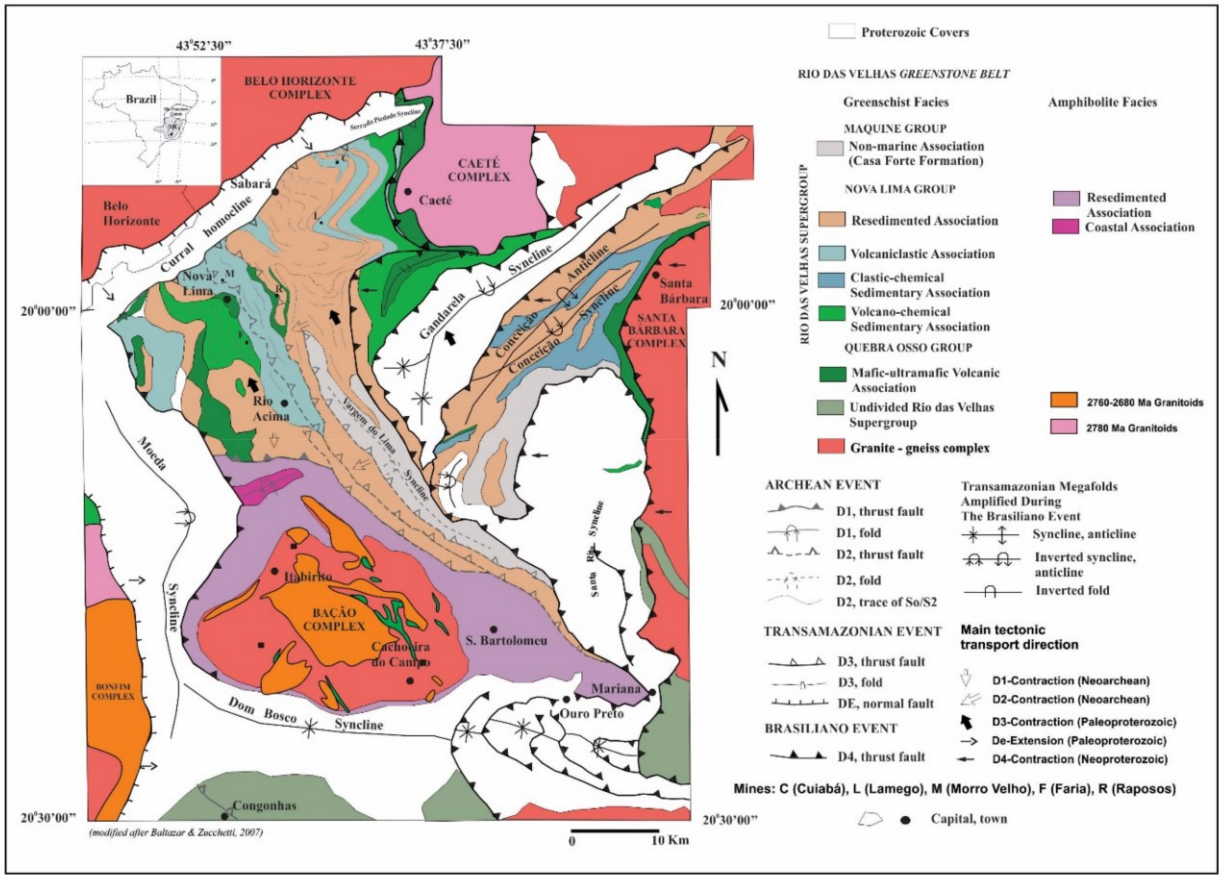

Figure 6. Geological map of the Quadrilátero Ferrífero region showing the Cuiabá Deposit in the Rio das Velhas Supergroup in detail (modified from Baltazar and Lobato, 2020).

3.4.1. *Geotectonic evolution of the Quadrilátero Ferrífero Region*

The Quadrilátero Ferrífero region constitutes the aggregation of Proterozoic and Archean terranes, consolidated at the end of the Minas orogeny, in the Trasamazonian orogenic cycle (Alkmim and Marshak, 1998; Baltazar and Lobato, 2020). The structural evolution of the QF region took place in three main periods during the Rio das Velhas orogeny: between 2.8 and 2.67 Ga, which relates to the evolution of the Rio das Velhas greenstone belt; 2.10 to 1.90 Ga, the Transamazonian event; and the Brasiliano orogeny (0.7 – 0.45 Ga), with fold and thrust belts verging to the west" (Baltazar and Zucchetti, 2007).

According to Rosière et al. (1990, apud Chamale Jr. et al.,1994), Chemale Jr. et al., (1994), Alkmim and Marshak (1998), Farina et al. (2015) and Baltazar and Lobato (2020), synformal mega folds define the geometry of the Quadrilátero Ferrífero region, truncated by N–S-directed thrust faults in its eastern portion (Figure 6). The western and southern borders are embodied by the Moeda and Dom Bosco synclines, respectively to the north, the Serra do Curral homocline represents the overturned limb of a large synclinal fold (Simmons, 1968; Dorr, 1969; Alkmim and Marshak, 1998; Sanglard, 2014; Baltazar and Lobato, 2020). To the east, the Gandarela, Ouro Fino, Conta História and Santa Rita synclines are disposed in an ample, N–S-directed arch, affected by Neoproterozoic shear zones of the Araçuaí orogeny (e.g. Ladeira and Viveiros, 1984; Marshak and Alkmim, 1989; Chemale et al., 1994; Alkmim and Marshak, 1998; Baltazar and Zucchetti, 2007; Baltazar and Lobato, 2020). All these synformal troughs are filled by metasedimentary rocks that originate from the Minas Supergroup and the Sabará and Itacolomi groups. One exception is the Vargem do Lima syncline where it is constituted by Rio das Velhas Supergroup lithotypes (Baltazar and Lobato, 2020).

The data and discussion presented below on the structural evolution of the QF are based on the work of Rosière et al. (1990, apud Chamale Jr. et al., 1994); Chemale Jr et al., 1994, Alkmim and Marshak (1998), Farina et al. (2015) and Baltazar and Lobato (2020). Five phases of structural, planar, and linear elements are recorded regionally within the QF. Collectively, these events involve four deformational, compressional phases (D1 to D4) and one extensional phase (DE), as summarized in (Table 1).

Baltazar and Lobato (2020) discourse about past decades, when works focusing on the structural progress of the Rio das Velhas Supergroup, near to gold districts. These authors suggest four deformation phases:

i. **D_{n1}** - mylonitic foliation parallel to the bedding, with isoclinal folds as well as mineral and intersection lineations, and with plunging to the east; folds are coaxial, with axes to E.
ii. **D_{n2} -** more pronounced foliation and lineation patterns, both related to a close-to-isoclinal folding of the bedding/foliation of D_{n1}; folds are coaxial, with axes to E; Thrust shear zones developed at the end of D_{n2}.
iii. **D_{n3} -** E–W/55N crenulation cleavage and an axial plane of open, normal-to-inclined folds, with axes plunging at a low angle to the E.
iv. **D_{n4}** - N–S/40–65E crenulation cleavage, an axial plane of gentle folds; S10W/30 to S10E/35 crenulation lineation.

Baltazar and Lobato (2020) still talk about that three phases of deformation are recognized in the Nova Lima Group, in the region of the gold district: (i) foliation parallel to the E–W bedding, of Archean age; (ii) penetrative NE–SW, Transamazonian foliation; and (iii) N-S crenulation cleavage related to the Brasiliano orogeny.

Almeida et al. (2004), Castro et al. (2020) and Endo et al. (2020) discuss how folds of various generations and styles, associated with different phases and tectonic events, characterize the structural framework of the Quadrilátero Ferrífero region: Nappe Curral with transport to N-NE, Ouro Preto Nappes System with transport to S-SW, and folds of the third generation resulting from amplification and/or refolding. According to these authors, the QF nappes system, although presenting opposite vergencies, has similar symmetry planes, whose poles, given by the disposition of the intersection lineation between the main schistosity and the bedding, are oriented around 095/45.

The mineral, mineral stretching, and pebble elongation lineation are oriented parallel to the intersection lineation and the fold axes at all scales in both the Nappe Curral and the Ouro Preto Nappes System. The Ouro Preto Nappes System is the product of coaxial folding during the Transamazonian event, generating a penetrative and oblique S2 axial plane schistosity to the bedding (Endo et al., 2005, Castro et al., 2020, Endo et al., 2020).

Table 1. Summary of QF deformation history, based on Baltazar and Lobato (2020).

Summary of regional QF deformation history. Based on Baltazar and Lobato (2020).				
Deformation Phase	**Regime**	**Structures**	**Units**	**OBS**
Pre-Rio das Velhas greenstone belt deformation	Ductile	Subvertical N–S foliation,	TTG basement	
D1	Ductile	**- S-verging, E–W oriented;** - The mylonitic axial-planar foliation associated with folding, arising in highly deformed zones. Its general orientation is E–W, with a high dip angle and a parallel mineral lineation that plunges to the north. N to S tectonic transport.	Nova Lima Group (Baltazar and Zucchetti, 2007).	- Rio das Velhas orogeny (Carneiro, 1992) of the Jequié orogenic cycle (Neoarchean); - Associated with the evolution of the Rio das Velhas greenstone belt.
D2	Ductile	**- SW-vergent, tight-to-isoclinal folds;** - mylonitic foliation, axial planar, with an average attitude of 060/35; - Along the foliation planes, the mineral lineation varies between 070/25 and 060/20; - NW–SE structures truncate and dislocate the D1 structures.	Maquiné and Nova Lima groups (Baltazar and Zucchetti, 2007).	
D3	Ductile-brittle	**- NE–SW-oriented, NW-vergent fold-thrust belt;** - SE to NW tectonic transport; - In the Nova Lima Group, the D3 foliation is recognized in the Nova Lima and Caeté gold districts.	Sabará Group, Minas Supergroup and Rio das Velhas Supergroup.	- Large-scale folded structures—such as the Serra do Curral homocline, the Serra da Piedade and - Gandarela synclines, and the Conceição anticline (Marshak and Alkmim, 1989; Alkmim and Marshak, 1998); - The D3 structures are attributed to the compressional phase of the Paleoproterozoic Transamazonian orogenic cycle (2,26 Ga - 1,86 Ga). - They correspond to the Minas accretionary orogeny in the extreme SE of the São Francisco Craton
DE	Ductile	**- Mylonitic, high-angle foliation, and a down-dip mineral lineation;** - Bação ascension also imprinted normal shear zones on its borders; - Normal faults WNW–ESE-oriented;	Bação Complex and Nova Lima Group	- DE structures are of extensional character and associated with the collapse phase of the Trasamazonian orogeny. - Related to the uplift of the basement complexes (Marshak and Alkmim, 1989; Alkmim and Marshak, 1998); - The Itacolomi Group is associated with the formation of intermontane basins during the DE phase (Alkmim and Marshak, 1998); - DE developed a dome-and-keel structure in the QF region (Marshak and Alkmim, 1989; Alkmim and Marshak, 1998); around 2095 Ma (whole-rock Sm-Nd; (Marshak et al., 1997). - Finally, the uplift of the basement blocks as metamorphic core complexes is proposed (Chemale et al., 1994; Baltazar and Zucchetti, 2007).
D4	Ductile	**- W-vergent, N–S-oriented fold-thrust belt;** - The D4 structures affect all Proterozoic; - Shear zones have a mylonitic foliation plunging to E; - Lineation, and kinematic markers indicating thrusting to W; - The W-vergent, isoclinal-to-tight folds, with axial-planar foliation and lineation following the dip direction associate with zones of high deformation; - Sub-horizontal mineral and stretching lineations; - N–S-directed fold-and-thrust belt, E–W and N–S folds and cleavages;	All Proterozoic as well as subjacent units	- D4 structures are related to the E–W compressional Neoproterozoic Brasiliano orogeny.

3.5. GEOLOGICAL CHARACTERISTICS OF THE CUIABA DEPOSIT

The Cuiabá mine is composed of a sequence of mafic and metasedimentary metavolcanic rocks in intermediate portion of the greenstone belt Rio das Velhas. The deposit structure is a cylindrical geometry, with a fold axis plunging to ESE represented by an overturned limb at north and an upright limb at south. Five main ore bodies are associated with sulphidation in the Banded Iron Formation (BIF), as seen in the map in Figure 7: in the southern flank, represented by the Serrotinho (SER) and Fonte Grande (FG) orebodies; on the northern flank, represented by Canta Galo (CGA), Balancão (BAL) and Galinheiro (GAL) orebodies. Other mineralized bodies are associated with the presence of quartz-carbonate veins and hydrothermal alteration in the metabasalts: Viana (VIA) and Galinheiro Footwall (GFW) are located in the upper metamafic unit; Veio de Quartzo (VQZ) are located in the lower metamafic unit, just inside the core and between the southern and northern limbs. The average gold grade for the deposit is 5.87 g/t, with maximum grades of up to 25g/t. It is worth mentioning that the main mineralization characteristics of these ore bodies are the same as those of the original characterization by Vial (1980), Vieira (1988), and Vieira (1992).

The Cuiabá deposit area (Figure 5 and Figure 6) is in the intermediate part of the Nova Lima Group, of the volcaniclastic and clastic sedimentary associations (Baltazar and Zucchetti, 2007). Cuiabá (*e.g.*, Lobato et al., 2005; Ribeiro Rodrigues et al., 2007) is a BIF-hosted gold deposit, marked by the contour of the large-scale Cuiabá fold.

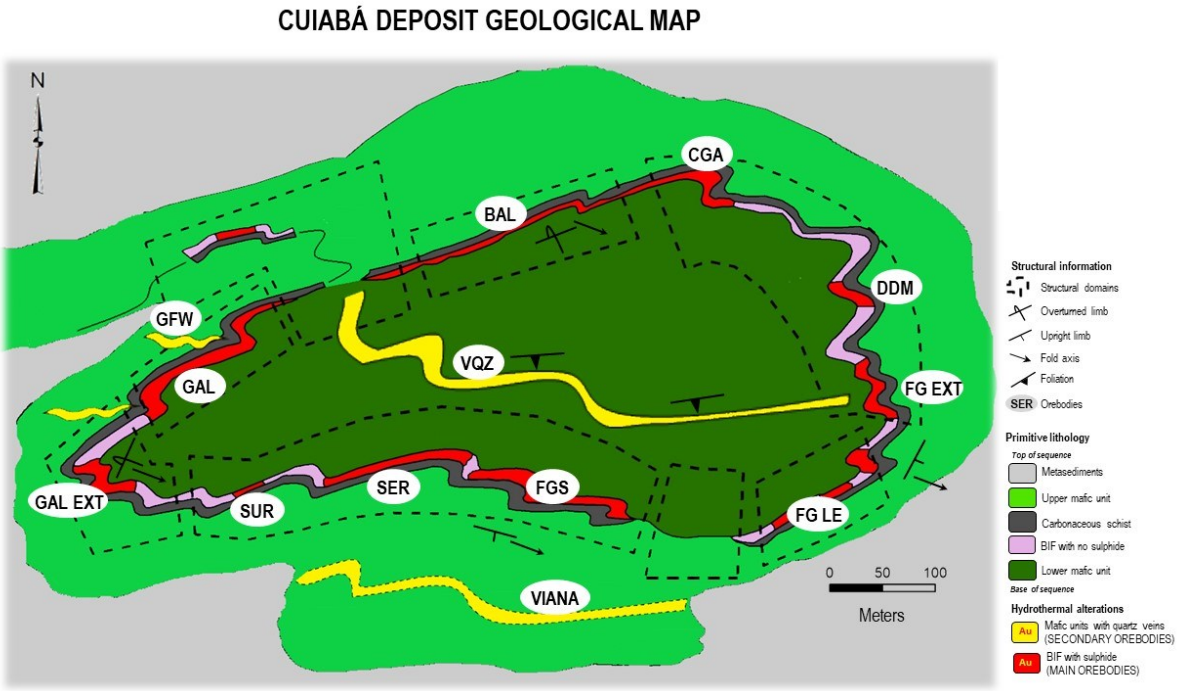

Figure 7. Schematic geological map based on level 11 to 16 of the Cuiabá Deposit (after Fernandes et al.,2016).

The lithological succession at Cuiabá (Figure 8) includes volcanic, volcaniclastic and other sedimentary rocks (Vial, 1980, Vieira, 1992, Toledo, 1997 and Ribeiro-Rodrigues et al., 2007). Primitive rock types are described, from base to top, as lower mafic volcanic rocks (MAN), the Cuiabá BIF, carbonaceous schists (XG), upper mafic volcanic rocks (MBA) and sedimentary rocks characterized by metapelites (X1) intercalated with metapsamites (XS) with volcaniclastic contribution. Mafic volcanic rocks are characterized by the presence of chlorite, epidote, plagioclase and actinolite and quartz as alteration minerals. The BIF is characterized by alternating dark (rich in carbonaceous matter), carbonate-quartz (± magnetite) and light quartz-carbonate bands. Algoma-type banded iron formations (BIFs) are thinly bedded, chemical sedimentary rocks, consisting of alternating layers rich in chert and iron-rich minerals (Araújo and Lobato, 2019). The upper unit is constituted of pelites alternating with volcaniclastics rocks. Post mineralization mafic dikes crosscut all rock types locally.

Vial (1980), Toledo (1997), Ribeiro-Rodrigues (1998) and Ribeiro-Rodrigues et al. *(*2007) considered the Cuiabá fold as a tubular structure, plunging 30º to ESE (Vial, 1980; Toledo, 1997). Cuiabá deposit hydrothermal alteration (Vieira, 1992, Toledo, 1997) at metamafic units (lower and upper) is divided by three main zones. It is classified as distal (epidote-chlorite schist, named as MANX for lower metandesitic basalt and MBAX for upper metamafic unit), intermediate (chlorite-carbonate schist, named as X2CL) and proximal zones (quartz-sericite schist, named as X2). At BIF´s the hydrothermal alteration is characterized by the presence of hydrothermal carbonate (ankerite) at intermediate zones and by sulphide zones at proximal domains. Hydrothermal alteration cut all rock types, following structural features (Figure 8).

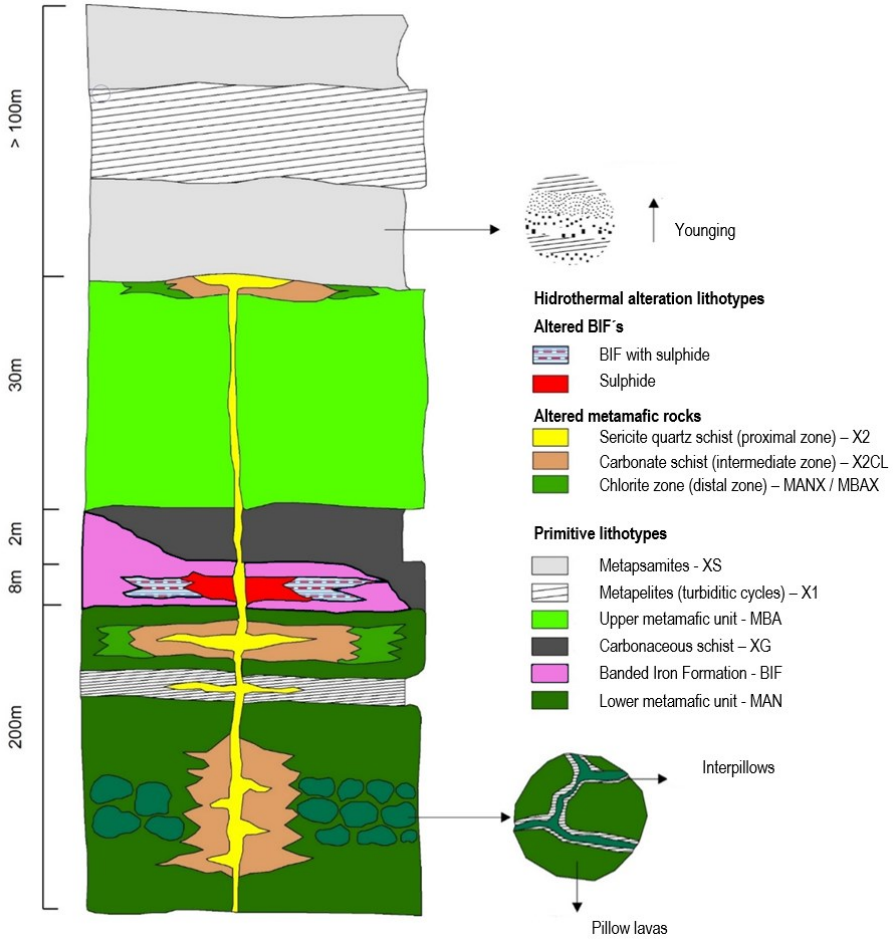

Figure 8. Simplified stratigraphic column at the Cuiaba mine. (modified from Fernandes et al., 2016).

According to Ribeiro-Rodrigues (1998) and Lobato et al. (2001a), metamafic units envelop mineralization hosted in BIF and ferruginous chert and mineralization in shear-zone-related quartz veins with disseminated sulfides associated with Fe-rich volcanic rocks. The recent discovered quartz-veins mineralized zones, hosted in the lower mafic unit, at the Cuiaba deposit are characterized by interconnecting quartz-carbonate veins related to the structurally controlled hydrothermal alteration of their host rock (Vitorino, 2017; Figure 7).

Three gold mineralization types are recognized at QF: i) Type 1: pyrrhothite dominant sulphidation of BIF stratigraphic horizon and lapa seca; ii) Type 2: pyrite dominant sulphidation inside BIF occurring as a replacement style at carbonatic layers; ii) Type 3: quartz veins with disseminated pyrite along its structures within the volcanic and sedimentary sequences. Cuiabá orebodies inside BIF are mainly associated to type-2 mineralization (Vieira, 1988).

3.6.METHODOLOGY

Cuiabá mine is being mapped since its beginning in industrial scale (1982). This work was obtained after 11 years of underground mapping (from 2009 to 2020). The mapping relied on the classical tools of structural geology, which joined together field and laboratory work with meso- and micro-structural studies. Geopetal and structural elements were observed, to understand the process of local topology. Geopetal features are used to determine top and bottom criteria and upright or overturned limb. They are characterized in the mine through stratigraphic studies (Vial, 1980, Vieira, 1988, Vieira, 1992, Toledo, 1997), which considered the rocks at the core of the deposit to be older than the external ones. As a way of confirming this hypothesis, stratigraphic criteria in turbiditic flows (Bouma, 1962) are also used in the portions external to the core. Linear and planar elements are obtained throughout symmetry plane analysis of folded systems (Ramsay & Huber,

1987, Cowan, J. 2016). During the field work a central ductile shear zone was recognized for the first time and described in Vitorino et al. (2020).

Field geologists have long known that the style and relationships of structures seen in a hand specimen, outcrop or drill core can mimic the style and relationships of much larger structures that formed during the same deformation but occur at the scale of a geological map or section. The axes and axial surfaces of minor folds of an area are congruent with those of the major fold structures of the same phase of deformation. This idea became known to several generations of geologists as Pumpelly's Rule (Pumpelly et al., 1894). Although strictly only a theory of fold and axial surface vergences, the Rule came to be associated with the idea that the general style of all minor structures was likely to mirror that of the major structures with which they were associated. A total of 52 underground galleries was mapped and geological field trips in different sites were done to complete this task. It was taken 2795 measurements (Figure 27) from level 07 (590m above sea level) to level 19 (200m below sea level). The 3D models allowed the construction of a more realistic geometry of the geological structures.

3.7. DEPOSIT SCALE STRUCTURAL ANALYSIS

The deposit is located between two important QF megastructures: the Serra do Curral homocline to the north and the Gandarela syncline to the south. The Cuiabá Deposit area has a transpressive transcurrent tectonic system with tectonic structures presenting a main NE-SW direction and dip to SE.

The main planar structures are characterized by the primary structures related to bedding (S_0; Figure 9) and axial-plane foliations (S_1, S_2, and S_3) associated with folding (D_1, D_2, and D_3). Linear structures are associated with fold axes and intersection lineations between planar structures (L_1, L_2, and L_3).

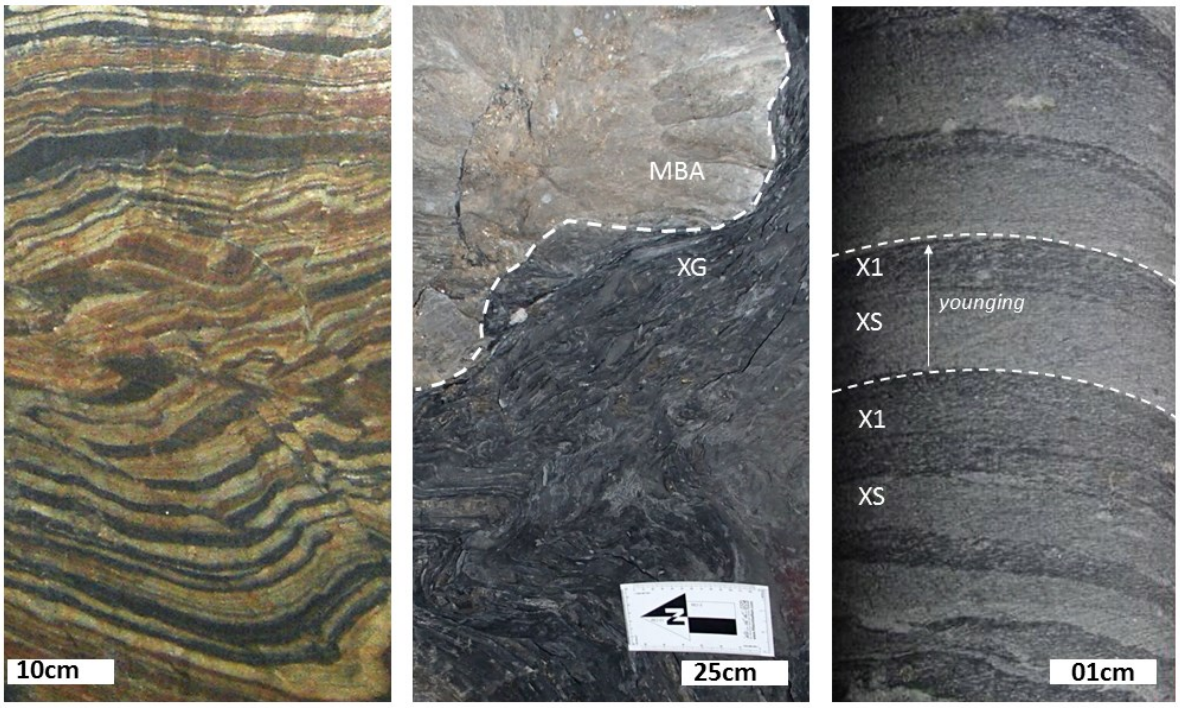

Figure 9. Different lithotypes representing the S0 phase of the Cuiabá deposit. LEFT: Compositional variation between carbonate, sideritic and quartz bands of BIF's. CENTER: Contact between different lithotypes (MBA: upper metabasalt; XG: carbonaceous schist). RIGHT. Gradational granulometric variation observed in the rhythmite (X1: metapelite; XS: metapsamite).

Kinematic indicators are observed along with all structures at different scales. Among the indicators associated with ductile rheology, the main ones are asymmetrical folds located in layers, or veins, (presenting asymmetry in Z, S, or M), SC foliation, and rotated porphyroblasts forming varied structures such as pressure shadows, fringes of pressure, and recrystallization tails, in sigma or delta structures. Among the indicators associated with ductile-brittle rheology are crenulation cleavage and deformed quartz veins associated with precipitation in zones of lower stress in gash veins.

3.7.1. *Deformation Structures*

3.7.1.1. *D_1 Phase Structures*

The structures of phases 1 and 2 are very difficult to distinguish on a deposit scale, due to the similarity and coaxial character between them. These structures were initially confirmed due to the local recognition of fold interference patterns (Figure 10) and different asymmetries of parasitic folds in the same limb. D_1 folds, L_1 fold axes, and S_1 axial plane foliation represent this ductile rheology phase. The D_1 structures present axial plane foliation usually dipping to SSE and a fold axis with moderate plunge to ESE, indicating a strike-slip tectonic transport with NNE-SSW direction.

D_1 folds have decimeter to decameter dimensions. They are characterized by inclined, flat folds (except in areas with fold interference patterns, as shown in Figure 10), cylindrical, similar, tight (with an interlimb angle ranging from 0 to 30 degrees), and in general asymmetrical. Locally, isocline folds with large amplitudes are observed.

The S_1 foliation is subparallel to the bedding in the fold limbs, corroborating the characterization of a tight to isocline fold. In schists, it is well marked and is characterized as a penetrative schistosity, composed by the orientation of phyllosilicates (chlorite and white mica) and carbonate porphyroblasts, which are the main building elements of this structure. In BIF's the S_1 foliation is recognized as axial-plane cleavages of D_1 folds, usually spaced and filled by chlorite, carbonate, and quartz.

The L_1 lineation is an intersection lineation between the S_1 foliation and the S_0 folded bedding, being parallel to D_1 fold axis. It is observed in the field that the mineral stretching lineation in carbonates and quartz is parallel to the D_1 fold axis, being represented in the same stereogram.

High concentration of quartz veins and the presence of mylonitic zones in the contact of upper metavulcanic, carbonaceous schist and mineralized BIF´s are well observed throughout the limbs.

3.7.1.2. *D2 Phase Structures*

Structures D2, together with D1, are the most pervasive and observed throughout the entire studied area of the deposit, representing the main structure of the deposit. These ductile to ductile-brittle structures are represented by D2 folds, L2 lineations (represented by fold axes, intersection lineations and mineral stretching lineations), S2 foliations and shear zones. In schists, the structures have a ductile character, while in BIF's, the axial-plane cleavage is spaced and pervasive, specially at hinge zones.

As mentioned above, D1 and D2 structures are difficult to distinguish due to their subparallelism at limbs. Even with little difference of rheology (as D1 are ductile and D2 are ductile to ductile-brittle) this distinction is not trivial. In rare cases where fold interference patterns are observed (Figure 10) it is possible to discriminate structural phases at D2 hinge zones. Thus, it was decided in this work to include them in the same stereograms and to name them S2-1 foliation and L2-1 lineation (Figure 14). S2-1 foliation is observed with a moderate dip to ESE and L2-1 fold axis with a moderate plunge to ESE, indicating strike-slip tectonic transport in the NE-SW direction. Due to the superposition of foldings, it is difficult to determine the vergence at first sight.

The D2 folds (Figure 11) have decimetric to decametric dimensions. They are characterized by inclined, flat, cylindrical, similar, tight (with an interlimb angle ranging from 10º to 30º), and asymmetrical folds. The L2 lineation is an intersection lineation from planar structures before this phase (bedding S0 or S1 foliation) and the S2 foliation, being parallel to the D2 fold axis and the stretching lineation of the carbonate and quartz minerals. In this way, as in D1, these structures are represented in the same stereogram.

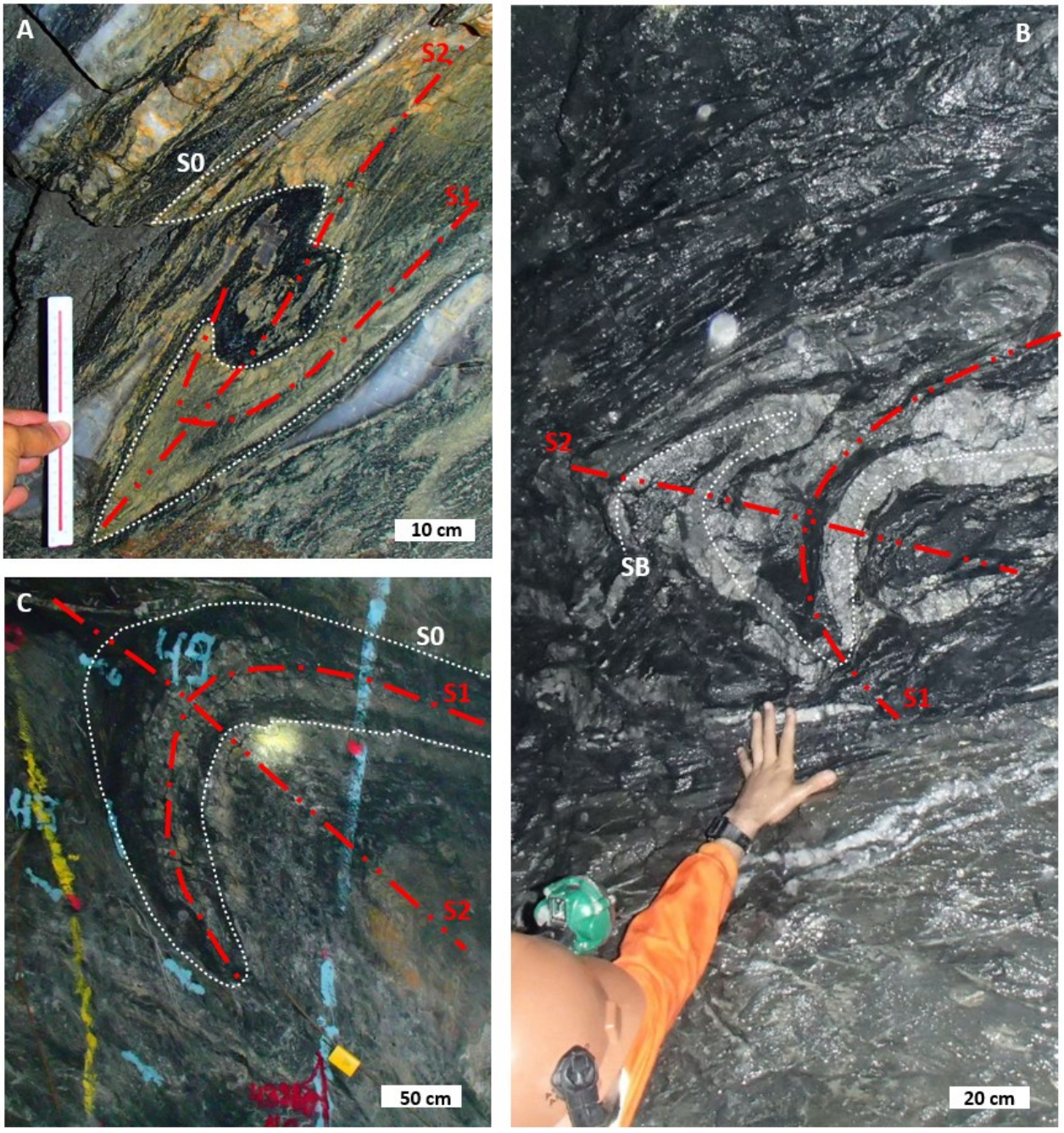

Figure 10. Structures related to interference patterns from D2 at D1 folds, generating coaxial hook-like geometry: A. Fonte Grande orebody (Center-South domain) level 15 (up-plunge view to NW); B. Balancão orebody (Center-North domain) level 10 (up-plunge view to NW); C. Galinheiro Extensão orebody (West domain) level 11 (down-plunge view to SE). Structural features: S0-bedding, SB-banding, S1-folded foliation from phase D1, S2-axial plane foliation from phase D2.

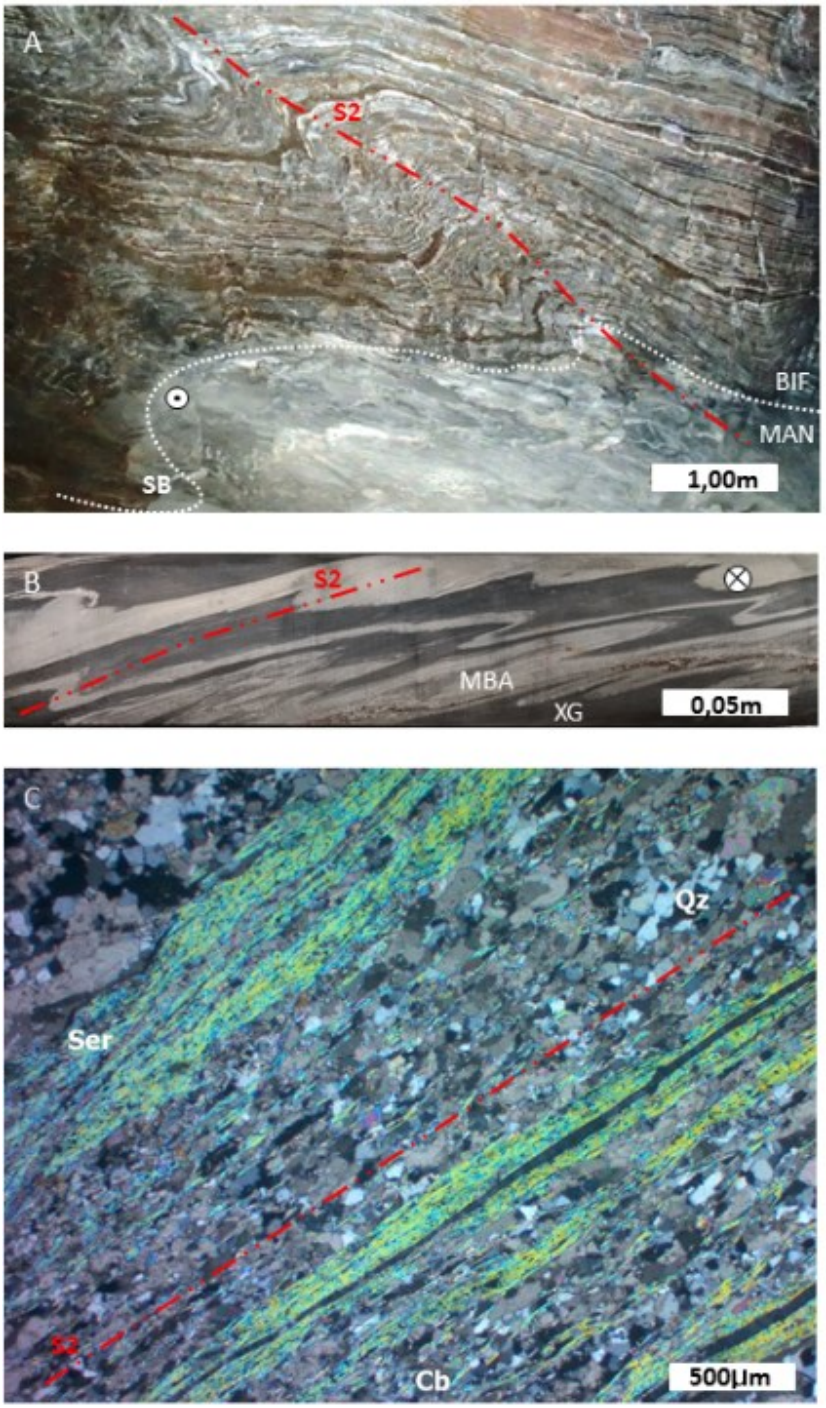

Figure 11. D2 structures. A. D2 folds (NW up-plunge view) with L2 lineation represented by the fold axis (represented by a small white circle) and S2 foliation characterized by the axial-plane cleavage at the contact between BIF and lower metandesite basalt (MAN); B. D2 folds (ESE down-plunge view), presenting L2 fold axis and S2 axial-plane foliation at the contact of carbonaceous schist (XG) and upper metabasalt (MBA); C. Photomicrograph of S2 foliation formed by orientation of phyllosilicates (sericite – ser) and elongated quartz (qz) and carbonate (cb) grains.

The S2 foliation is marked in all rocks in the deposit, being parallel to the axial plane of the D2 folds. In the most competent rocks (BIFs and metabasalts) the S2 foliation is less penetrative and centimetric to subdecimetric spaced. In general, this structure is represented as an axial plane cleavage (Figure 11A). In BIFs, the presence of S2 foliation planes filled with chlorite and quartz can be noticed. In less competent rocks, such as hydrothermally altered metavolcanic rocks and schists of sedimentary origin (carbon shales and metaritmites), the S2 foliation is characterized as a penetrative foliation (Figure 11B), with millimeter spacing, forming a schistosity through the preferential orientation of the phyllosilicates (chlorite and white mica), carbonate porphyroblasts, and quartz, being these minerals the main building elements of this structure (Figure 11C).

It is observed concentrations of quartz veins and the presence of mylonitic zones in the axial planes of D2 folds.

3.7.1.3. *D3 Phase Structures*

Features related to D3 structures are less frequent and sparser than D1 and D2. D3 structures are brittle-ductile to brittle, registering shallower crustal levels. Folds (D3), crenulation lineation (L3), crenulation cleavage (S3), and partially filled cavities, materialize this deformation phase. The S3 foliation has a moderate to strong dip to E and the L3 fold axis registers a smooth plunge to S (Figure 14).

D3 folds (Figure 12A), millimeter to metric, show crenulation along its overturned limbs. They are flat, cylindrical, harmonic, and closed to smooth folds, with an interlimb angle ranging from 30 to 70 degrees. The D3 folds are vergent to W.

The crenulation lineation, L3 (Figure 12B), is defined by the D3 microfold axes with the foliation S3. L3 has an N-S direction with a moderate plunge to S.

The S3 foliation (Figure 12C and Figure 12D) is pervasive in rocks with a higher composition of phyllosilicates (graphitic schist and metaritmites) and defined by the discontinuity of the previous planar structures (S2, S1, or S0). It is penetrative, sigmoidal, and spaced, forming crenulation cleavages with centimetric to subcentimetric spacing. The crenulation cleavage, tension gashes filled by milky quartz veins (Figure 12E) and the rupture of BIF's layers (Figure 12F) are the most representative structures.

The D3 phase records cavities (geodes) with decimetric to metric dimensions (Figure 12G), partially filled by euhedral quartz, carbonate, chlorite, and pyrrhotite crystals. Rare centimetric needles of rutile (Figure 12H) included, or not, in quartz crystals, are observed.

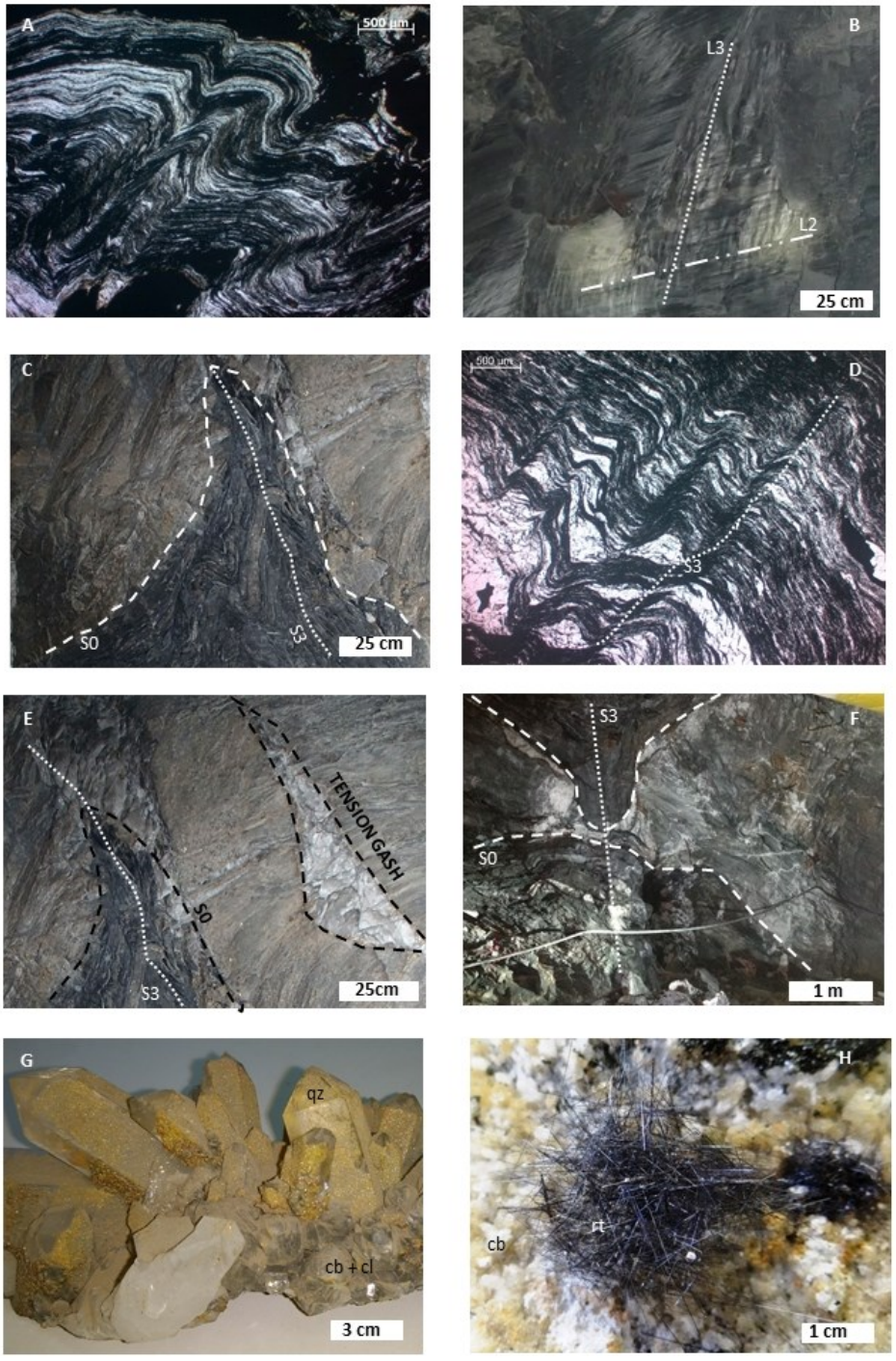

Figure 12. D3 structures. A. D3 folds with vergence to W (view to S); B. L3 fold axis presenting crenulated aspect (view to S); C. S3 foliation (mesoscopic view for N); D. Foliation S3 (microscopic view to S); E. Tension gashes of milky quartz veins associated with shear zones of the S3 foliation (N view); F. Disruption of BIF's layers associated with D3 phase (view to N); G. Cavities partially filled by euhedral crystals of quartz (qz), carbonate (cb) and chlorite (cl); H. Rare acicular crystals of rutile (rt) associated with cavities in carbonate matrix (cb).

3.7.2. *Structural domains*

For a better understanding of the relationship between the structural features in phases D1 and D2, which are difficult to individualize, structural domaining for Cuiabá deposit are presented, described (Figure 13; Table 2) and differentiated (Figure 14). The division into domains is based on topology and structural location of the fold (overturned limb, upright limb or hinge zone) and based on the styles and asymmetries of D1 or D2 folds. Folds D1 and D2 are similar in morphology and geometry, creating difficulty in mapping differentiation. Therefore, the generation of these folds will not be discussed in these domains.

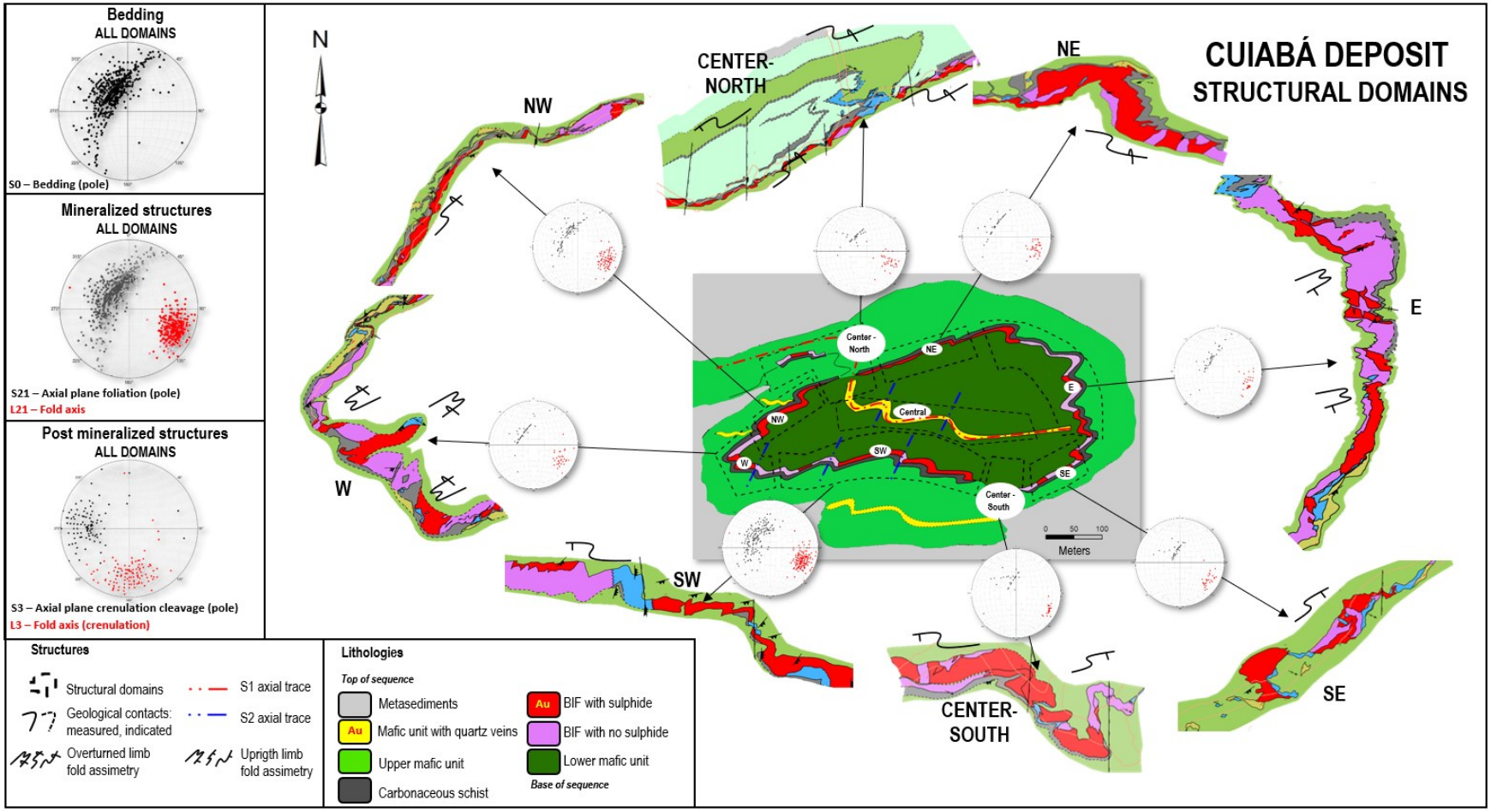

Figure 13. Maps of defined structural domains. Note that on the south and east flank the domains are classified as normal flank, while on the north and west flank the domains have an inverse flank.

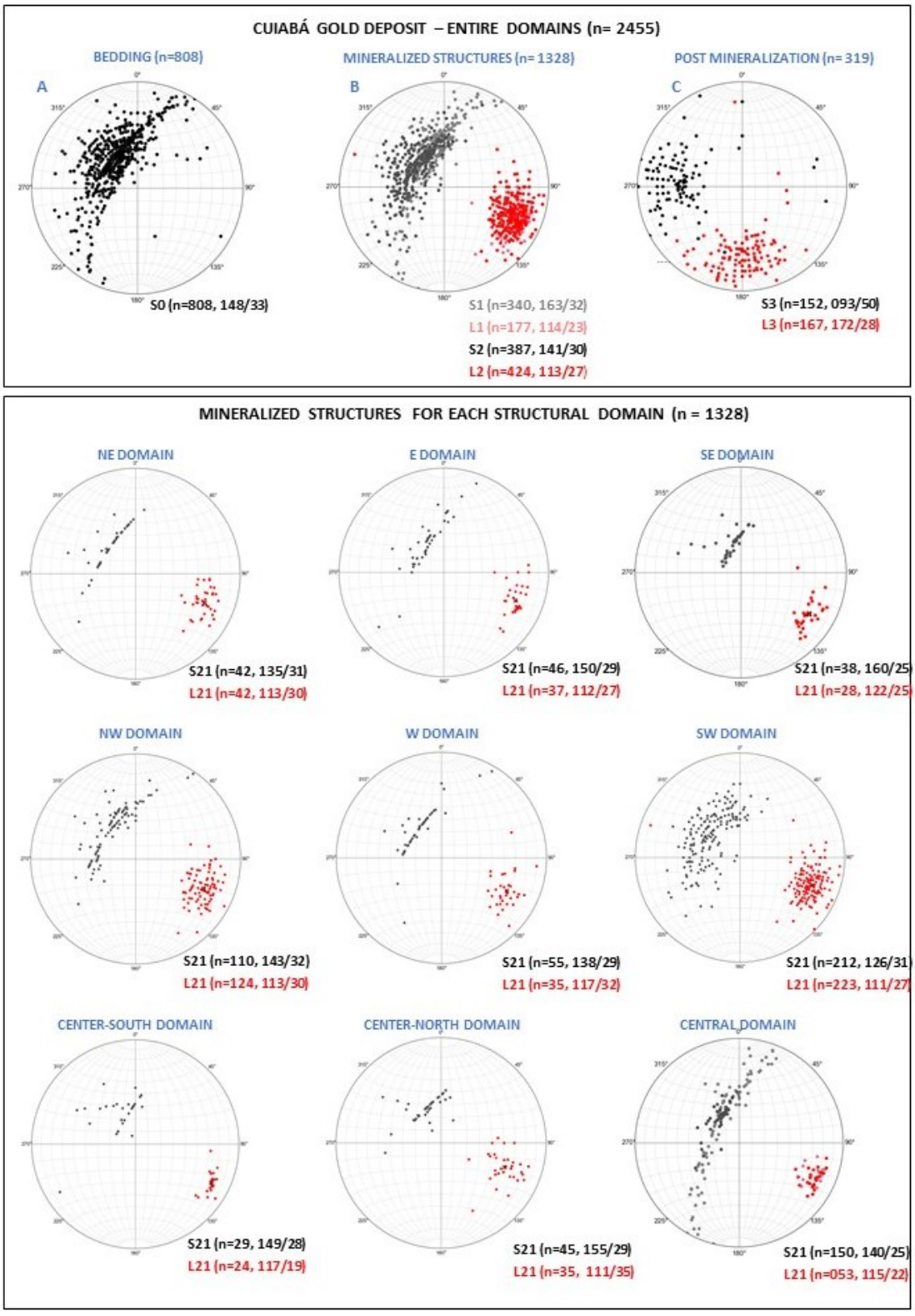

Figure 14. Stereograms of mineralized structures in the Cuiabá deposit, individualized by structural domains. Red dots represent the fold axes. Black dots represent the poles of axial-plane foliation.

3.7.2.1.*Center-North Domain*

Applying Pumpelly's Rule (Pumpelly et al., 1894), the asymmetry of the folds (Figure 13) and the continuity of the BIF layer were analyzed. Through this study regions with repetitions of carbonaceous schist layers, and the presence of a mineralized body called Galinheiro Foot Wall can be noticed.

However, it is noted that there is a subdecimetric mineralized BIF layer located in the Foot Wall of the NW Domain. Through geological information (mapping and drilling holes), it is possible to observe the continuity of this structure in-depth, from the surface to level 21.

3.7.2.2.*NE Domain*

As observed in Table 2, as one approaches Domain E, the evolution of folds with asymmetry initially in Z (indicative of clockwise vorticity to this domain) to asymmetry in Z and M is noticed. This change in the asymmetry pattern indicates the transition from the overturned limbs to the hinge zone. An inverted stratigraphic relationship in the domains is observed, where the carbonaceous schist occurs in the Foot Wall of the BIF, in an inverted position (Figure 13).

3.7.2.3.*E Domain*

In the boundary region with the NE Domain, Z-folds and overturned limbs are observed, transitioning to M; in the boundary region with the SE Domain, S-folds and upright limbs are observed, transitioning to M (Figure 13). The fold asymmetry in this domain is indicative of hinge zone.

3.7.2.4.*SE Domain*

As we approach Domain E (Figure 13), we can see the evolution of folds from initially S asymmetry to M asymmetry, indicative of counterclockwise vorticity to this domain. This change

in the asymmetry pattern indicates the proximity of the hinge zone to the main fold, with continuity to the north. The normal stratigraphic relationship is evident in the SE domains, where the carbonaceous schist is observed in the Hanging Wall of the BIF layer (Figure 13).

3.7.2.5. *Center-South Domain*

This domain area is characterized by upright limbs. Some peculiar characteristics are observed in this domain as it goes deeper into the deposit, parallel to the plunge of main fold axis; (Figure 13). Between the surface and level 11, it is observed in this domain, the continuity of the BIF layer along the strike, reaching about 15 meters of apparent horizontal thickness. This increase in thickness occurs due to the fold interference pattern with Z-folds asymmetry in the western limit and S-folds asymmetry in the eastern limit of its domain. This region is considered one of the areas with the highest metallic content in gold (between levels 05 to 11), due to high contents associated with a thick BIF layer.

Between levels 12 and 13 (Figure 15) the BIF layer, still continuous and thick due to the interference of folds, undergoes a duplication associated with the presence of smoky quartz veins near the Hanging Wall. This duplication is responsible for the increase in the thickness of the mineralized layer, including the presence of smoky quartz veins, reaching up to 25 meters of apparent horizontal thickness at this location. Although the gold content has decreased slightly in relation to the upper levels, it is observed that the metallic content is still high due to the increase in the thickness of the mineralized horizon.

Below level 13, the BIF layer disappears in this domain, showing ruptures of approximately 75 meters in length along the strike. This feature is observed down to level 28, where there is geological information to date. The gold metallic content, and the BIF layer, at these levels decreases considerably.

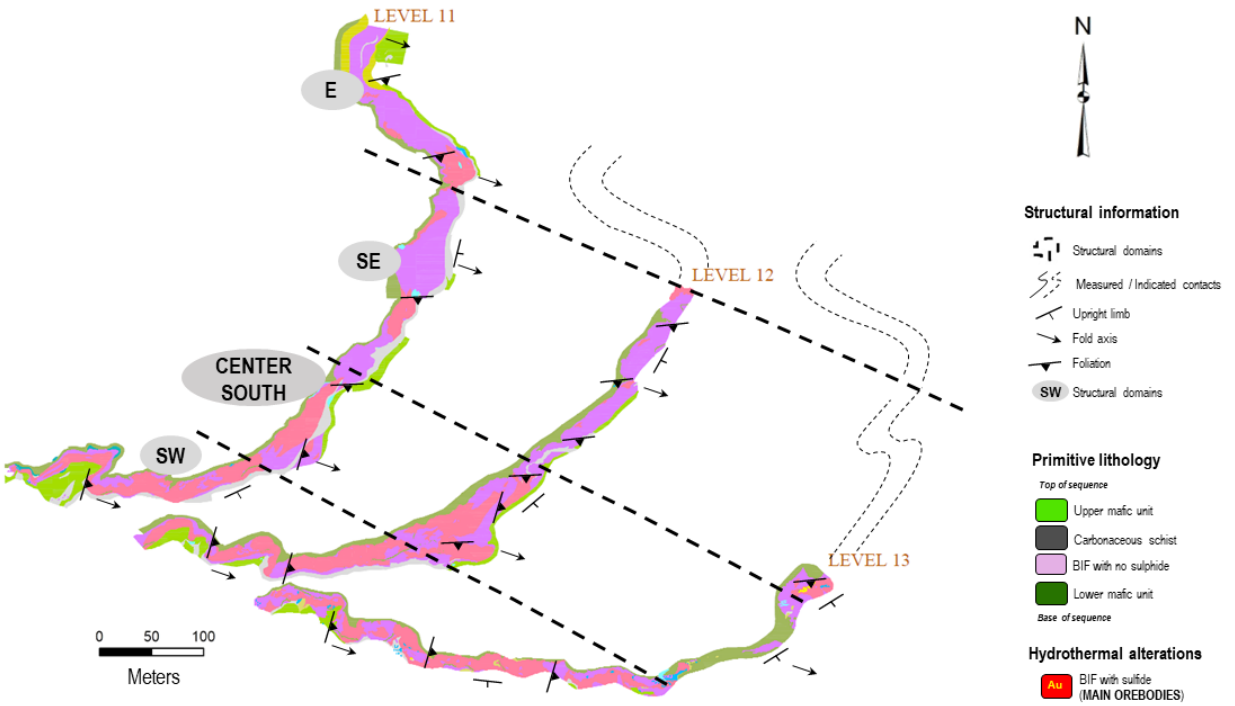

Figure 15. Level 11, 12 and 13 composite maps from Fonte Grande orebody at Center-South domain showing local duplication of BIF´s at this site.

In the southern-most portion of the deposit, at about 100 meters in the Hanging Wall of Fonte Grande orebody, it is noted the presence of submetric to metric quartz veins inside hydrothermalized zones of metabasalt (Viana orebody). This domain is apparently continuous with the Baú oredody, both with E-W trend. Further investigations are necessary after its development, since the Viana orebody has locally presented rocks with characteristics similar to BIF at level 19 and 20.

3.7.2.6. *SW Domain*

The Z-fold asymmetry (indicative of clockwise vorticity) and normal limbs in this domain allow to observe the closing of this structure towards W Domain, being consistent with Pumpelly's Rule. However, the continuity of the structure in the transition between the SW and SE domains is inconsistent with this rule, as described in the SE Domain, indicating more than one deformation phase (Figure 13).

3.7.2.7. *W Domain*

The overturned limb and M-fold asymmetry in this domain (Figure 13) indicates a hinge zone. Fold interference pattern at this location is also notorious, characterizing by local refolding elements where foliations S1 and S2 are observed in the same outcrop (Figure 10C). Fold concavity plunging to the core of Cuiabá deposit nuclei (Figure 13) indicating a synform-anticline is another important evidence that reinforces the presence of fold interference patterns at the domain.

3.7.2.8.*NW Domain*

As seen in Figure 13, as it approaches the W Domain, the evolution of folds with asymmetry initially in S (indicative of sinistral cinematics) to asymmetry in S and M is observed inside a overturned limb. This change in the asymmetry pattern indicates the transition from the limb to the hinge zone of the main fold, closing toward W Domain.

3.7.3. *Structural features of the vein systems (Central Domain) Structural Domains*

The central zone of the Cuiabá deposit is represented by the quartz vein ore body (VQZ) associated with lower andesitic metabasalts metamafic rocks. The main structures associated with this domain are the S1 and S2 foliations (Figure 14), where quartz veins are hosted within the proximal alteration zones (sericite zone) mainly along S1 foliation, where higher gold grades are placed. This is the only domain of the deposit where it is possible to clearly distinguish the two mineralized phases.

The S1 foliation (Figure 14), is characterized by a highly tectonized and folded foliation, whose are mainly formed by sericite and quartz, in the proximal zone, being the main builder elements of this structure. It is also noted that this shear zone cut the BIF at East domain (observed at L17 throughout development inspection) and at the Center-North domain, where BIF layer is silicified (observed throughout geological mapping at Level 09, 10, 11, 12, 13 and 14). Within the veins, a

small proportion of sulfides is observed, characterized mainly by millimetric to subcentimetric crystals of pyrrhotite stretched parallel to the fold axis. It is also observed, in a less constant way, subhedral to euhedral crystals of sphalerite and galena of subcentimetric to centimetric size.

The S2 foliation (Figure 14), is the most penetrative structure and is observed in the zones of intermediate (carbonate zone) and distal (chlorite zone) alteration, reaching the point of obliterating the previous features. It is characterized by the alignment of phyllosilicate (chlorite and sericite), carbonates, and quartz, being the main builder elements of this structure. Locally, quartz veins and proximal hydrothermal alteration can be observed contained in the S2 foliation, which is parallel to the axial plane of the folded quartz veins contained in the S1 foliation. In the veins associated to S2 foliation, it is observed a small proportion and disseminated sulfides characterized mainly by euhedral to subhedral pyrite crystals of milimetric to subcentimetric size.

Two types of quartz veins are verified: (1) smoky quartz, more present in the S1 foliation, and (2) quartz-carbonate veins, more present in the S2 foliation. However, smoky quartz is also observed in the S2 foliation in minor proportion. Both quartz veins are related to gold occurrences. S2 foliation hosts gold inside quartz veins with lower gold grades and small length (2 to 4 g/t in average and at most 40 m along strike), probably remobilized from D1 mineralized zones (Figure *17*.A) where gold grade is higher and more continuous (4 to 10 g/t in average and at least 150 m along strike). Visible gold (Figure *17*.B) occurs rarely only in the S1 foliation, usually associated with sphalerite and galena.

The S1 foliation is folded and has a moderate dip to SSE. The S2 foliation is axial-plane of the S1 folded foliation and has a moderate dip to SE and a fold axis with a moderate plunge to ESE. Phase 1 folds, in quartz veins inside lower mafic unit, are asymmetrical with Z-asymmetry (Figure *16*).

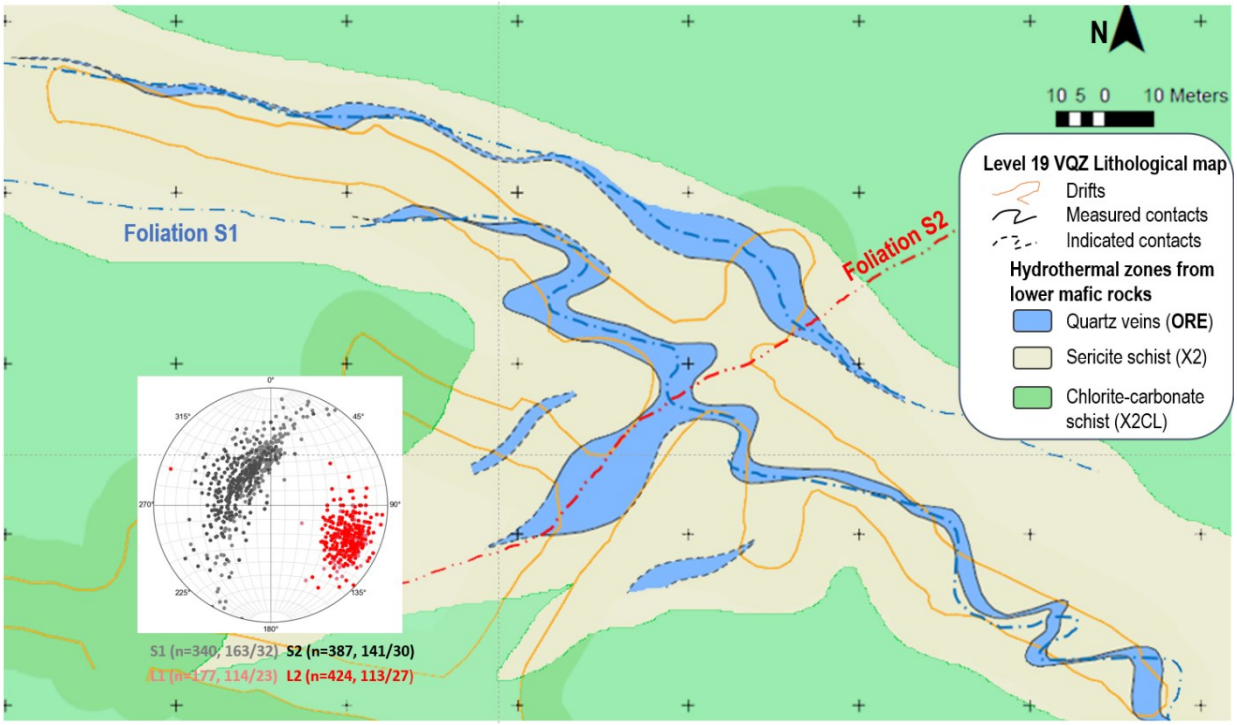

Figure 16. Level 19 VQZ orebody lithological map, showing the location of high grades and folded quartz veins at proximal hydrothermal zones (X2) sericite schist along S1 foliation. Secondary quartz vein at axial plane S2 foliation is observed with small length and lower grades. Stereographic projection is related to all mineralized structures measured from this paper.

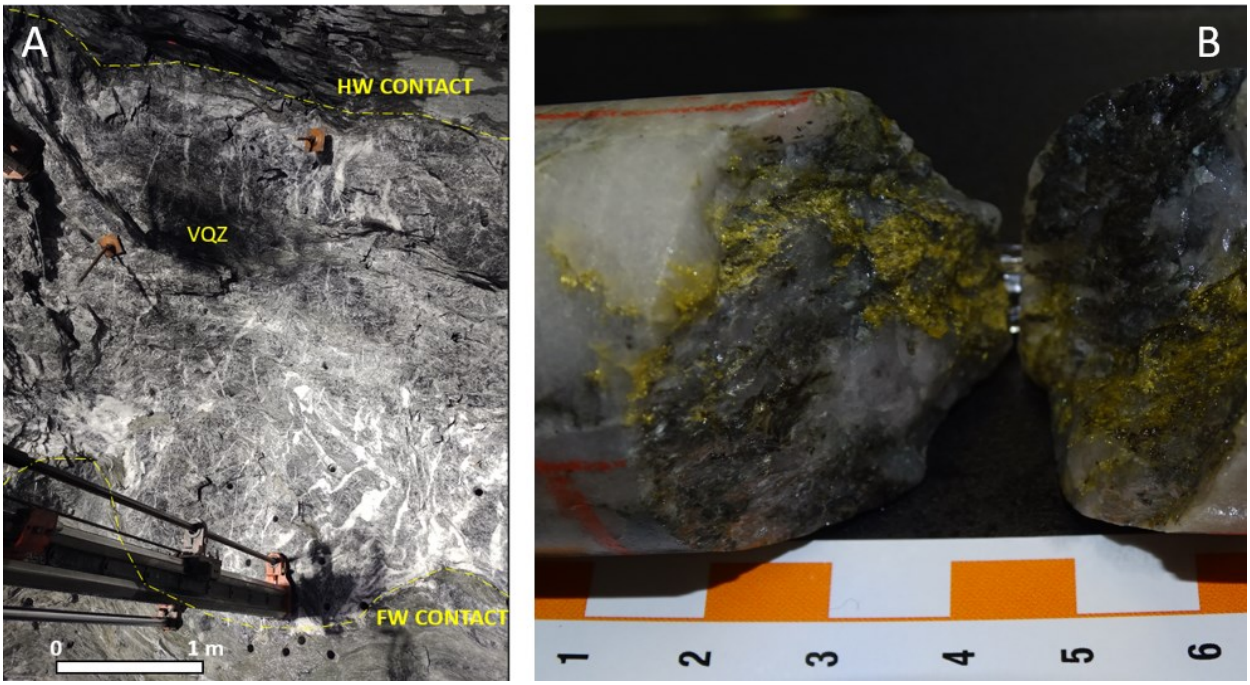

Figure 17. Quartz veins at metamafic examples: (A) outcrop scale at level 18 VQZ (up-plunge view to NW) with of 3 m thick smoky quartz vein surrounded by contacts represented by proximal alteration zone at (yellow sericite schist -X2) along S1 foliation where high gold grades (4 to 10 g/t) are placed; (B) Drill core (35 mm of diameter) showing quartz vein with visible gold at foliation S1 (from level 18 VQZ.

3.7.4. *Structural phase distinction at Cuiabá domains*

After structural domains characterization inside Cuiabá deposit, it is noteworthy that the D1 and D2 mineralized structures were locally distinguishable through 3 criteria: (i) Central Domain (VQZ orebody), where quartz veins is folded along S1 foliation and where S2 foliation represents its axial-plane; (ii) Fold interference patterns observed locally at refolded BIF layers, inside the W, Center-South, and Center-North domains and (iii) S1 foliation is more observed in NE, E and SE domains, dipping to SSE. On the other hand, S2 foliation is more penetrative in the NW, W and SW domains dipping to SE (Figure 14).

Thus, the Cuiabá deposit can be divided into two large structural compartments: The Western compartment (W) and the Eastern compartment (E). Compartment E encompasses the previously described NE, E, and SE domains. It refers to deformation zones associated with phase 1, presenting very tight to isocline recumbent folds, with foliation dipping to SSE. The W compartment encompasses the Center, North-Central, NW, W, SW and South-Central domains, with folding zones mainly associated with phase 2 as clearly observed at Center Domain, with foliation dipping to SE. Locally it is possible to observe fold interference pattern from D1 and D2 folds, as observed in Center-South and W domains. These criteria are helpful to understand the whole deposit and classify the phase predominance at each domain as described at Table 2.

Table 2. Summary of structural domains of Cuiabá Deposit.

Table 2. Summary of structural domains of Cuiabá Deposit

Structural Domains							
Domain	**Location**	**Compartment**	**Tectonic phase definition**	**Extension**	**Structures**	**Tectonic Features**	**Observation**
Mid-North Intermediate Domain	Junction of the Northwest (NW) and Northeast (NE) Domains.	W	D1 and D2	50 m	Tectonic foliation paralleled with banding, inclined recumbent folds and fold interference zones, ruptured BIF replaced by metric smoky quartz venulations interspersed with carbonaceous schist.	Folds: foliation with moderate dip for SE and fold axis with moderate dip for ESE.	When moving away from the tectonized zone, it is observed the appearance of folds with S asymmetry in the NW Domain and folds with Z asymmetry in the NE Domain.
NE	East-central Balancão (BAL) ore body	E	D1	300 m	Axial-plane foliation and inclined to reclining, recumbent and asymmetric Z-folds	Folds: foliation with moderate dip to SSE and fold axis with moderate plunge to ESE. Stretch marks: sub-horizontal with NE-SW direction. Z-folds, indicative of a dextrally moving fold flank.	Inverted stratigraphic relationships, where the carbonaceous schist. appears on the foot wall of the ore body. Locally the presence of tectonic stretch marks located in the carbonaceous schist. lithology.
E	Canta Galo (CGA; very high gold content), Dom Domingos (DDM) and the eastern end of the Fonte Grande (FG) ore body.	E	D1	300 m	Inclined to isoclinal recumbent, symmetrical, M type folds.	Folds: foliation with moderate dip to SSE and fold axis with moderate plunge to ESE. M-folds, indicating fold hinge zone.	*
SE	Fonte Grande (FG) ore body.	E	D1	200 m	Inclined to reclined, asymmetrical folds in S.	Folds: foliation with moderate dip for SSE and fold axis with moderate plunge to ESE. S-folds, indicative of sinistral strike-slip movement for the SE Domain.	Normal stratigraphic relationships, where carbonaceous schist appears in the Hanging Wall of the ore body.
Central-South Intermediate Domain	Junction of the Southeast (SE) and Southwest (SW) Domains.	W	D1 and D2	100 m	Inclined recumbent folds with varying asymmetry. Towards the SE Domain there is asymmetry in S. Towards the SW Domain there is asymmetry in Z	Folds: folded foliation S1 dipping to SSE, foliation S2 dipping to SE and fold axis with moderate plunge to ESE	*
SW	West segment of Fonte Grande orebody (FG); Serrotinho (SER) and Surucucú (SUR) ore bodies.	W	D2	600 m	Inclined to reclined, asymmetrical Z folds. Axial-plane foliation. Locally with tectonic stretch marks in the carbonaceous schist.	Folds: foliation with moderate dip for ESE and fold axis with moderate plunge to ESE. Sub-horizontal tectonic SE. Stretch marks, with NE-SW direction.	This domain is the richest region of the deposit, with ore bodies with high grades (generally above 10 g/t in the SER and FG bodies) and actual thicknesses varying between 7 and 15 meters.
W	West of the Galinheiro ore body, called Galinheiro Extension (GAL EXT)	W	D2	200 m	Folds inclined to reclined, symmetrical in M and axial-plane foliation.	M- to Z-folds, indicative of hinge zone related to D2 tectonic	*
NW	Galinheiro ore body (GAL), with the exception of the western segment, and the western portion of the Balancão body (BAL).	W	D2	300 m	Inclined folds with S asymmetry and plane-axial foliation on bending.	Folds: foliation with moderate dip for SE and fold axis with moderate plunge to ESE. S-folds, indicative of sinistral movement.	Inverted stratigraphic relationships, where carbonaceous schist appears on the foot wall of the ore body
Central Domain	The Cuiabá Central Domain is represented by the quartz vein ore body (VQZ) associated with lower metamafic rocks (andesitic metabasalts).	W	Folded D1 and axial plane D2	250 m (inside lower metamafic unit)	The S1 foliation is characterized by a highly tectonized and folded foliation. The S2 foliation is the most pervasive structured, obliterating the previous features.	It is possible to perceive a clear relationship between S1 and S2 in the VQZ zone. S1 is folded and has a moderate dip for SSE. The S2 foliation is plane-axial of the folds of S1 and has a moderate dip for SE and a fold axis with moderate slope for ESE. Phase 2 bends in quartz veins are asymmetrical with Z-symmetry.	Two types of quartz veins are verified: (1) smoky quartz, more present in the S1 foliation and (2) quartz-carbonate veins more present in the S2 foliation. However, smoky quartz is also observed in the S2 foliation in minor proportion. Key domain for understand the whole deposit.

3.8. STRUCTURAL EVOLUTION OF THE CUIABÁ DEPOSIT

Previous works attribute the tubular fold or sheath fold model as a hypothesis for the structural evolution of the Cuiabá deposit (Vial, 1980; Vieira, 1992; Toledo, 1997; Ribeiro-Rodrigues, 1998;Figure 18**).**

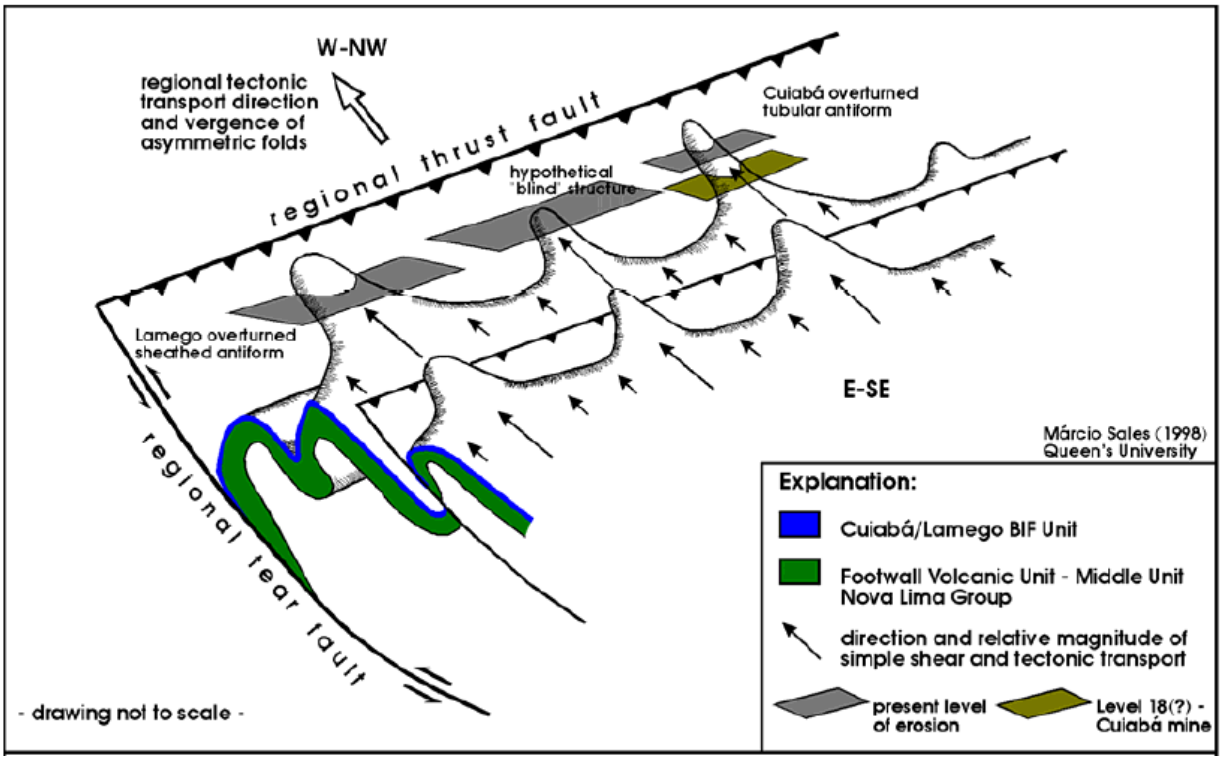

Figure 18. Structural sheath fold evolution model accordingly to Sales (1998) and Ribeiro Rodrigues (2007).

However, the arguments presented here contradict this previous hypothesis and reinforce the model of structural evolution by refolding:

i. Absence of sheath folds in the Cuiabá mine at outcrop scale during underground geological mapping.

ii. Presence of parasitic folds with linear (fold axes) and planar (plane-axial foliation) structures with constant values, dipping SE, forming a small stereographic distribution. Conical stereographic behaviors, distributed in circular shapes, are expected for sheath fold models.

iii. The presence of superposition of coaxial folds was observed on a mesoscopic scale, as observed in the W and Center-South domains.

iv. The intense shearing (which is one of the causes of sheath fold, according to Skjernaa, 1989) is contradicted by the presence of preserved magmatic (e.g., pillow lavas at metamafic units) and sedimentary structures (e.g., graded bedding or load casts in rhythmites).

Holcombe and Coughlin (2003) and Rankin (2006) also corroborate the evolution of the deposit model here proposed.

The structural evolution of the Cuiabá mine is divided into three phases of deformation as Figure 19. The structures referring to phases D1 and D2 are coaxial and possibly have a progressive behavior, considered inserted in the same tectonic event (Event 1). The structures of phase D1 were generated in the ductile regime, while those of phase D2 were generated in the ductile to the ductile-brittle regime. The structures referring to the D3 phase are non-coaxial, non-progressive concerning the previous phases, and were generated in a brittle-ductile regime, in another tectonic event (Event 2).

3.8.1. *Event 1 – Phase 1*

Phase 1 structures are locally characterized by a ductile deformation with tectonic transport from SW to NE, represented by closed and inclined folds with fold axis plunging to ESE and sinistral "S" vorticity (Figure 19A). The parallelism between stretching lineation and L1 indicates type "b" lineation (Sander, 1970, Ramsay, 1967, Sullivan, 2013), indicative of a regional hinge zone.

3.8.2. *Event 1 - Phase 2*

Phase 2 (Figure 19B) of the first recorded deformation event is characterized by a ductile to ductile-brittle deformation with tectonic transport from NE to SW, coaxial and progressively with phase

1. Tight and inclined folds represent this phase, with a fold axis plunging to ESE and dextral "Z" vorticity that refolds the layers already folded in phase 1, generating a hook-like geometry folding which consist in a "type-3 fold interference pattern" from Ramsay and Huber (1987). This phase presents local transposition, as observed in the rupture of the BIF layer in the Central-South Domain, and in the Central-North Domain, generating shear zones, characterized by highly developed S2 foliation, subparallel to the bedding. The parallelism between stretching lineation and L_2 indicates type "b" lineation (Sander, 1970, Ramsay, 1967, Sullivan, 2013), indicative of a regional hinge zone as well as the relationship between L_1 intersection and stretching lineations. S1 and S2 foliations are well observed at Central domain, being able to make analogies to the other structural domains to the point of understanding the structural framework.

3.8.3. *Event 2 - Phase 3*

Phase 3 (Figure 19C), which characterizes the second deformation event, and is characterized by a brittle-ductile convergent deformation of the "fold and thrust belt" type with tectonic transport from E to W, dipping to E. Crenulation cleavages and shear zones associated with the short flanks of the fold represent this phase. The oblique to orthogonal variation between fold axis and axial planes from this phase to preceding ones can generates dome-and-basin geometry folding, associated to a "type-1 fold interference pattern" from Ramsay and Huber (1987).

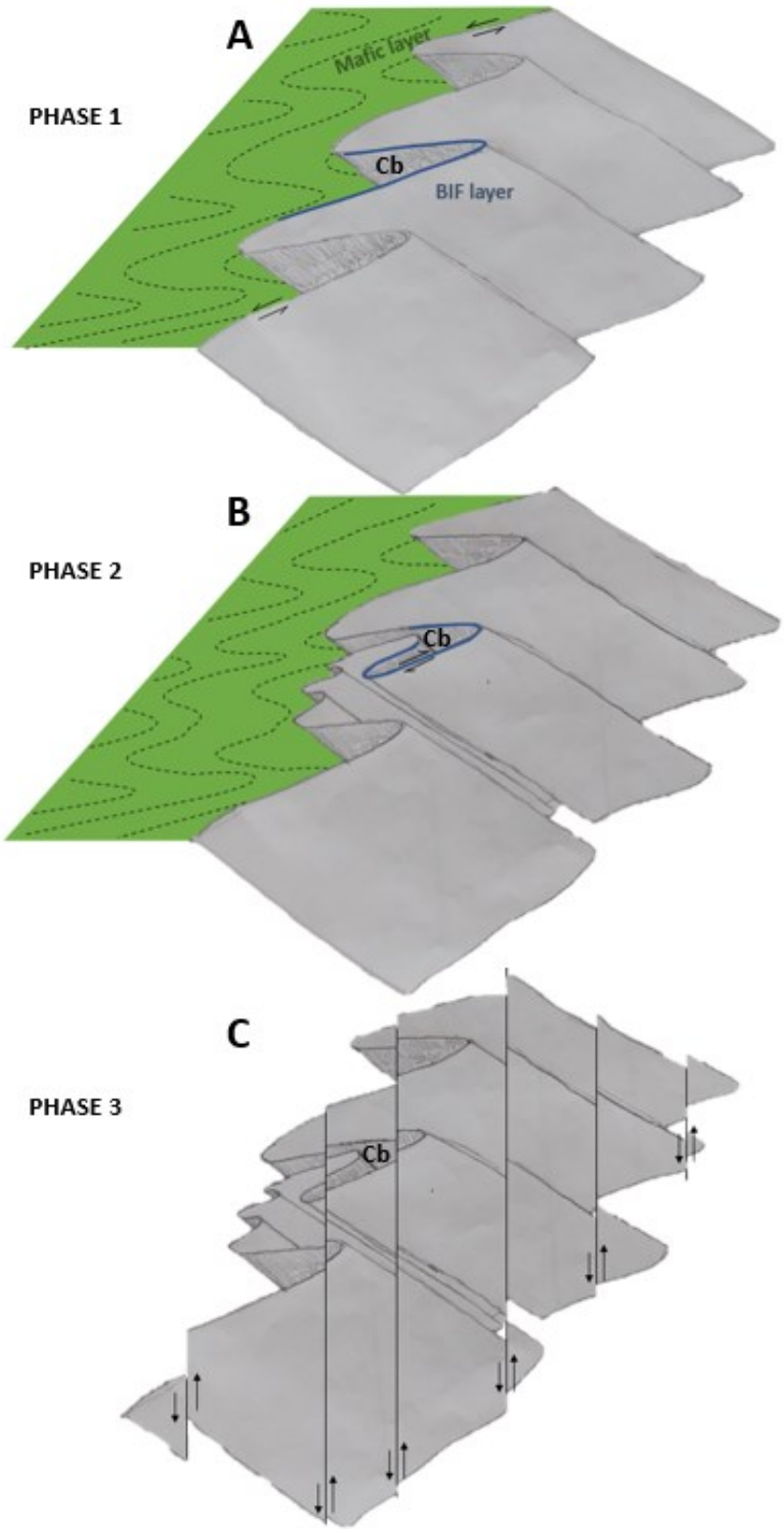

Figure 19. Synthesis of the structural evolution for the Cuiabá (CB) deposit.

A. Event 1 – Phase 1 with ductile strike-slip tectonic transport with ENE-WSW direction and counterclockwise vorticity.

B. Event 1 – Phase 2, with ductile to ductile-britle strike-slip tectonic transport with NE-SW direction and clockwise vorticity, generating "hook-like" geometry folding associated to "type 3-fold interference patterns" from Ramsay & Huber (1987).

C. Event 2 – Phase 3, with inverse tectonic transport with W vergence, with possible generation of local dome-and-basin folding associated to "type-1 fold interference pattern" from Ramsay & Huber (1987).

3.9. STRUCTURAL CONTROL ON ORE FORMATION

As mentioned above, the Cuiabá deposit has 11 ore bodies. Of this total, 7 are related to mineralization in the BIF, with a thickness between 1 and 15 meters (Canta Galo, Balancão, Galinheiro, Surucucú, Serrotinho, Fonte Grande, and Dom Domingos), and 4 orebodies are related to mineralization in quartz-sulfide schist at the metavolcanic rocks (Galinheiro Footwall, Viana, Baú and VQZ). In addition, the quartz vein mineralization is still in the detailing phase by the brownfields exploration team and is hosted in sulfide quartz-schist. The VQZ mineralization is present inside the Cuiabá nuclei, at the lower metabasalts just between normal and overturned limbs (Figure 7). The ore controlling structure is associated with the D1 and D2 phases. At D1 mineralization, there is a WNW-ESE trend with dip to SSE associated to S1 foliation and fold axis plunging to ESE. At D2 mineralization, there is a NE-SE trend dipping to SE and fold axis plunging to ESE. It is noteworthy that plunge from both phases decrease its plunge with depth, as can be seen at Figure 27.

The gold mineralization inside BIF and quartz veins at the Cuiabá deposit is directly associated with the presence of sulfides (Figure 20**Erro! Fonte de referência não encontrada.**). In this work, it is chosen to distinguish the generations of these mineral-ores. Macroscopically, 4 generations of sulfides can be observed in the Cuiabá deposit inside these rocks and are now described in ascending chronological order (Figure 22). All generations of sulfides, except the last, are mineralized into gold. Kresse et al. (2018) identified the main ore-stage pyrite types as Py2 and Py3.

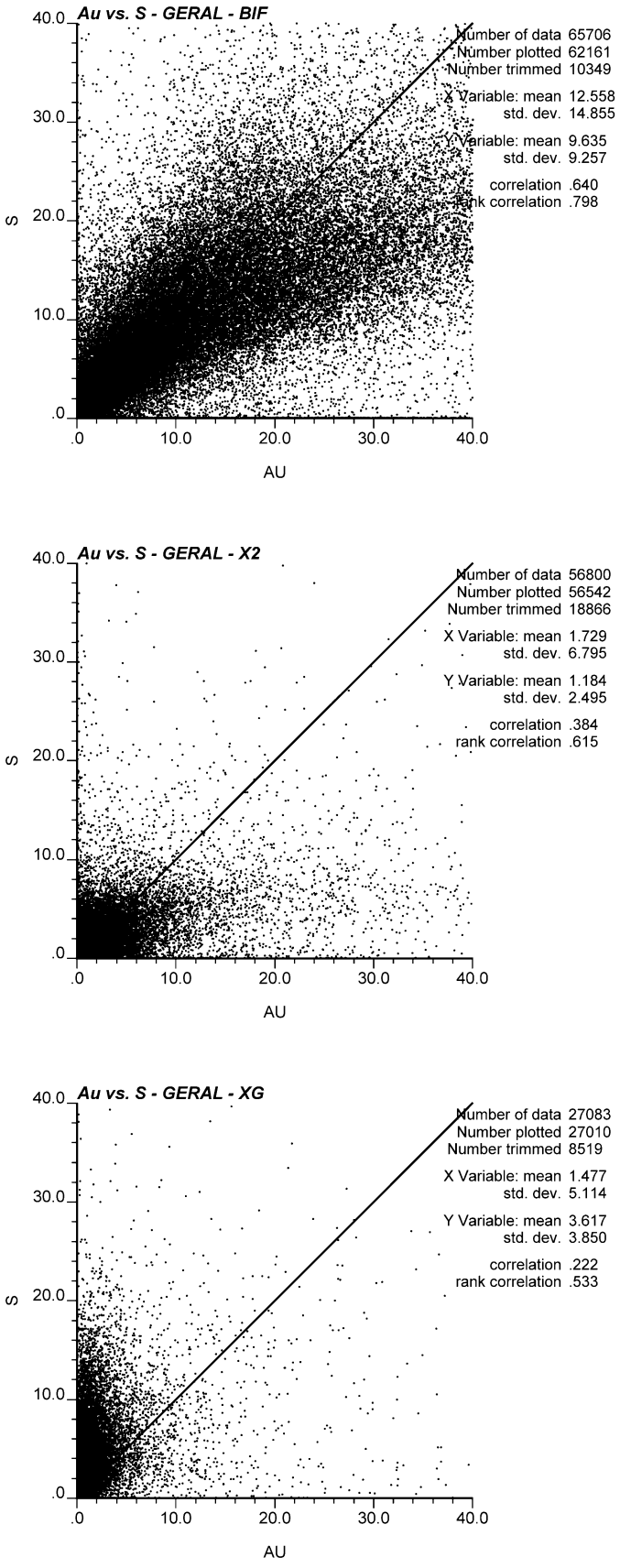

Figure 20. Au x S correlation charts for different lithologies. BIF – Banded Iron Formation; X2: metamafic schist; XG: carbonaceous schist. Data obtained from AngloGold Ashanti internal laboratory analysis (methodology of Au measurement is Fire Assay, while for S measurement is LECO).

3.9.1. *D1 sulfidation*

The D1 sulfidation (Figure 22) is observed in all structural domains of the deposit, especially in the Central, NE and E domains; but with a much smaller proportion compared to D2 syn-tectonic sulfidation. It is characterized inside BIF´s by millimeter to submillimeter bands of grained and massive pyrrhotite deformed in ductile regime by phase 1. The pyrrhotite of this generation is crystallized in the axial planes of D1 folds and is concordant to the BIF bedding along D1 limbs (domains NE and SE) and orthogonal to bedding in D1 hinge zones (domain E). Microscopic (submillimeter) crystals of euhedral arsenopyrite disposed inside pyrrhotite is observed at this stage. Inside quartz veins at metabasalts associated to D1 structural phase (usually smoky quartz veins), it is observed disseminated and deformed crystals of submillimeter pyrrothite and sporadic millimeter to subcentimeter subhedral sphalerite and galena deformed in a ductile regime and associated with veins containing quartz, ankerite, chlorite, and sericite.

The mineralization associated with the tectonic phase D1 is directly associated with pyrrhotitic "type-1" ore defined by Vieira (1988), with the presence of medium to coarse-grained gold (between 50 and 500μm) precipitated at the sulfide edges.

3.9.2. *D2 syn-tectonic sulfidation*

Subhedral pyrite bands with very fine grains characterize D2-syntectonic sulfidation (Figure 22. Hand sample (left) and microscopic scale (right) from different types of sulphidation observed at Cuiabá deposit. Note that D1 and D2 sulphidation are mineralized. D3 sulphidation has no gold observed.). The pyrites of this generation are mineralized into gold, corresponding to the main ore in the deposit. This type of mineralization is abundant and is observed in all domains but is quite prominent in the SW and NW domains. In places where there is not an abundance of this mineralization, "Christmas-tree" type hydrothermal replacement textures inside BIF are observed.

In the richest places, the great concentration of pyrite obliterates the primary features and possibly the early-tectonic D1 sulfide. In quartz veins at metabasalts, this sulfidation is disseminated in millimeter blasts of subhedral to euhedral pyrite as can be noticed inside Central domain (VQZ ore body). This mineralization can be associated with pyritic "type-2" ore defined by Vieira (1988) where gold was precipitated as inclusion in pyrite and is fine-grained (between 10 and 100μm).
It is locally noted the correspondence between the structural phases D1 and D2 and the relationship between sulfides pyrrhotite related to D1 axial planes and pyrite related to D2 (Figure 21). The D2 phase is associated with syn-D2 pyritic sulfidation along the axial planes of these folds.

3.9.3. *D2 late tectonic sulfidation*

Late tectonic D2 sulfidation (Figure 22) is characterized by subhedral to euhedral coarse-grained pyrite poikiloblasts with centimeter to subcentimeter size. Locally, this type of sulfidation is observed in BIF, especially in the NE and NW structural domains.

3.9.4. *D3 late tectonic sulfidation*

Late tectonic D3 sulfidation (Figure 22) is characterized by submetric to metric discordant milky quartz veins filling voids in D3 phase structures, containing very coarse sub-centimeter to centimeter-grained euhedral mineral aggregates, composed mainly of pyrite and pyrrhotite, in addition to accessory minerals, as chlorite and rutile. This association has no gold mineralization.

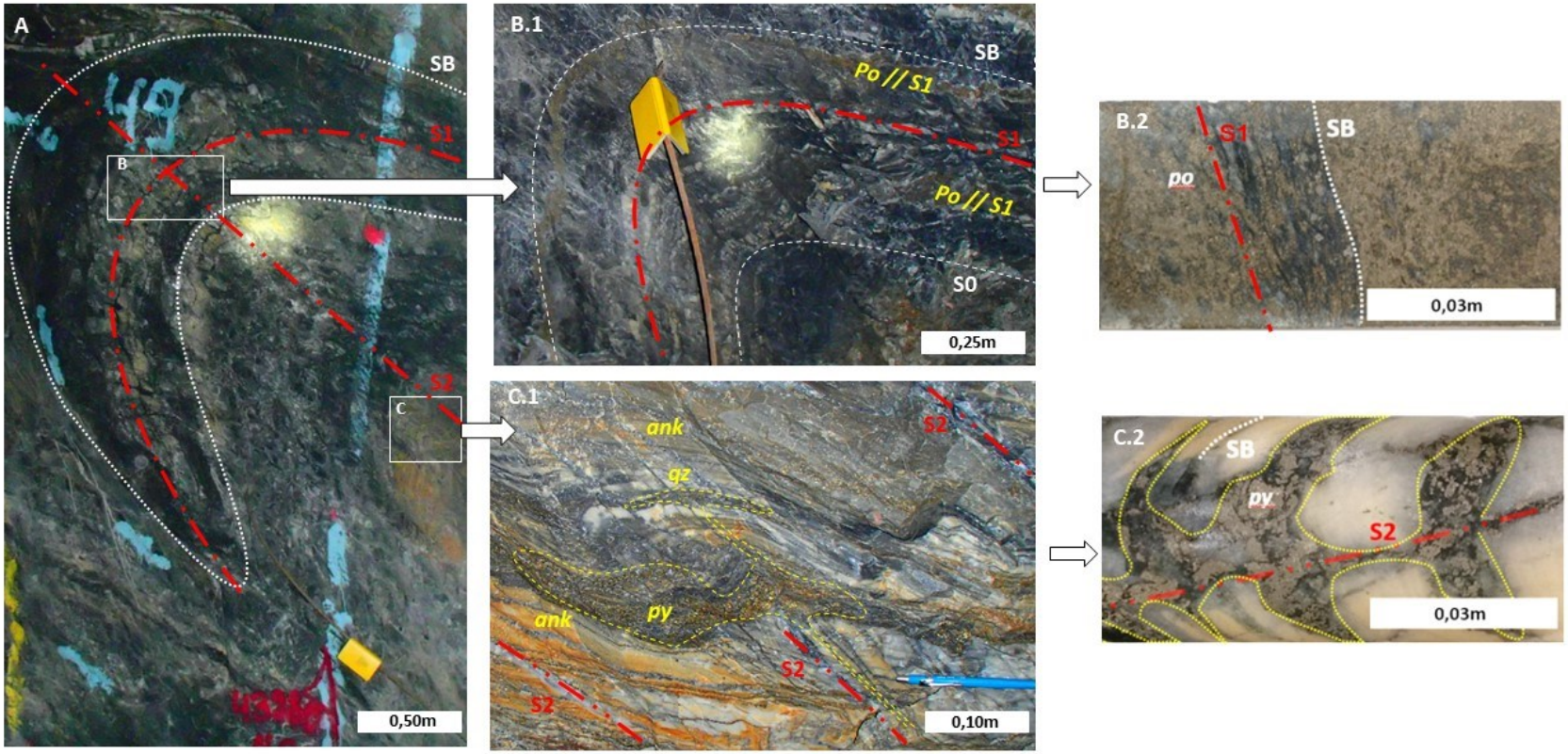

Figure 21. Correspondence between deformational phases and gold mineralization inside BIF. A. Overview of structural phases D1 and D2, where bedding (SB) is refolded and foliation S1 is folded by foliation S2; B. D1 pyrrhotitic (po) mineralization parallel to S1 axial plane foliation; C. Syn-D2 pyritic mineralization parallel to the S2 axial plane (replacement textures of carbonate bands (ank) by pyrite (py) are observed). The images were taken to L1 and L2 down-plunge view (to ESE). Level 11 GAL EXT orebody, structural domain W.

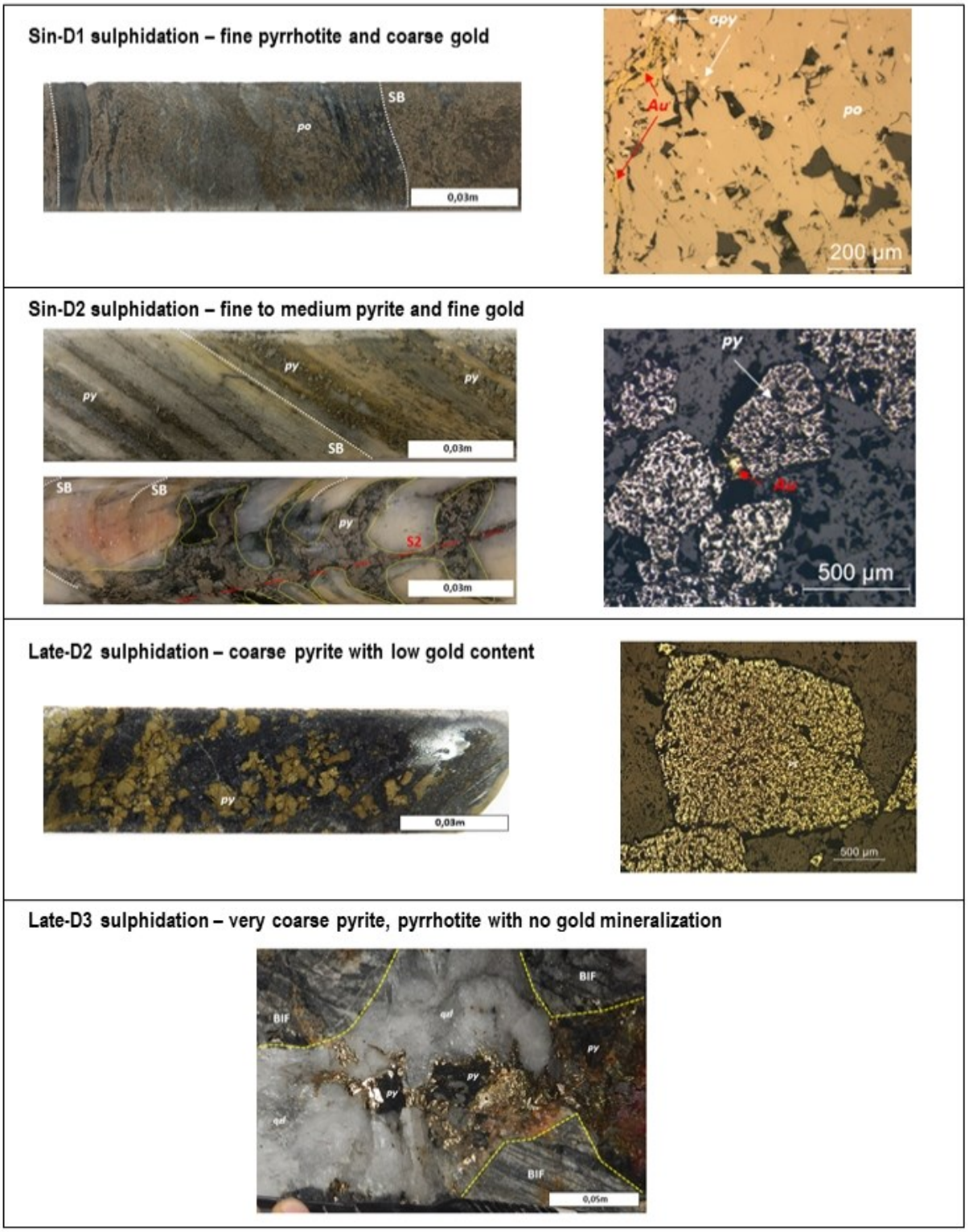

Figure 22. Hand sample (left) and microscopic scale (right) from different types of sulphidation observed at Cuiabá deposit. Note that D1 and D2 sulphidation are mineralized. D3 sulphidation has no gold observed.

3.9.5. *Structural implications for gold metallogenesis*

Based on the correlation between sulfide and deformation, mineralization at the Cuiabá mine is divided into 3 phases (Figure 23). The D1 tectonic phase mineralization is directly related to type 1 ore defined by Vieira (1988). It is characterized essentially by pyrrhotite with the presence of medium to coarse-grained gold precipitated at the sulfide edges. As it is observed to be concordant with the axial plane of D1 folds and is contained in the phase 1 foliation, a tectonic D1 generation is suggested. It is proposed that the pyrrhotite was formed under different physicochemical conditions from the later phase, in an environment with relatively low $\int O2$ and S, as shown in the diagram in Figure 24.

The D2 syn-tectonic mineralization is directly related to type 2 ore defined by Vieira (1988) and comes from fluids formed by an association of quartz, ankerite, chlorite, and sericite. This fluid percolated through the rock through openings in the axial plane of the D2 folds during small stages of tectonic quietude during the D2 deformation and that enabled the formation of substitution textures in the sideritic bands of the BIF's (Vieira, 1988, Lobato, 2001b). It is suspected that the fold interference with same asymmetry between phases D1 and D2 (S or Z-folds from D2 interfering S or Z-folds from D1, respectively) allows an increase in the gold content of the mineralization due to the amplification of the folds, as in the case of the boundary between the domains NE and E (Z-fold asymmetry from D1 amplified by Z-fold asymmetry from D2) and the NW domain (S-fold asymmetry from D1 amplified by S-fold asymmetry from D2). The gold at this stage was precipitated as inclusion in pyrite and is fine-grained.

The late-tectonic D2 sulfide is directly associated with mineralized zones with subhedral and coarse pyrites, with a lower presence of gold and a low correlation between this element and sulfur, quite observed in the NW and NE domains. McClay & Ellis (1983) describe a directly proportional

relationship between mineral growth and the increase in metamorphic grade, which is probably associated with this type of sulfide.

Table 3 summarizes the chronological relationship between mineralization and deformation structures.

Table 3 Chronological relationship between mineralization and deformation phases. Note the greater presence of gold in the syn-D2 tectonic phase, associated with pyrite and arsenopyrite.

Ore minerals x tectonic phases	TECTONIC PHASES								
	D1			D2			D3		
	EARLY	SIN	LATE	EARLY	SIN	LATE	EARLY	SIN	LATE
Pyrrhotite									
Pyrite									
Arsenopyrite			Needles		Aggregates				
Chalcopyrite									
Sphalerite									
Galena									
GOLD		50 - 500 µm			10 - 100 µm	<5 µm			

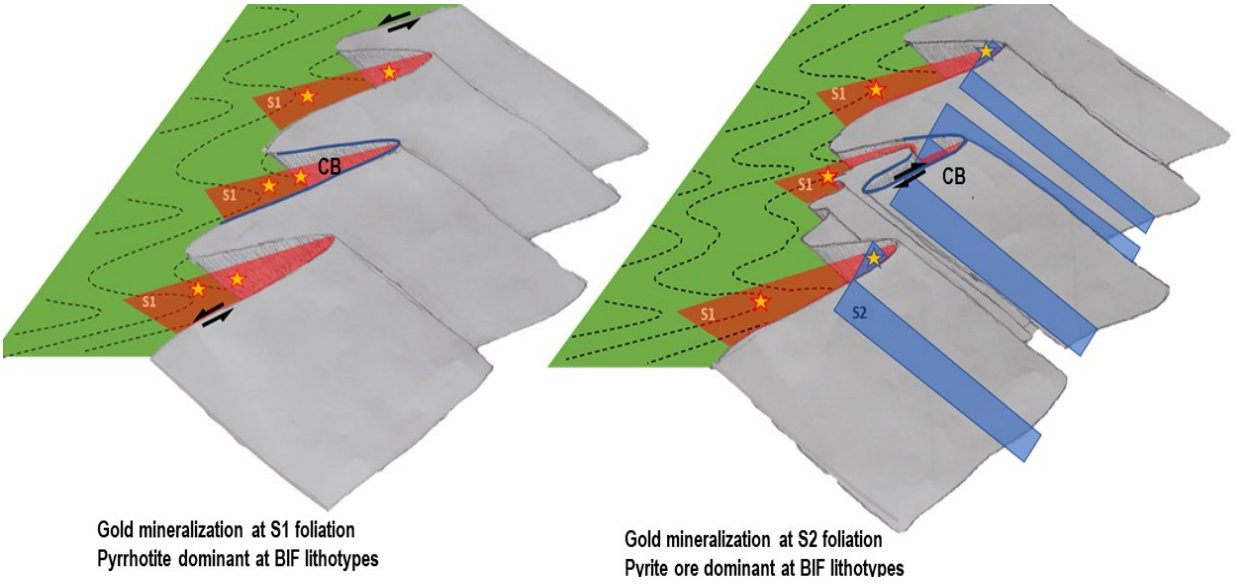

Figure 23. 3D schematic cartoon showing relationship from structural evolution and gold mineralization inside Cuiabá deposit (CB).

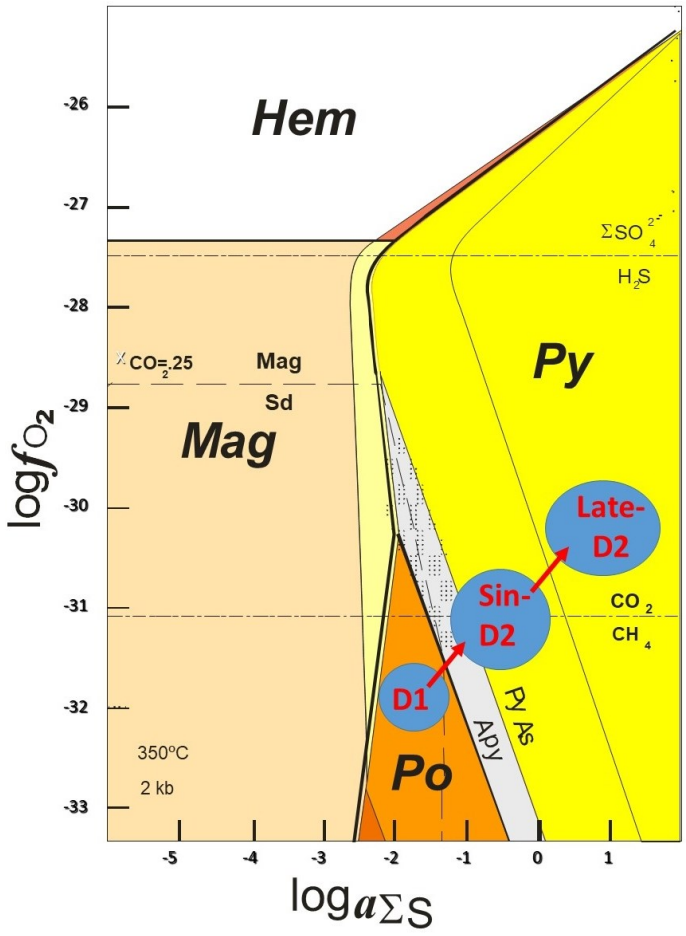

Figure 24. Diagram ∫S2 versus ∫O2 for sulfide formation in S-based complexes, for temperature of 350ºC and pressure of 2kb (extracted from Mikucki and Ridley, 1993). The formation of D1 pyrrhotitic ore would be associated with relatively low ∫O2 and S conditions in relation to syn and late-D2 pyritic ore.

3.10. DISCUSSION

Based on the deformational model proposed here for the Cuiabá gold deposit, some modifications are made concerning the known historical model. The continuity at the extreme W of the deposit, which refers to the extrapolation of BIF in the NW domain, has a strong tendency to connect with the Lamego deposit, located about 5km SW of Cuiabá.

The continuity to the extreme NW of the Cuiabá mine, referring to the extrapolation of BIF in the NE domain, was inferred from the hypothesis of structural evolution, not being observed in detail inside the Cuiabá deposit, probably due to some displacement of the layer due to the beginning of transposition.

3.10.1. *Structural geochronology hypothesis*

Albeit two mineralized structures are observed at the Cuiaba gold deposit (associated with D1 and D2 phases), it is not yet possible to determine their relative age. Although geochronological works are indicating the Archean age of mineralization (Silva, 2006; Lobato, 2001) and other works associating mineralized structures to a single and progressive event (Vieira, 2000), the hypothesis of a potential Paleoproterozoic age cannot be despised (Vieira, 2000). Thus, it is suggested to carry out geochronological analysis of the structures to confirm whether the relationship between D1 and D2 is progressive or not.

3.10.2. *New proposed model and lateral continuities*

After the structural characterization of phases and domains, the Cuiabá deposit structural model is proposed. It is related to a type-3 fold interference pattern from Ramsay & Huber (1987), with a hook-like geometry, which characterizes the first phase of deformation in the eastern portion of the Cuiabá deposit (associated with the NE, E, and SE domains; Figure 13), refolded by the western portion in the second phase (represented by the SW, W, and NW domains; Figure 13). Thus, the model of tectonic evolution by coaxial refolding for the Cuiabá deposit is more satisfactory than tubular or sheath fold. Continuity of the main reef (the BIF layer) outside the deposit limits is proposed using as reference the Center-North domain where the BIF layer in the overturned limb splits into two distinct paths. While the BIF layer of the NW domain is folded and continues to SW towards the Lamego gold deposit (5km away from Cuiabá; Figure 25) the NE domain BIF layer keeps in the NE direction toward the Descoberto gold target (2km away from Cuiabá). In addition, ENE-WSW trend related to D1 foliation can be another secondary exploration target.

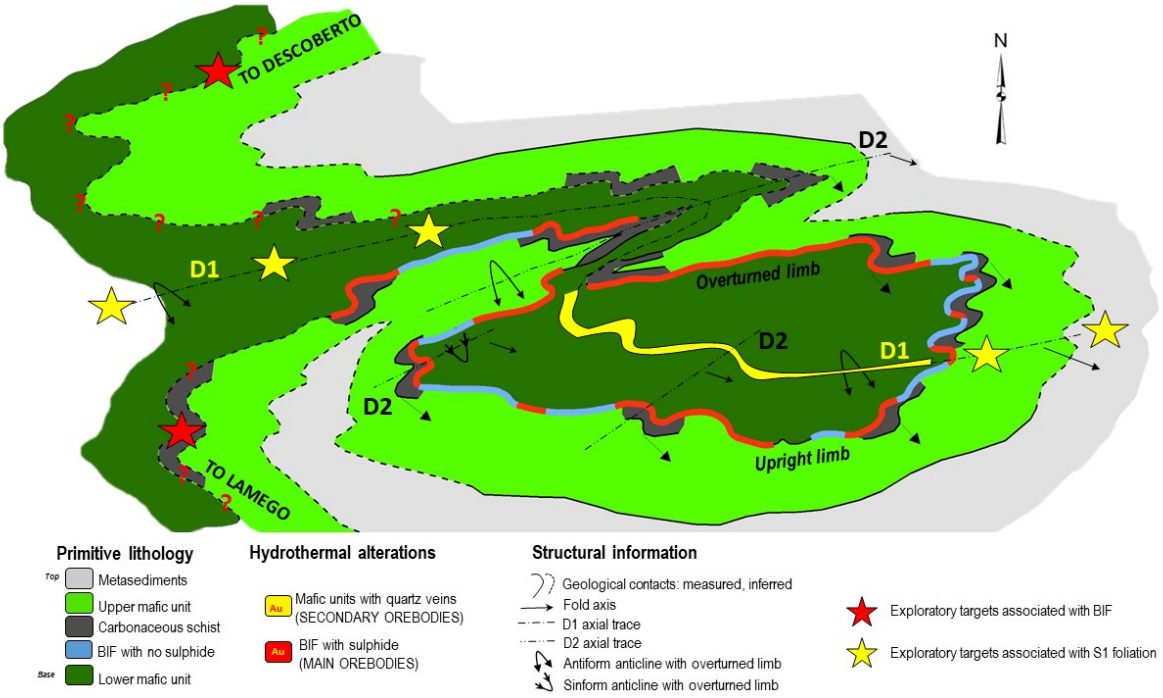

Figure 25. Proposed continuity of the main mineralized guide-horizon (BIF) outside of the Cuiabá Deposit (Fernandes et al., 2016). The continuity to the west end of the deposit has a strong tendency to connect with the Lamego gold deposit, located 5km SW of Cuiabá. In addition, D1 foliation can be a potential exploration target at ENE-WSW trend.

The continuity, and similarities, of the layers and structures, outside the deposit limits, is suggested using as reference Cuiabá, Lamego, Raposos, Morro Velho, Faria, Bicalho, Descoberto, Córrego dos Sítio 1 and Córrego dos Sítio 2 deposits (Figure 26, Table 4).

Finally, the post mineralized structures associated to D3 phase form fold and thrust belts orthogonal to previous-and-mineralized structures, with local displacement by crenulation cleavage. Due to its orthogonality from different phases, it is possible to form local dome-and-basin refolding outcrops, characterized by type-1 fold interference pattern from Ramsay & Huber (1987).

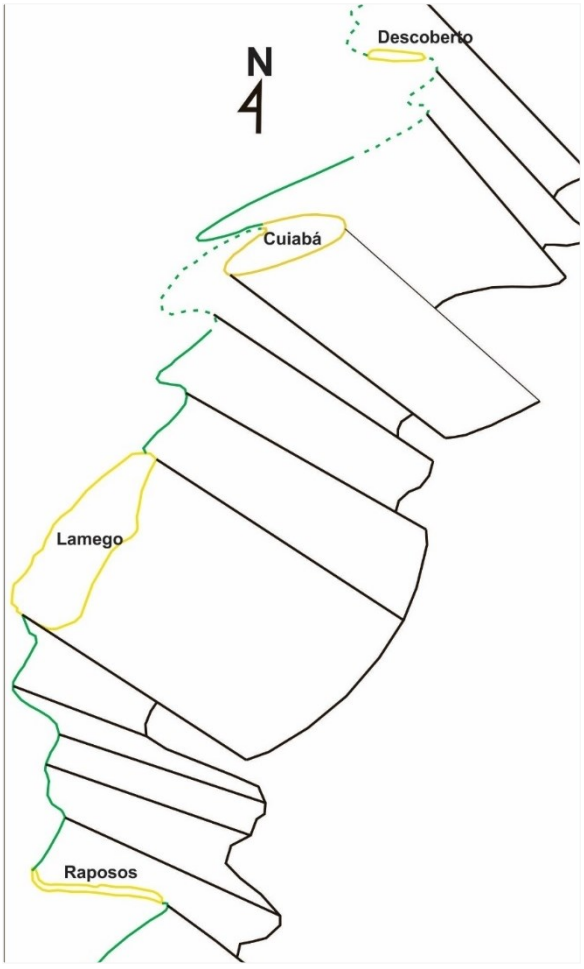

Figure 26. Suggested continuity of layers and structures in the Descoberto, Cuiabá, Lamego and Raposos deposits region.

3.10.3. *Similarities with other deposits inside QF*

3.10.3.1. *Parallelism of fold axis and stretching lineation*

All gold deposits from RVGB (Table 4) have their stretching lineation parallel to the fold axis, where gold mineralization is located (Ladeira, 1991; Toledo, 1997; Ribeiro-Rodrigues, 1998; Vieira, 2000; Lobato et al., 2001; Baltazar and Zucchetti, 2007; Vial, 2007; Roncato et al., 2015; Martins et al., 2016; Baltazar and Lobato, 2020 and Ferraz da Costa et al., 2022). The same structural features described above are consistent for iron ore deposits at Minas Supergroup (Endo et al., 2005, Piassa, 2018, Castro et al., 2020). This fact is a strong indicative of tectonic environment where deformation ellipsoid is predominantly prolate.

Several structural and tectonic models explain the deformation mechanisms where these structures are parallel (e.g. Cobbold and Quinquis 1980, Ridley, 1986, Skjernaa, 1989, Alsop and Holdsworth 2004, Alsop and Holdsworth 2006). However, the presence of these mechanisms is not observed in the Cuiabá deposit such as: fold axis with stereographic conical arrangement, intense shearing obliterating primary structures and formation of sheath folds.

Thus, it is suggested the parallelism between linear elements was originally formed in this way, concomitant to a constrictional deformation system, with the stretching lineation being associated with a "b" type lineation (Ramsay, 1967; Sander, 1970 and Sullivan, 2013). This observation is in line with the regional geology of the QF where there are no reports of sheath folds or intense shearing mechanisms responsible for rotation or parallelism of these structures (Almeida, 2002; Endo, 2005; Piassa, 2018 and Castro, et al., 2020). Thus, it is likely that mineral stretching lineation trend in the Cuiabá deposit would not represent the tectonic transport direction.

3.10.3.2. *Fold interference pattern*

Type-3 fold interference pattern (Ramsay and Huber, 1987), as aforementioned, is observed in many deposits from RVGB (Table 4), such as Faria, Raposos, and Morro Velho gold deposits (Vieira, 2000; Baltazar and Lobato, 2020), besides Lamego deposit as well (Martins, 2016). One visible feature is observed in the maps from Lamego (Martins, 2016), which is related to a synform-anticline located at the SW side of the deposit (Cabeça de Pedra orebody). This structure must be observed only in refolded terrains and is analogue to the synform-anticline observed in the western domain at the Cuiabá deposit (Galinheiro Extensão ore body).

Table 4. Similarities from gold deposits in Rio das Velhas Greenstone Belt (RVGB).

SIMILARITIES FROM GOLD DEPOSITS IN RVGB					
GOLD DEPOSITS	**MAIN FOLD AXIS PLUNGE**	**STRETCHING LINEATION**	**ORE PLUNGE**	**FOLD INTERFERENCE PATTERN OBSERVED?**	**DEPTH (m)**
CUIABA	ESE	Parallel to main fold axis	Parallel to main fold axis	Type-3	1450
LAMEGO	ESE			Type-3	750
RAPOSOS	ESE			Type-3	1500
MORRO VELHO	ESE			Type-3	2400
FARIA	ESE to ENE			Type-3	500
BICALHO	ESE			Not observed yet	600
CÓRREGO DO SÍTIO 1	NE			Type-3	500
CÓRREGO DO SÍTIO 2 (SÃO BENTO DEPOSIT)	ESE (POSSIBILITY TO NE?)			Not observed yet	1200

3.10.3.3. *Fold axis flattening in higher depths*

It is observed in deeper deposits (Cuiabá, Lamego, Raposos, Morro Velho, Faria, Bicalho, Descoberto, Córrego do Sítio 1 and Córrego dos Sítio 2 deposits) that the main fold axis related to gold mineralisation is steeper in lower depths (plunging over than 25º above 750m deep) and smoothed in higher depths (plunging lower than 25º below 750m deep; **Figure 27**). In the same context, all gold deposits from RVGB have ore plunging to E (Table 4), usually to ESE, with exception of the Córrego do Sítio Deposit, where ore and fold axis plunge to NE (Ladeira, 1991; Vieira, 2000; Lobato et al., 2001; Baltazar and Zucchetti, 2007; Vial, 2007; Roncato et al., 2015; Martins et al., 2016; Baltazar and Lobato, 2020). One possible hypothesis for this flattening in depth is regarded to younger D3 crenulation cleavage local interference at older rocks, creating a series of small and local thrust systems (Figure 19.C). As GBRV gold deposits deepen to E, they would get closer to the Neoproterozoic Araçuaí belt (Almeida, 1977), where D3 crenulation cleavage tend to be more intense and abundant.

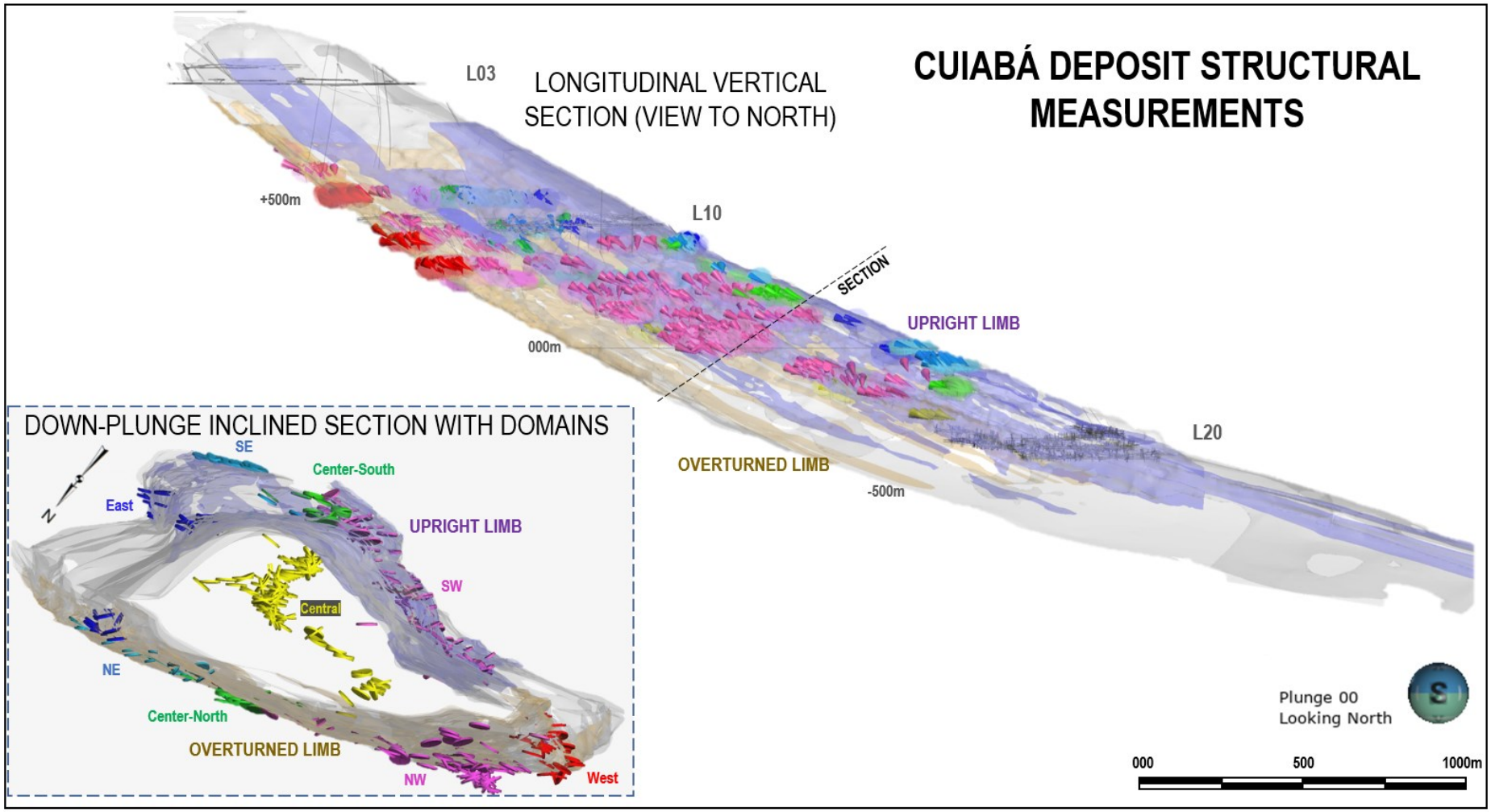

Figure 27. Longitudinal vertical section (view to north) and down-plunge inclined section with domains of Cuiabá deposit.

3.11. CONCLUSION

The data presented provide some structural similarities on regional and deposit scale models, where the Cuiabá is representative of the folded BIF-hosted gold deposits. Based on the integration of the detailed geological mapping and structural analysis of the Cuiabá deposit, the following aspects are concluded below.

The structural geology of the deposit is characterized by 3 deformational phases possibly related to 2 tectonic events. The first event has two progressive ductile deformational phases (D1 and D2), with a NE-SW strike-slip convergent transport direction, generation of coaxial and hook-like cylindrical geometry fold associated with a "type-3" refolding patterns (Ramsay and Huber, 1987) with fold axis plunging to ESE, being the main contributor for the structural framework and gold mineralization in the deposit. The second event is a brittle-ductile to brittle deformational phase (D3) with a W-verging convergent tectonic direction, with no gold mineralization associated and possibly associated with the Brasiliano Pan-African orogeny at the edge of the São Francisco Craton as confirmed by other works (Endo et al., 2005, Martins et al. 2016, Baltazar & Lobato, 2020; Castro et al. 2020; Endo et al., 2020 and Gonçalves Dias et al., 2022).

Gold mineralization is associated with quartz veins and sericite zones at metamafic units with low sulphide and sulfide-rich bearing zones at BIF layers, both associated to hydrothermal fluid introduction through D1 and D2 axial-plane foliation. Phase D1 is pyrrhotite-associated mineralization, with coarse gold presence (ranging from 50 to 500 micrometers). D2 phase has pyrite-associated mineralization with fine gold, ranging from 10 to 100 micrometers. There is no gold in phase D3, although it has late-tectonic sulphide formation. It is suggested to carry out geochronological analysis of the types of sulphide to corroborate the relative age the 2 main phases of mineralization associated with different phases of tectonic deformation.

Even having been reported in previous works (Vieira, 1992, Toledo, 1997, Ribeiro-Rodrigues, 1998, Ribeiro-Rodrigues, 2007), there are no field elements that prove the presence of tubular or sheath folds in the Cuiabá deposit. These arguments are reinforced by (i) not observation of tubular folds or sheath folds during geological field work, (ii) persistence of mineralized fold axis plunging to ESE at stereographic projections, (iii) the presence of coaxial refolding at mesoscopic scale and (iv) the presence of primary structures (e.g. pillow lavas at metamafic units) and sedimentary structures inside the deposit indicating the absence of intense shearing, which is one of the causes of sheath fold. In addition, the mineral stretching lineation, is a “b” type lineation and is associated with constriction environments (Ramsay, 1967; Sander, 1970 and Sullivan, 2013), therefore it is likely that its trend would not represent the tectonic transport direction.

Fold interference patterns associated to deposit morphology suggests SW and N prospective targets, with strong possibility of structural connection amongst other gold deposits, such as Lamego and Descoberto targets. In addition, ENE-WSW S1 foliation can be another secondary exploration target.

4. CONSIDERAÇÕES FINAIS

4.1. MECANISMOS DE DEFORMAÇÃO ASSOCIADO AO DEPÓSITO

A partir do mapeamento geológico no depósito Cuiabá, é possível estabelecer algumas considerações a respeito dos mecanismos de deformação associados localmente.

4.1.1. Paralelismo entre o eixo de dobramento e a lineação mineral das fases 1 e 2

Observa-se um paralelismo entre o eixo de dobramento, lineação de interseção e lineação mineral no depósito Cuiabá, onde ambos possuem caimento para ESE, sempre associado a foliação plano-axial com mergulho para SE. Embora essa relação não tenha sido observada nesse trabalho, trabalhos anteriores evidenciam esse paralelismo neste depósito (Toledo, 1997; Ribeiro-Rodrigues, 1998; Ferraz da Costa *et al.*, 2022) e em outros depósitos auríferos do QF (Ladeira, 1991; Vieira, 2000; Lobato *et al.,* 2001; Baltazar e Zucchetti, 2007; Vial, 2007; Roncato *et al.,* 2015; Martins *et al.,* 2016; Baltazar e Lobato, 2020) indicando um ambiente tectônico onde o elipsoide de deformação é predominantemente prolato.

Diversos modelos estruturais e tectônicos explicam o mecanismo de deformação associado ao processo com que essas estruturas se paralelizam (Cobbold e Quinquis 1980, Ridley, 1986, Skjernaa, 1989, Alsop e Holdsworth 2004, Alsop e Holdsworth 2006). Entretanto, não se observa no depósito Cuiabá a presença desses mecanismos: disposição cônica no estereograma dos eixos de dobramentos principais, eixos de dobras com direções intermediárias a direção final paralelizada e nem cisalhamento intenso a ponto de se obliterar as estruturas primárias e formar dobras em bainha.

Assim, propõe-se que o paralelismo entre os elementos lineares das fases mineralizadas 1 e 2 tenha sido formado originalmente desse modo, concomitante a um sistema de deformação

constricional, sendo a lineação mineral associada a uma lineação do tipo “b” (Sander, 1970; Ramsay, 1967; Sullivan, 2013). Esta observação está de acordo com a geologia regional do Quadrilátero Ferrífero onde não há relatos de dobras em bainha ou mecanismos de cisalhamento intenso que pudessem promover a rotação e paralelismo durante o processo de formação dessas estruturas (Almeida *et al.,* 2002, Endo *et al.,* 2005, Piassa *et al.,* 2018, Castro *et al.,* 2020 e Endo *et al.,* 2020). Desta forma, é bem provável que a direção de estiramento mineral no depósito Cuiabá não represente a direção do transporte tectônico.

4.1.2. Modelo tectônico para o depósito em contexto de um sistema convergente do tipo *strike-slip* associado a eixo de dobramentos com caimento para ESE

Assumindo-se a premissa acima discutida, que as dobras não foram rotacionadas por mecanismos anteriormente explicados é possível dessa forma analisar o transporte tectônico através da análise da estrutura em seu correto plano de simetria (Cowan, 2016a) ou plano de verdadeira grandeza. O transporte tectônico de uma zona de convergência deve ser concomitantemente contido no plano AC da estrutura (Figura 3) e possuir eixo de transporte sub-horizontal (caso contrário teríamos estruturas extensionais). Desta forma, o correto plano de simetria da estrutura de Cuiabá é um plano de direção NNE-SSW com mergulho de alto ângulo para WNW (Figura 28). Sendo assim, sugere-se que o transporte tectônico do depósito Cuiabá tenha ocorrido de forma sub-horizontal ao longo deste plano indicando um sistema convergente do tipo *strike-slip* e com direção NNE-SSW.

Desta forma, o modelo geológico é aderente às observações em campo deste trabalho e de Fernandes *et al.* (2016), conforme a metodologia científica proposta por Feynman (1964) e reforçada em Cowan (2016b). Nota-se também que a direção de transporte tectônico definida neste

trabalho é similar ao proposto por Almeida *(*2004), Endo *et al. (*2005), Castro *et al.,* (2020) e Endo *et al.* (2020).

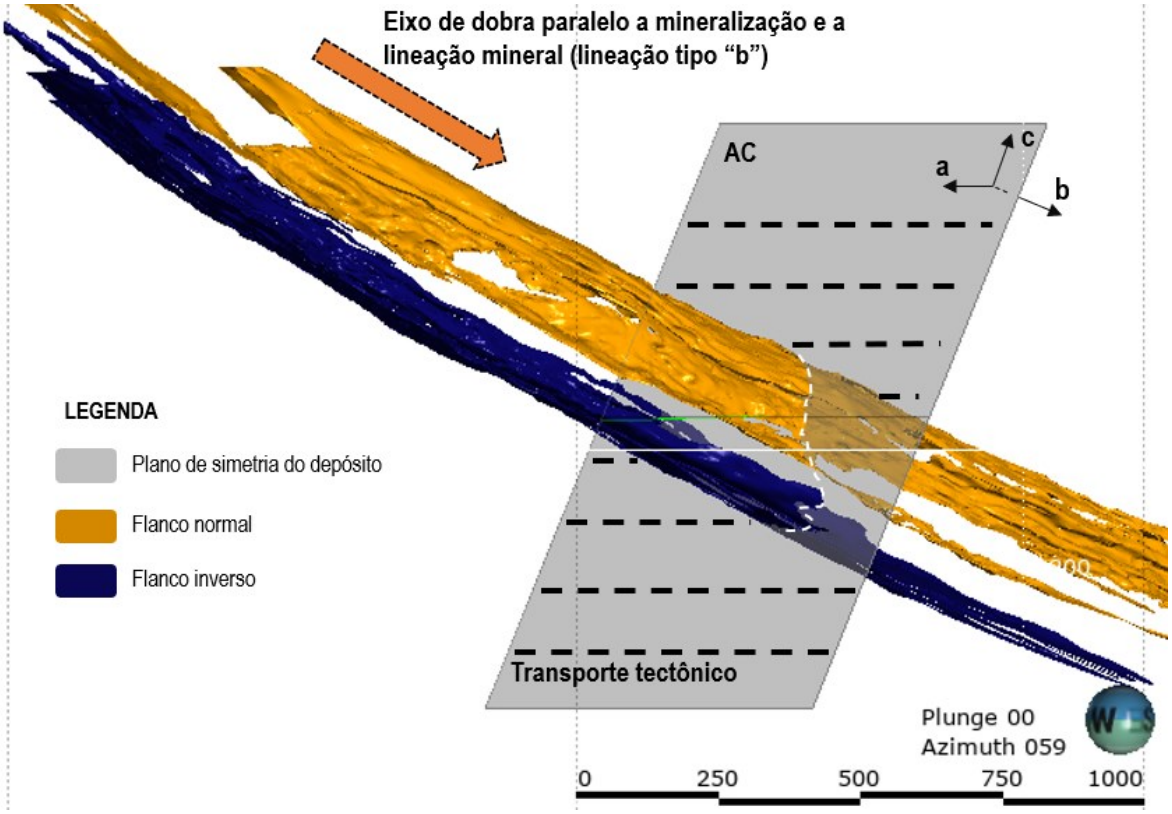

Figura 28. Plano de simetria (AC) para o depósito Cuiabá com direção NE-SW e mergulho para NW (visada para ENE). Esta superfície representa o plano de movimento para o depósito Cuiabá conforme a metodologia descrita em Cowan (2016a) e Ramsay e Huber (1987). Considerando que a tectônica convergente possui o tensor principal de deformação sub-horizontal e contido no plano de movimento, é esperado que a direção de transporte esteja subparalela ao vetor $\vec{a}$, com direção NE-SW, associado a um sistema tectônico convergente do tipo *strike-slip.*

4.2. CONCLUSÕES GERAIS

Com base na integração do mapeamento geológico de detalhe e a análise estrutural do depósito Cuiabá, conclui-se os seguintes aspectos abaixo.

- A geologia estrutural do depósito é caracterizada por 3 fases deformacionais relacionadas a 2 eventos tectônicos. O primeiro evento possui duas fases deformacionais

progressivas dúcteis (D1 e D2), com tectônica convergente do tipo *strike-slip* e direção de transporte tectônico NNE-SSW, com geração de padrões de interferência de dobras coaxiais associadas a padrões de redobramentos do tipo 3 de Ramsay e Huber (1987) com geometria cilíndrica e caimento de eixo para ESE, sendo este evento o agente formador da estrutura principal e da mineralização aurífera no depósito. O segundo evento possui uma fase deformacional rúptil-dúctil a rúptil (D3) com tectônica inversa e vergência para W, não mineralizado em ouro e sendo associado possivelmente à tectônica brasiliana na borda do Cráton São Francisco.

- A mineralização aurífera está associada a veios de quartzo e zonas de sericita em unidades metamáficas com baixo teor de sulfetos e zonas ricas em sulfetos nas camadas de BIF, ambas associadas à introdução de fluidos hidrotermais através da foliação plano-axial das fases D1 e D2. A fase D1 é uma mineralização associada à pirrotita, com presença de ouro grosso (variando de 50 a 500 μm). A fase D2 possui mineralização associada à pirita com ouro fino, variando de 10 a 100 μm. Não há ouro na fase D3, embora tenha formação de sulfeto tectônico tardio.

- Mesmo tendo sido reportado em trabalhos anteriores, não há elementos em campo que comprovem a presença de dobras em bainha no depósito Cuiabá. Além disso, a lineação de estiramento mineral por ser uma lineação do tipo “b”, associada a ambientes constricionais, não corresponde portanto, à direção de transporte tectônico, sendo ortogonal a este movimento.

4.3. PERSPECTIVAS EXPLORATÓRIAS FUTURAS

Com base no modelo deformacional proposto para a mina Cuiabá, é proposta uma nova etapa de trabalho para se confirmar a continuidade do principal horizonte-guia mineralizado (BIF), conforme **Erro! Fonte de referência não encontrada.**.

A continuidade a extremo W da mina Cuiabá desta camada (que se refere a extrapolação da BIF no domínio NW) possui forte tendência de conexão com a mina Lamego, cujo núcleo está distante 7km a SW de Cuiabá.

A continuidade a extremo NW da mina Cuiabá desta camada (referindo-se à extrapolação da BIF no domínio NE) foi inferida a partir da hipótese de evolução estrutural, não sendo observado com detalhe dentro da mina Cuiabá (provavelmente devido a algum rompimento da camada devido à início de transposição). Caso ela realmente exista, possui forte tendência de continuidade estrutural para N da mina, com provável conexão ao alvo Descoberto.

Para avaliar a continuidade destas duas camadas-guia, sugere-se a seguir os procedimentos exploratórios abaixo:

(i) Estudos petrofísicos em afloramentos conhecidos (de preferência dentro da mina) para se conhecer o comportamento geofísico de diferentes litologias com intuito de se obter uma base de dados confiável durante o levantamento geofísico semi-regional;

(ii) Geofísica de detalhe (escala 1:2.000) ao redor das minas Cuiabá, Lamego e a norte, que facilite correlacionar com as camadas e estruturas geológicas de maneira confiável e em 3D;

(iii) Amostragem de solo de detalhe (escala 1:2.000) e mapeamento geológico nas anomalias geofísicas. Muito importante a utilização de levantamento estrutural e topológico idêntico a este trabalho;

(iv) Amostragem de trincheira nas anomalias de solo mais pronunciadas;

(v) Sondagem diamantada nas trincheiras com resultados positivos. Os furos devem ser realizados na capa (*hanging-wall*) da anomalia e sempre ortogonais ao plano da foliação associada a mineralização principal.

4.4. LACUNAS NO CONHECIMENTO GEOLÓGICO

Sugere-se que trabalhos acadêmicos futuros sejam realizados com o intuito de se aumentar ainda mais o conhecimento geológico da mineralização aurífera ao redor deste depósito, tais como:

(i) Efetuar a geocronologia das estruturas planares mineralizadas (S1 e S2) em Cuiabá com o intuito de se confirmar se a mineralização é apenas de idade arqueana ou se há indícios de fluidos mineralizantes posteriores associados ao paleproterozoico.

(ii) Executar um trabalho de entendimento geológico estrutural para o depósito Lamego e Descoberto, visando corroborar a analogia com a hipótese de evolução estrutural de Cuiabá proposta neste trabalho e perspectivas exploratórias de conexão entre ambos, considerando que os mecanismos de evolução estrutural sejam semelhantes. Embora haja trabalhos no depósito de Lamego (*e.g.* Martins, *et al.,* 2016) algumas questões importantes ainda permanecem sem resposta tais como: (1) o mecanismo de deformação para geração de dobramentos, (2) a maneira como sua geometria cilíndrica foi formada e (3) o possível local de abertura do horizonte principal (BIF) para além dos domínios do depósito.

5. REFERÊNCIAS

Alkmim, F.F., Marshak, S. 1998. Transamazonian orogeny in the Southern São Francisco Craton region, Minas Gerais, Brazil: evidence for Paleoproterozoic collision and collapse in Quadrilátero Ferrífero. Precambrian Research, 90, 29-58.

Almeida, F.F.M. 1977. O Cráton do São Francisco. Revista Brasileira de Geociências, 7: 349-364.

Almeida L. G., Endo I., Fonseca M. A. 2002. Sistema de nappes na porção meridional do Quadrilátero Ferrífero, MG. In: SBG, Congresso Brasileiro de Geologia, 41, João Pessoa, Anais, p. 615.

Almeida, L. G. 2004. Estratigrafia e geologia estrutural da porção central do Sinclinal Dom Bosco, Quadrilátero Ferrífero, Minas Gerais. Universidade Federal de Ouro Preto, M.Sc. Thesis 117 p.

Alsop, G.I., Holdsworth, R.E. 2004. The geometry and topology of natural sheath folds: a new tool for structural analysis. Journal of Structural Geology 26, 1561-1589.

Alsop, G.I. & Holdsworth, R.E. 2006. Sheath folds as discriminators of bulk strain type. Journal of Structural Geology. 28, 1588-1606.

AngloGold Ashanti 2021. AngloGold Ashanti South America. Internal technical report.

Araújo, J.C.S. 2018. Modelo deposicional das formações ferríferas bandadas hospedeiras de ouro no greenstone belt arqueano Rio das Velhas, Quadrilátero Ferrífero, com base em geoquímica e análises in situ de magnetita por ablação a laser via ICP-MS. Dissertação de Mestrado. Universidade Federal de Minas Gerais, Belo Horizonte, Brazil, pp. 183.

Araújo, J.C.S; Lobato, L.M. 2019. Depositional model for banded iron formation host to gold in the Archean Rio das Velhas greenstone belt, Brazil, based on geochemistry and LA-ICPMS magnetite analyses. Journal of South American Earth Sciences 94, 102205.

Baltazar, O.F., Lobato, L. M. 2020. Structural Evolution of the Rio das Velhas Greenstone Belt, Quadrilátero Ferrífero: Influence of Proterozoic Orogenies on its Western Archean Gold Deposits. Minerals, 2020, 10, 983.

Baltazar O.F., Zucchetti M. 2007. Lithofacies associations and structural evolution of the Archean Rio das Velhas greenstone belt, Quadrilátero Ferrífero, Brazil: a review of the setting of gold deposits. Ore Geology Reviews 32, 471-499.

Bouma, A.H. 1962. Sedimentology of Some Flysch Deposits: A Graphic Approach to Facies Interpretation. Elsevier, Amsterdam, 168 p.

Castro, P.T.A., Endo, I., Gandini, A. L. 2020. Quadrilátero Ferrífero: avanços do conhecimento nos últimos 50 anos. 480 p. il. 3i Editora. Belo Horizonte. ISBN 978-65-990542-8-0. www.qfe2050.ufop.br

Chemale Jr, F., Rosière, C.A., Endo, I. 1994. The tectonic evolution of the Quadrilfitero Ferrifero, Minas Gerais, Brazil. Precambrian Research 65, 25-54.

Cobbold, P.R., Quinquis, H. 1980. Development of sheath folds in shear regimes. Journal of Structural Geology 2, 119-126.

Costa, M.N.S. 2001. Estudo dos isótopos de carbono e oxigênio e caracterização petrográfica em corpos de minério da mina Cuiabá. Quadrilátero Ferrífero, Minas Gerais. Dissertação de Mestrado, IGC/UFMG.

Cowan, J. 2014. 'X-ray Plunge Projection'— Understanding Structural Geology from Grade Data. AusIMM Monograph 30: Mineral Resource and Ore Reserve Estimation — The AusIMM Guide to Good Practice, second edition, p. 207-220.

Cowan, J. 2016a. Why I Give Geological Cross Sections the cold shoulder. In: http://www.orefind.com/blog/orefind_blog/2016/05/06/why-i-give-geological-cross-sections-the-cold-shoulder

Cowan, J. 2016b. If Richard Feynman was a geologist… In: http:// www.orefind.com/blog/orefind_blog/2016/09/25/if-richard-feynman-was-a-geologist-

Cowan, J. 2017. The fundamental reason why your geological models may be completely wrong. In: https://www.linkedin.com/pulse/fundamental-reason-why-your-geological-models-maybe-completely-cowan/

Cowan, J. 2018. Structural Geology—a forgotten discipline in mineral exploration. In: https://www.linkedin.com/pulse/structural-geologya-forgotten-discipline-mineral-jun-cowan

Dorr II, J.V., Gair, J.E., Pomerene, J.B., Rynearson, G.A. 1957. Revisão da estratigrafia pré-cambriana do Quadrilátero Ferrífero, Brasil. Departamento Nacional da Produção Mineral, Divisão de Fomento da Produção Mineral, Avulso, vol. 81. 31 pp.

Dorr II, J.V. 1969. Physiographic, stratigraphic and structural development of the Quadrilátero Ferrífero, Minas Gerais, Brazil. United States Geological Survey Professional Paper 614-A. 110 pp.

Endo, I., Oliveira, A. H., Peres, G. G., Guimarães, M. L. V., Lagoeiro, L. E., Machado, R., Zavaglia, G., Rosas, C. F., Melo, R. J. 2005. Nappe Curral: Uma megaestrutura alóctone do Quadrilátero Ferrífero e controle da mineralização. 4th International Symposium On Tectonics, Curitiba. Boletim de Resumos Expandidos, p. 279-282.

Endo, I., Galbiatti, H. F., Delgado, C. E. R., Oliveira, M. M. F. de, Zapparoli, A. de C., Moura, L. G. B. de, Peres, G. G., Oliveira, A. H. de, Zavaglia, G., Danderfer F,º A., Gomes, C. J. S., Carneiro, M. A., Nalini, Jr. H. A., Castro, P de T. A., Suita, M. T. de F., Tazava, E., Lana, C. de C., Martins-Neto, M. A., Martins, M. de S., Ferreira F,º F. A., Franco, A. P., Almeida, L. G., Rossi, D. Q., Angeli, G., Madeira, T. J. A., Piassa, L. R. A., Mariano, D. F., Carlos, D. U. 2019. Mapa Geológico do Quadrilátero Ferrífero, Minas Gerais, Brasil. Escala 1:150.000: Uma celebração do cinquentenário da obra de Dorr (1969). Ouro Preto, Departamento de Geologia da Escola de Minas – UFOP - Centro de Estudos Avançados do Quadrilátero Ferrífero: www.qfe2050.ufop.br. p.236-263.

Endo, I., Machado, R., Galbiatti, H. F., Rossi, D. Q., Zapparoli, A de C., Delgado, C. E. R., Castro, P. T. A., Oliveira, M. M. F. de., 2020. Estratigrafia e Evolução Estrutural do Quadrilátero Ferrífero, Minas Gerais. In: Castro P. T. de A. & Endo I., Gandini A. L. (eds.). O Quadrilátero Ferrífero: Avanços do conhecimento nos últimos 50 anos. Departamento de Geologia da Escola de Minas – UFOP - Centro de Estudos Avançados do Quadrilátero Ferrífero: www.qfe2050.ufop.br. p.70-113.

Farina, F., Albert, C., Lana, C. 2015. The Neoarchean transition between medium- and high-K granitoids: Clues from the Southern São Francisco Craton (Brazil). Precambrian Research 266, p. 375–394.

Fernandes, R.C., Endo, I., Pereira, R.M.P, Rivarola, I., de Souza, J.C. 2016. Geologia e evolução estrutural do depósito aurífero Cuiabá: Novas perspectivas para a exploração mineral. In: VII Simpósio Brasileiro de Exploração Mineral, Ouro Preto, 2016.

Ferraz da Costa, M., Kyle, J.R., Lobato, L.M., Ketcham, R.A., Figueiredo e Silva, R.C., Fernandes, R.C. 2022. Orogenic gold ores in three-dimensions: A case study of distinct mineralization styles at the world-class Cuiabá deposit, Brazil, using high-resolution X-ray computed tomography on gold particles, Ore Geology Reviews, 140, 104584.

Feynman. R., 1964. Feynman sobre o método científico – aula na Universidade de Cornell em https://www.youtube.com/watch?v=EYPapE-3FRw&t=178s.

Gair, J.E. 1962. Geology and ore deposit of the Nova Lima and Rio Acima quadrangles, Minas Gerais, Brazil. United States Geological Survey Professional Paper 341-A, 67 pp.

Gonçalves Dias, T., Figueiredo e Silva, R.F., Lobato, L.M., Caxito, F.A., Hagemann, S., Santos, J.O.S., Barrote, V. 2022. Ediacaran - Cambrian fluid flow in Archean orogenic gold deposits: Evidence from U–Pb SHRIMP hydrothermal monazite ages of the metaturbidite-hosted Córrego do Sítio and Pilar deposits, Quadrilátero Ferrífero, Brazil, Journal of S. Am. Earth Sciences, Vol. 116. 103844.

Herz, N. 1970. Gneissic and igneous rocks of the QuadriláteroFerrífero, Minas Gerais, Brazil. U.S. Geological. Survey Professional. Paper, 641(B):1-58.

Holcombe, R., Coughlin, T. 2003. Structural observations in the northern Quadrilatero Ferrifero and implications for gold mineralization. AngloGold Ashanti South America. Internal technical report.

Kresse, C., Lobato, L.M., Hagemann, S.G., Figueiredo e Silva, R.C. 2018. Sulfur isotope and metal variations in sulfides in the BIF-hosted orogenic Cuiaba gold deposit, Brazil: implications for the hydrothermal fluid evolution. Ore Geol. Rev. 98, 1–27.

Kresse, C., Lobato, L.M., Figueiredo e Silva, R.C., Hagemann, S.G., Banks, D., Vitorino, A.L.A. 2020. Fluid signature of the shear-zone controlled Veio de Quartzo ore body in the world-

class BIF-hosted Cuiabá gold deposit, Archaean Rio das Velhas greenstone belt, Brazil: A fluid inclusion study. *Mineralium. Deposita*, *55*, 1–26.

Ladeira, E. A. 1980. Metallogenesis of gold at the Morro Velho Mina and in the Nova lima District, Quadrilátero Ferrífero, Minas Gerais, Brazil. Unpublished PhD thesis, University of Western Ontario, Canada.

Ladeira, E.A. Viveiros, J.F.M. 1984. Hipótese sobre a estruturação do Quadrilátero Ferrífero com base nos dados disponíveis. In *Sociedade Brasileira de Geologia*; Boletim Especial. Belo Horizonte, Minas Gerais, Brasil. 4: 1–14.

Ladeira, E. A. 1991. Genesis of gold Quadrilátero Ferrífero: A remarkable case of permanency, Recycling and inheritance - a tribute Djalma Guimarães, Pierre Routhier and Hans Ramberg. In: Ladeira, E.A. (Ed.): Brazil gold'91 - the economics, geology, geochemistry and gensis of gold deposits, Proceedings, 11-30, Rotterdam (Balkema).

Lana, C., Alkmim, F.F., Armstrong, R., Scholz, R., Romano, R., Nalini Jr., H.A. 2013. The ancestry and magmatic evolution of Archaean TTG rocks of the Quadrilátero Ferrífero province, southeast Brazil. Precambrian Research 231, 157–173.

Lobato L.M., Vieira F.W.R. 1998. Styles of hydrothermal alteration and gold mineralization associated with the Nova Lima Group of the Quadrilátero Ferrífero: Part II, the Archean mesothermal gold-bearing hydrothermal system. Rev. Bras. Geoc., 28: 355-366.

Lobato, L.M., Ribeiro Rodrigues, L.C., Vieira, F.W.R. 2001a. Brazil's premier gold province: Part II. Geology and genesis of gold deposits in the Archean Rio das Velhas greenstone belt, Quadrilátero Ferrífero. Mineralium Deposita 36, 249–277.

Lobato, L.M., Ribeiro Rodrigues, L.C., Zucchetti, M., Noce, C.M., Baltazar, O.F., Silva, L.C., Pinto, C.P. 2001b. Brazil's premier gold province: Part I. The tectonic, magmatic, and structural setting of the Archean Rio das Velhas greenstone belt, Quadrilátero Ferrífero. Mineralium Deposita 36, 228–248.

Lobato, L.M., Baltazar, O.F., Reis, L.B., Achtschin, A.B., Baars, F.J., Timbó, M.A., Berni, G.V., Mendonça, B.R.V., Ferreira, D.V. 2005. Projeto Geologia do Quadrilátero Ferrífero - integração e correção cartográfica em SIG com nota explicativa. Belo Horizonte, CODEMIG. 1 CD-ROM.

Lobato, L.M., Santos, J.O.S., McNaughton, N.J., Fletcher, I.R., Noce, C.M. 2007. U–Pb SHRIMP monazite ages of the giant Morro Velho and Cuiabá gold deposits, Rio das Velhas greenstone belt, Quadrilátero Ferrífero, Minas Gerais, Brazil. Ore Geology Reviews. 32, 674-680.

Machado, N., Carneiro, M.A. 1992. U–Pb evidence of late Archean tectono-thermal activity in the southern São Francisco shield, Brazil. Canadian Journal of Earth Science 29, 2341–2346.

MacKin, J. H., 1950. The down-structure method of viewing geological maps. The Journal of Geology, 58:55–72.

Marshak, S., Alkmim, F. F. 1989. Proterozoic contraction/extension tectonics of the southern São Francisco region, Minas Gerais, Brazil. Tectonics, v., 8, n. 3, p. 555-571.

Martins, B.S., Lobato, L.M., Rosière, C.A., Hagemann, S.G., Santos, J.O.S., Villanova, F.L.S.P. 2016. The Archean BIF-hosted Lamego deposit, Rio das Velhas greenstone belt, Quadrilátero Ferrífero: Evidence for Cambrian structural modification of an Archean orogenic gold deposit. Ore Geology Reviews. 72, 963–988.

Martins, R. 2000. Caracterização petrográfica e geoquímica mineral dos corpos de minério Fonte Grande Sul e Galinheiro, nível 11, mina de ouro de Cuiabá, Quadrilátero Ferrífero, Minas Gerais. Dissertação de Mestrado, IGC/UFMG.

McClay, K.R., Ellis, P.G. 1983. Deformation and recrystallization of pyrite. Mineral Mag. 47, 527-538.

McClay, K.R. 1987. The Mapping of Geological Structures. Geological Society of London Handbook. New York, John Wiley, 161p.

Mikucki, E.J., Ridley, J.R. 1993. The hydrothermal fluid of Archæan lode-gold deposits at different metamorphic grades: compositional constraints from ore and wallrock alteration assemblages. Mineral. Deposita, 28, 469-481.

Moreira, H.S., Lana, C., Nalini, H. 2016. The detrital zircon record of an Archaean convergent basin. Precambrian Research 275, 84-99.

Noce, C.M., Machado, N., Teixeira, W. 1998. U-Pb geochronology of gneisses and granitoids in the Quadrilátero Ferrífero (southern São Francisco craton): age constraints for Archean and

Paleoproterozoic magmatism and metamorphism. Revista Brasileira de Geociências 28, 95–102.

Noce, C.M., Tassinari, C.G., Lobato, L.M. 2007. Geochronological framework of the Quadrilátero Ferrífero, with emphasis on the age of gold mineralization hosted in Archean greenstone belts. Ore Geology Reviews 32, 500–510.

Piassa L. R. A. 2018. A Falha do Engenho revisitada: Sul do Quadrilátero Ferrífero, Minas Gerais. Departamento de Geologia da Escola de Minas da Universidade Federal de Ouro Preto, Ouro Preto, Minas Gerais, Dissertação de Mestrado. 156p.

Pluijm, B.A.V.D., Marshak, S. 2004. Earth Structure: – Second Edition. W.W. Norton and Company Ltd.

Pumpelly R., Wolf, J. E., Dale, T. N. 1894. Geology of the Green Mountains. USGS Mem., 23, 1-157

Ramsay, J.G. 1967. Folding and fracturing of rocks. New York, McGraw-Hill, 568 p.

Ramsay, J.G., Huber, M.I. 1987. The techniques of modern structural geology, volume 2: folds and fractures. Academic Press.

Rankin, L.R. 2006. Quadrilatero Ferrifero Project Southern Brazil: Structural controls on gold mineralisation ant targeting. Geoterp internal technical report for AngloGold Ashanti.

Ribeiro-Rodrigues L.C. 1998. Gold in Archean banded iron-formation of the QuadriláteroFerrífero, Minas Gerais, Brazil. The Cuiabá Mine. Unpublished PhD thesis, Aachen University, Aachen, Germany.

Ribeiro Rodrigues, L.C., Oliveira, C.G., Friedrich, G. 2007. The Archean BIF-hosted Cuiabá Gold deposit, Quadrilátero Ferrífero, Minas Gerais, Brazil. Ore Geology Reviews 32, 543–570.

Ridley, J. 1986. Parallel stretching lineations and fold axes oblique to a shear displacement direction - a model and observations. Journal of Structural Geology, 8, 647-653.

Romano, R., Lana, C., Alkmim, F.F., Stevens, G.S., Armstrong, R. 2013. Stabilization ofthe southern portion of the São Francisco Craton, SE Brazil, through a long-livedperiod of potassic magmatism. Precambrian Research 224, 143–159.

Roncato Jr., J.G., Lobato, L.M., Lima, L.C., Porto, C.G., Figueiredo e Silva, R.C. 2015. Metaturbidite-hosted gold deposits, Córrego do Sítio Lineament, Quadrilátero Ferrífero, Brazil. Brazilian Journal of Geology 45: 5-2. https://doi.org/10.1590/23174889201500010001.

Roncato, J., Almeida, A.L.C., Macedo, B., Oliveira, M. 2020. A geophysical analysis of the Conceição River region Quadrilátero Ferrífero, based on field, petrographic, aerial images and airborne data. São Paulo, UNESP, Geociências, v. 39, n. 1, p. 47 – 63. DOI: https://doi.org/10.5016/geociencias.v39i1.14613.

Ruchkys, U. A., Machado, M. M. M. 2013. Patrimônio geológico e mineiro do Quadrilátero Ferrífero, Minas Gerais - caracterização e iniciativas de uso para educação e geoturismo. Boletim Paranaense de Geociências, Curitiba, v.70, p. 120-133. DOI: http://dx.doi.org/10.5380/geo.v70i0.31541.

Sales, M. 1998. The Geological Setting of the Lamego Iron-Formation Hosted Gold Deposits, Quadrilátero Ferrífero District, Minas Gerais, Brazil. Master's Thesis, Queen's University, Geological Sciences, Kingston, ON, Canada.

Sander, B. 1970. An Introduction to the Study of Geological Bodies. Pergamon Press Ltd., Oxford, London.

Sanglard J. C. D., Rosiere, C.A., Santos, J.O.S., McNaughton, N.J., Fletcher, I.R. 2014. A estrutura do segmento oeste da Serra do Curral, Quadrilátero Ferrífero, e o controle tectônico das acumulações compactas de alto teor em Fe. Geologia USP. Série Científica 13:81–95. DOI: 10.5327/Z1519-874X201400010006

Schorscher, H.D. 1978. Komatiítos na estrutura "Greenstone Belt" Série Rio das Velhas, Quadrilátero Ferrífero, Minas Gerais, Brasil. 30th Congresso Brasileiro de Geologia. Sociedade Brasileira de Geologia, Recife, pp. 292–293.

Schorscher H.D., Carbonari F.S., Polonia J.C., Moreira J. M. P. 1982. Quadrilatero Ferrífero - Minas Gerais State: Rio das Velhas Greenstone Belt and Proterozoic Rocks. In: International Symposium On Archean And Early Proterozoic Crustal Evolution And Metallogenesis - ISAP - Excursion Guide (Annex.). CPM-SME. Salvador, Bahia, 46 p.

Sepulveda, G., Novo, T. A., Roncato, J. 2021. Characteriation and geochronology os Archean metasedimetary sequences in the eastern portiom of Rio das Velhas Greenstone Belt, Quadrilátero Ferrífero, Brazil. Journal of South American Earth Sciences 102, 102962. https://doi.org/10.1016/j.jsames.2020.102962.

Sena, N.C., Figueiredo E Silva, R.C., Lobato, L.M., Duarte, V.N., Martins, B.S. 2021. Paleoenvironmental reconstruction of gold-bearing BIF from the Archean Cuiabá deposit based on petrographic and geochemical studies. Journal of South American Earth Sciences, 108, June 2021, 103223 https://doi.org/10.1016/j.jsames.2021.103223

Simmons, G.C. 1968. Geology and iron deposits of the westem Serra do Curral, Minas Gerais, Brazil. Washington: USGS, Prof. Paper, 341-g, a. 57 p.

Silva, C.M.G. 2006. Aplicação de isótopos radiogênicos na mineralização de ouro da mina Cuiabá, Greenstone Belt Rio das Velhas, MG. Master thesis, University of São Paulo Geosciences Institute.

Skjernaa, L. 1989. Tubular folds and sheath folds: definitions and conceptual models for their development, with examples from the Grapesvare area, northern Sweden. Journal of Structural Geology 11, 689–703.

Sullivan W. A. 2013. L tectonites. Journal of Structural Geology, 50:161-175.

Toledo C.L.B. 1997. Controle estrutural da mineralizacão aurifera na mina de Cuiabá, setor noroeste do Greenstone Belt Rio das Velhas, Quadrilátero Ferrifero. Universidade Estadual de Campinas, M.Sc. Thesis, 166p.

Vial, D.S. 1980. Mapeamento Geológico do Nível 3 da Mina de Cuiabá. Relatório interno da Mineração Morro Velho S.A. 21p.

Vial, D.S. 2007. Smaller gold deposits in the Archean Rio das Velhas greenstone belt, Quadrilátero Ferrífero, Brazil. Ore Geology Reviews 32, 651-673.

Vieira F.W.R. & Oliveira G.I. 1988. Geologia do distrito aurífero de Nova Lima, Minas Gerais. In: C. Schobenhaus-Filho, C.E.S. Coelho (eds) Metais básicos não ferrosos, ouro e alumínio. Principais depósitos minerais do Brasil 3. DNPM/CVRD, Brasília, Brasil, p. 377-391.

Vieira F.W.R. 1992. Geologia da Mina de Cuiaba, Niveis 03 e 04. Internal Report, Mineracao Morro Velho S. A., Nova Lima, pp. 23.

Vieira, F.W.R. 2000. Controle estrutural das mineralizações auríferas do Grupo Nova Lima. Workshop Quadrilátero Ferrífero AngloGold. Internal report.

Vitorino, A.L.A. 2017. Mineralizacao aurifera associada aos veios quartzo-carbonaticos hospedados na unidade mafica basal da jazida Cuiaba, greenstone belt Rio das Velhas, Quadrilatero Ferrifero, Minas Gerais, Brasil. Unpublished M.Sc. thesis, Universidade Federal Minas Gerais, Brazil.

Vitorino, A.L.A., Figueiredo e Silva, R., Lobato, L.M. 2020. Shear-zone-related gold mineralization in quartz-carbonate veins from metamafic rocks of the BIF-hosted world-class Cuiaba deposit, Rio das Velhas greenstone belt, Quadrilatero Ferrifero, Brazil: Vein classification and structural control. Ore Geology Reviews 127.

Xavier RP, Toledo CLB, Taylor B, Schrank A. 2000. Fluid evolution and gold deposition at the Cuiabá mine, SE Brazil: fluid inclusions and stable isotope geochemistry of carbonates. Rev Bras Geogr 30:337– 341.

Zucchetti M., Baltazar O.F. 2000. Rio das Velhas Greenstone Belt lithofacies associations, Quadrilátero Ferrífero, Minas Gerais, Brazil. In: 31th International. Geological. Congress, Rio de Janeiro. CD-ROM.

ANEXO A – Comprovante de submissão de artigo

Journal of South American Earth Sciences

STRUCTURAL MODEL AND FEATURES OF THE WORLD-CLASS CUIABÁ OROGENIC GOLD DEPOSIT, RIO DAS VELHAS GREENSTONE BELT, QUADRILÁTERO FERRÍFERO REGION, BRAZIL

--Manuscript Draft--

Manuscript Number:	SAMES-D-22-00548R2
Article Type:	Review Article
Section/Category:	Economic geology, metallogenesis and hydrocarbon genesis and reservoirs
Keywords:	Orogenic gold deposit, fold interference pattern, structural model, structural metallogenesis.
Corresponding Author:	Raphael do Carmo Fernandes, BSC Federal University of Minas Gerais Geosciences Institute BELO HORIZONTE, MG BRAZIL
First Author:	Raphael do Carmo Fernandes, Bachelor
Order of Authors:	Raphael do Carmo Fernandes, Bachelor
	Jorge Roncato, Doctoral degree
	Rodrigo Sérgio de Paula, Doctoral degree
Abstract:	The structural architecture of an orogenic deposit is essential for its metallogenetic understanding, as both subjects are interconnected in this type of environment. Cuiabá gold deposit, located in Archean rocks from Rio das Velhas Greenstone Belt, is the subject of numerous studies focused mainly on metallogenetic issues. From the point of view of structural characterization, two divergent models have been studied: the sheath-fold model and the refolding model. Such hypothesis is different in terms of defining an exploratory research plan and, therefore, the detailed structural characterization is still not well understood. As a way of filling this gap, the main objective of this work is to propose a structural characterization of the entire deposit in order to demonstrate evidence for a new model of tectonic evolution. For this, the methodologies applied for this work were: underground geological mapping in all available ore galleries and definition of geological-structural domains whose main criteria are related to down-plunge view of fold asymmetry and stratigraphic indicators. Structural geology is characterized by 3 deformation phases related to 2 tectonic events. The first event has two ductile-progressive deformation phases (D1 and D2), with NE-SW strike-slip direction of transport associated coaxial fold interference patterns with cylindrical geometry plunging to ESE, which represents the main structure at the mine. The second event is a brittle-ductile deformational phase (D3) with W-verging reverse fault systems, probably associated to Brasiliano Pan-African Orogeny. Gold mineralization is associated with silica and sulfide-rich hydrothermal fluid introduction through D1 and D2 axial-plane foliation. Phase D1 is pyrrhotite-associated mineralization, with coarse gold presence. D2 phase has pyrite-associated mineralization with fine gold. There is no gold in phase D3, although it has late-tectonic sulphides formation. Therefore, there is no field evidence that corroborate the existence of sheath folds for the deposit. Fold interference patterns associated to deposit morphology suggests SW and N prospective targets, with strong possibility of structural connection between other gold deposits, such as Lamego and Descoberto targets.

ANEXO B - Comprovante de publicação no periódico Journal of South American Earth Sciences

ELSEVIER

Journal of South American Earth Sciences
Volume 123, March 2023, 104201

Structural model and features of the world-class Cuiabá orogenic gold deposit, Rio das Velhas greenstone belt, Quadrilátero Ferrífero region, Brazil

Raphael do Carmo Fernandes [a b], Jorge Roncato [b], Rodrigo Sérgio de Paula [b]

[a] Anglogold Ashanti, Cuiabá Mine, Estrada Mestre Caetano, S/n Cuiabá, Sabará, MG, 34505-320, Brazil

[b] Instituto de Geociências-Centro de Pesquisa Manoel Teixeira da Costa, Departamento de Geologia, Universidade Federal de Minas Gerais, Av. Antônio Carlos 6627, Campus Pampulha, 30130-009, Belo Horizonte, Minas Gerais, Brazil

Received 20 October 2022, Revised 10 January 2023, Accepted 15 January 2023, Available online 23 January 2023, Version of Record 28 January 2023.

Check for updates

Show less

+ Add to Mendeley Share Cite

https://doi.org/10.1016/j.jsames.2023.104201

Get rights and content